TESIS DOCTORAL: Programa de doctorado en Medicina

NUEVAS METODOLOGÍAS PARA LA SELECCIÓN NO INVASIVA DE EMBRIONES HUMANOS EN TRATAMIENTOS DE REPRODUCCIÓN ASISTIDA: INTRODUCCIÓN DE LA INTELIGENCIA ARTIFICIAL EN LOS LABORATORIOS DE FECUNDACIÓN IN VITRO.

Lorena Bori Arnal

Directores:

Dr. Marcos Meseguer Escrivá

Dra. Thamara Alexandra Viloria Samochin

Dr. José Alejandro Remohí Giménez

VNIVERSITAT DE VALÈNCIA
Facultat de Medicina i Odontologia

Valencia, Noviembre 2022

“No es la especie más fuerte, ni la más inteligente la que sobrevive. Es la que más se adapta al cambio.”

Charles Darwin

NUEVAS METODOLOGÍAS PARA LA SELECCIÓN NO INVASIVA DE EMBRIONES HUMANOS EN TRATAMIENTOS DE REPRODUCCIÓN ASISTIDA: INTRODUCCIÓN DE LA INTELIGENCIA ARTIFICIAL EN LOS LABORATORIOS DE FECUNDACIÓN IN VITRO.

NEW METHODOLOGIES FOR THE NON-INVASIVE SELECTION OF HUMAN EMBRYOS IN ASSISTED REPRODUCTION TREATMENTS: INTRODUCTION OF ARTIFICIAL INTELLIGENCE IN IN VITRO FERTILIZATION LABORATORIES.

Lorena Bori Arnal

Directores de tesis: Dr. Marcos Meseguer Escrivá, Dra. Thamara Alexandra Viloria Samochin y Dr. José Alejandro Remohí Giménez.

Tesis doctoral

Programa de Doctorado 3139 Medicina: Obstetricia, ginecología y medicina regenerativa.

Facultat de Medicina i Odontologia

Valencia, Noviembre 2022

Don Marcos Meseguer Escrivá, doctor en biomedicina por la Universitat de Valencia, embriólogo en IVI Valencia y supervisor científico de IVIRMA Global.

Doña Thamara Alexandra Viloria Samochin, doctora en ciencias biológicas por la Universitat de Valencia y embrióloga supervisora del laboratorio de fecundación in vitro en IVI Valencia.

Don José Alejandro Remohí Giménez, catedrático de pediatria, obstetricia y ginecología de la Universitat de Valencia y presidente de IVIRMA Global.

CERTIFICAN:

Que la presente memoria, titulada "*Nuevas metodologías para la selección no invasiva de embriones humanos en tratamientos de reproducción asistida: introducción de la inteligencia artificial en los laboratorios de fecundación in vitro.*", corresponde al trabajo realizado bajo su dirección por Dña. Lorena Bori Arnal, para su presentación como Tesis Doctoral en el Programa de Doctorado en Medicina de la Universitat de València.

Y para que conste firman el presente certificado en Valencia, a 28 de noviembre de 2022.

Fdo.: Dr. Marcos Meseguer Escrivá	Fdo.: Dra. Thamara Viloria Samochin	Fdo.: Dr José Alejandro Remohí Giménez
		

Agradecimientos

Con estas líneas me gustaría expresar mi más sincero agradecimiento a todas las personas que han ayudado a que este trabajo de investigación haya salido adelante, por su soporte científico y/o humano.

Quiero agradecer en primer lugar a mis directores de tesis Dr. Marcos Meseguer, Dra. Thamara Viloria y Dr. José Remohi que han hecho posible la ejecución de los estudios presentados en esta memoria.

Nunca hubiese pensado que realizaría la tesis bajo la supervisión de un referente en el mundo de la embriología, Marcos. Cuando te escribí el primer e-mail para colaborar en uno de tus miles de proyectos, no me imaginaba todo este trayecto. Gracias por confiar en mí todos estos años. Recorrer este camino contigo me ha brindado muchísimas experiencias, de las que siempre he aprendido algo nuevo. Te agradezco todas las reuniones, congresos, viajes, e incluso, tus audios de WhatsApp. Gracias por todo el aprendizaje y enriquecimiento personal.

Tammy, gracias por estar siempre dispuesta a ayudar.

A los compañeros que he ido conociendo durante estos años. Aunque no pueda nombrarlos a todos, gracias por hacer más fácil el día a día.

Lu, gracias por acogerme desde el primer día. ¡Quién me iba a decir que la primera persona con la que hablé del FIV sería con la que más conectaría! Admiro la pasión y delicadeza que tienes por tu trabajo. Aunque sin duda, los mejores momentos los hemos vivido (y viviremos) fuera del laboratorio.

Marta, eres el ejemplo de que tener miedo no significa no ser valiente. Porque no hay nada que se te resista. Agradezco a la vida que nos uniera en Valencia para compartir parte de este camino. Siempre recordaré nuestras tertulias matutinas, gracias por todos tus consejos amiga.

Ángel, gracias por haber formado parte en esta travesía. Me alegro de que empezáramos esta etapa juntos, porque los años en IVI 2 son imborrables. Eres un gran profesional y mejor persona.

Nandito, no podría haber llegado alguien mejor al equipo MM. Siempre me recuerdas que el primer día te pregunté “qué eras”. No me imaginaba que desde ese

día ibas a ser un gran apoyo. Gracias por hacer que los momentos más estresantes acabaran en risas.
Marian, pasamos de convivir en 2 m^2 a no vernos en semanas. Y, aun así, sé que siempre estás ahí. Gracias por echarme una mano cuando la necesitaba y por todo lo que he aprendido contigo.
Elena, gracias por enseñarme tanto, aun hablando distinto "idioma". Muy agradecida de conocerte, dentro y fuera del trabajo.
Irene, quería que tu nombre estuviese entre estas líneas. Porque, aunque no pasaste mucho tiempo en nuestro equipo, fue suficiente para darme cuenta de lo grande que eres.
Nuria, gracias por tu naturalidad. Por tu entusiasmo en cada tema que hablamos. Agradezco conocer a alguien tan especial.
A todo el equipo de IVIRMA Valencia y Fundación IVI. Sobre todo, al laboratorio de FIV. Gracias a todas las personas que han colaborado directa o indirectamente en este trabajo.

A mis amigas, que sin darse cuenta me han ayudado a desconectar cuando más lo necesitaba. Gracias por estar siempre ahí: Aida, Africa, Elena, Julia, Laura, Lewis y Paola. Y a mi amigo Javier. Os quiero.
A mi hermana y a mi Lili, por sacarme una sonrisa en cualquier momento. Muy feliz de convertirme en tía en esta etapa de mi vida. Os quiero.
A mis padres. No existen palabras de agradecimiento para vosotros. Sois los máximos responsables de que haya llegado hasta aquí. Gracias por los valores que me habéis transmitido y por hacer que todo sea más fácil. Os quiero.
A mi chico, mi gran compañero desde el principio. No podría haber elegido una persona mejor. Gracias por enseñarme que soy más fuerte de lo que creo. Por todo lo que me das. Te quiero.

ÍNDICE

Símbolos, abreviaturas y siglas

AI: Inteligencia artificial, del inglés *artificial intelligence*

ANN: Red neuronal artificial, del inglés *artificial neural network*

ASEBIR: Asociación para el estudio de la biología de la reproducción

AUC: Área bajo la curva

BC: Blastocisto cavitado

BE: Blastocisto expandido

BEd: Diámetro de expansión del blastocisto

BH: Blastocisto eclosionado

BHi: Blastocisto eclosionando

BT: Blastocisto temprano

CCL23: Ligando de quimiocina 23

ccTroph: Ciclo celular del trofoectodermo

CD: grupo de diferenciación

CX3CL1: Quimioquina ligando 1

CXCL: Ligando de quimioquinas con motivo C-X-C

D+2: Segundo día de desarrollo embrionario

D+3: Tercer día de desarrollo embrionario

D+4: Cuarto día de desarrollo embrionario

D+5: Quinto día de desarrollo embrionario

D+6: Sexto día de desarrollo embrionario

DL: Aprendizaje profundo, del inglés *deep learning*

DNER: Receptor relacionado Delta/Notch-like EGF

DS: Desviación estándar

EIM: Consorcio europeo de fecundación in vitro

EMMPRIN: Inductor de inductor de la metaloproteinasa de la matriz

EpCAM: Molécula de adhesión de células epiteliales

ESHRE: Sociedad europea de reproducción humana y embriología

FIV: Fecundación in vitro

Flt3L: Ligando de la tirosina quinasa 3 tipo FMS

GM-CSF: Factor estimulante de colonias de granulocitos y macrófagos

h: Horas

hCG: Hormona gonadotropina coriónica

HE-4: Proteína 4 del epidídimo humano

HLA-G: Antígeno leucocitario humano G

IA: Inteligencia artificial

IC: Íntervalo de confianza

ICMa: Área de la masa celular interna

ICSI: Inyección intracitoplasmática

IFN-α2: Interferón-α2

IL: Interleucina

IMC: Índice de masa corporal

IVF: Fecundación in vitro, del inglés *in vitro fertilization.*

KID: Datos de implantación conocidos

KiSS: Kisspeptina

MCI: Masa celular interna

MCP-1: proteína quimiotaxis aceptante de metilo

MIP-1β: Proteína inflamatoria de macrófagos-1β

ML: Aprendizaje automático, del inglés *machine learning*

MMP1: Metalopeptidasa de matriz 1

MSP-α: Proteína estimulante de macrófagos-α

NPX: Expresión proteica normalizada

OR: Odds ratio

PEA: Ensayo de extensión por proximidad, del inglés *proximity extensión assay*

PGT-A: Test genético preimplantatorio para aneuploidías

PGT-M: Test genético preimplantatorio para enfermedades monogénicas

PLGF: Factor de crecimiento placentario

PN: Pronúcleos

PNm: Migración de los pronúcleos

PZD: Perforación parcial de la zona pelúcida

RNV: Recién nacido vivo

SCF: Factor de células madre

SET: Transferencia de un único embrión, del inglés *single embryo transfer*

SI: Sistema internacional

SP1: Glicoproteína P-1 específica del embarazo

SUZI: Inseminación subzonal

t2: Tiempo de división a dos células

t3: Tiempo de división a tres células

t4: Tiempo de división a cuatro células

t5: Tiempo de división a cinco células

t6: Tiempo de división a seis células

t7: tiempo de división a siete células

t8: Tiempo de división a ocho células

tB: Tiempo de formación de blastocisto

tBEd: Tiempo de la medición BEd

TE: Trofoectodermo

tEB: Tiempo de blastocisto expandido

tHib: Tiempo de inicio de eclosión

tICMa: Tiempo de la medición ICMa

TL: Lapso de tiempo, del inglés *time-lapse*

tM: Tiempo de formación de mórula

TNF: Factor de necrosis tumoral

TNFRSF9: Miembro de la superfamilia del receptor del TNF 9

tPNa: Tiempo de aparición de los pronúcleos

tPNf: Tiempo de desaparición de los pronúcleos

TRA: Técnicas de reproducción asistida

TRAIL: Ligando inductor de apoptosis relacionado con TNF

TRAIL-R3: Receptor para el ligando citotóxico TRAIL

tSB: Tiempo de inicio de blastulación

tSC: tiempo de inicio de compactación

uPA: Activador del plasminógeno urocinasa

v1: Primera versión

v2: Segunda versión

v3: Tercera versión

VEGFA: Factor de crecimiento endotelial vascular

µm: Micrómetros

Lista de figuras

Figura 12. Gráfico de columnas agrupadas del artículo II que representa la media del valor NPX obtenido mediante la técnica PEA para las 25 proteínas útiles analizadas en los medios de cultivo de 81 embriones generados a partir de óvulos autólogos.

Lista de tablas

Resumen

Resumen

La evaluación y selección de embriones en los tratamientos de fecundación in vitro (FIV) se realiza manualmente de forma convencional, mediante observaciones puntuales bajo el microscopio durante el desarrollo del embrión in vitro. Dicho análisis altera las condiciones de cultivo, pudiendo afectar a las tasas de éxito del tratamiento de reproducción asistida. La introducción de la microscopía de lapso de tiempo o *time-lapse* ha hecho posible un seguimiento continuo de los embriones in vitro. De esta forma, se obtiene rutinariamente gran cantidad de información en formato de imágenes grabadas. Hoy en día, el análisis de este material todavía se realiza manualmente, y las imágenes se utilizan sobre todo cualitativamente.

Otra fuente de información acerca de la viabilidad de los embriones in vitro es el medio de cultivo en el que se incuban durante su desarrollo. Numerosos estudios avalan la importancia de la interacción entre el embrión y el tracto reproductor femenino mediante ligandos y receptores durante la fase preimplantacional. Actualmente, el avance en las técnicas de análisis de proteómica permite conocer los valores de numerosos marcadores simultáneamente en el medio de cultivo embrionario.

Nosotros hipotetizamos que se podría considerar el uso de herramientas y técnicas computacionales para aprovechar esta gran cantidad de datos y mejorar la evaluación de los embriones. Mediante el uso de la inteligencia artificial (IA) se podrían identificar particularidades conocidas y desconocidas que caractericen un embrión con alto potencial de implantación. Información resultante de la incubación in vitro (tanto las imágenes *time-lapse*, como el perfil secretómico), podría medirse con esta tecnología, ya que es capaz de analizar cantidades masivas de datos.

El objetivo general de esta tesis es definir nuevas metodologías no invasivas como herramienta de apoyo en los laboratorios de fecundación in vitro para seleccionar qué embrión transferir a la paciente, desarrollando y aplicando innovadoras tecnologías como la inteligencia artificial para automatizar y mejorar la evaluación

in vitro. Para ello, se plantearon los siguientes objetivos específicos: a) describir parámetros del desarrollo embrionario y su relación con el potencial de implantación; b) identificar marcadores no invasivos del secretoma embrionario y su asociación con el éxito de un tratamiento de reproducción asistida; c) desarrollar modelos basados en inteligencia artificial para predecir resultados clínicos; y d) evaluar herramientas para la automatización de la selección embrionaria en los laboratorios de fecundación in vitro.

La presente investigación de tesis doctoral se presenta como un compendio de tres publicaciones con datos relevantes para avanzar en la selección embrionaria con métodos no invasivos, señalando a la inteligencia artificial como herramienta de apoyo fundamental en los laboratorios de fecundación in vitro. Los siguientes artículos componen este compendio:

I. Novel and conventional embryo parameters as input data for artificial neural networks: an artificial intelligence model applied for prediction of the implantation potential. Bori L, Paya E, Alegre L, Viloria TA, Remohi JA, Naranjo V, Meseguer M. Fertil Steril. 2020 Dec;114(6):1232-1241. doi: 10.1016/j.fertnstert.2020.08.023. Epub 2020 Sep 8. PMID: 32917380. 5-year impact factor: 8,109.

El objetivo principal de este estudio fue predecir el potencial de implantación del embrión utilizando nuevos parámetros no invasivos observados con sistemas *time-lapse*. Para ello, propusimos algunos parámetros morfodinámicos del embrión, que no habían sido evaluados hasta el momento, y analizamos su asociación con la probabilidad de implantación. Finalmente, desarrollamos un modelo utilizando redes neuronales artificiales para predecir el éxito de la implantación.

II. An artificial intelligence model based on the proteomic profile of euploid embryos and blastocyst morphology: a preliminary study. Bori L, Dominguez F, Fernandez EI, Del Gallego R, Alegre L, Hickman C, Quiñonero A, Nogueira MFG, Rocha JC, Meseguer M. Reprod Biomed

Online. 2021 Feb;42(2):340-350. doi: 10.1016/j.rbmo.2020.09.031. Epub 2020 Oct 8. PMID: 33279421. 5-year impact factor: 4,603

El objetivo del presente estudio era desarrollar un modelo de predicción de nacimientos vivos basado en la inteligencia artificial. Se utilizaron datos procedentes del análisis de imagen de blastocistos e información proteómica del medio de cultivo embrionario para predecir el potencial de un embrión euploide para dar lugar a un nacimiento vivo.

III. The higher the score, the better the clinical outcome: retrospective evaluation of automatic embryo grading as a support tool for embryo selection in IVF laboratories. Bori L, Meseguer F, Valera MA, Galan A, Remohi J, Meseguer M. Hum Reprod. 2022 May 30;37(6):1148-1160. doi: 10.1093/humrep/deac066. PMID: 35435210. 5-year impact factor: 5,632

El objetivo principal de este estudio fue evaluar la utilidad de una puntuación embrionaria automática como herramienta de apoyo a la toma de decisiones en los laboratorios de FIV. En primer lugar, analizamos la asociación entre la puntuación del embrión y una serie de resultados clínicos, como la ploidía, el embarazo, la implantación y el nacimiento vivo. En segundo lugar, cuantificamos la contribución de la puntuación del embrión en los resultados de implantación y nacimiento vivo en diferentes escenarios en un contexto individualizado.

Summary

Summary

Embryo evaluation and selection in in vitro fertilization (IVF) treatments is performed manually in a conventional way, through specific observations under the microscope during the embryo development in vitro. Such analysis alters the culture conditions and may affect the success rates of assisted reproduction treatment. The introduction of time-lapse microscopy has made it possible to continuously monitor embryos in vitro. In this way, a large amount of information is routinely obtained in the form of recorded images. Today, the analysis of this material is still performed manually, and the images are mostly used qualitatively.

Another source of information about the viability of in vitro embryos is the culture medium in which they are incubated during their development. Numerous studies support the importance of the interaction between the embryo and the female reproductive tract by means of ligands and receptors during the preimplantation phase. Currently, advances in proteomic analysis techniques make it possible to know the values of numerous markers simultaneously in the embryo culture medium.

We hypothesize that the use of computational tools and techniques could be considered to take advantage of this large amount of data and improve embryo evaluation. Using artificial intelligence (AI), known and unknown particularities that characterize an embryo with high implantation potential could be identified. Information resulting from in vitro incubation (both time-lapse images and secretomic profiling) could be measured with this technology, as it can analyze massive amounts of data.

The general objective of this thesis is to define new non-invasive methodologies as a support tool in in vitro fertilization laboratories to select which embryo to transfer to the patient, developing and applying innovative technologies such as artificial intelligence to automate and improve in vitro evaluation. To this end, the following specific objectives were proposed: a) to describe parameters of embryo development and their relationship with implantation potential; b) to identify non-

invasive markers of the embryonic secretome and their association with the success of assisted reproduction treatment; c) to develop models based on artificial intelligence to predict clinical outcomes; and d) to evaluate tools for the automation of embryo selection in in vitro fertilization laboratories.

The present doctoral thesis is presented as a compendium of three publications with relevant data to advance embryo selection with non-invasive methods, highlighting artificial intelligence as a key support tool in in vitro fertilization laboratories. The following articles make up this compendium:

I. Novel and conventional embryo parameters as input data for artificial neural networks: an artificial intelligence model applied for prediction of the implantation potential. Bori L, Paya E, Alegre L, Viloria TA, Remohi JA, Naranjo V, Meseguer M. Fertil Steril. 2020 Dec;114(6):1232-1241. doi: 10.1016/j.fertnstert.2020.08.023. Epub 2020 Sep 8. PMID: 32917380. 5-year impact factor: 8,109.

The main aim of this study was to predict embryo implantation potential using new non-invasive parameters observed with time-lapse systems. For this purpose, we proposed new morphodynamic parameters of the embryo, which had not been evaluated so far, and analyzed their association with the probability of implantation. Finally, we developed a model using artificial neural networks to predict implantation success.

II. An artificial intelligence model based on the proteomic profile of euploid embryos and blastocyst morphology: a preliminary study. Bori L, Dominguez F, Fernandez EI, Del Gallego R, Alegre L, Hickman C, Quiñonero A, Nogueira MFG, Rocha JC, Meseguer M. Reprod Biomed Online. 2021 Feb;42(2):340-350. doi: 10.1016/j.rbmo.2020.09.031. Epub 2020 Oct 8. PMID: 33279421. 5-year impact factor: 4,603

The aim of the present study was to develop an artificial intelligence-based live birth prediction model. Data from blastocyst image analysis and proteomic

information from the embryo culture medium were used to predict the potential of a euploid embryo to lead to a live birth.

III. The higher the score, the better the clinical outcome: retrospective evaluation of automatic embryo grading as a support tool for embryo selection in IVF laboratories. Bori L, Meseguer F, Valera MA, Galan A, Remohi J, Meseguer M. Hum Reprod. 2022 May 30;37(6):1148-1160. doi: 10.1093/humrep/deac066. PMID: 35435210. 5-year impact factor: 7,736

The main objective of this study was to evaluate the usefulness of an automated embryo score as a decision support tool in IVF laboratories. First, we analyzed the association between embryo scoring and several clinical outcomes, such as embryo ploidy, pregnancy, implantation, and live birth. Second, we quantified the contribution of embryo score on implantation and live birth outcomes in different scenarios in an individualized context.

Compendio de artículos que avalan esta tesis

Esta tesis se basa en tres publicaciones a modo de compendio en las que la candidata es la primera autora. El texto completo de las publicaciones se muestra a continuación.

Bori L, Paya E, Alegre L, Viloria TA, Remohi JA, Naranjo V, Meseguer M. Novel and conventional embryo parameters as input data for artificial neural networks: an artificial intelligence model applied for prediction of the implantation potential. Fertil Steril. 2020 Dec;114(6):1232-1241. doi: 10.1016/j.fertnstert.2020.08.023. Epub 2020 Sep 8. PMID: 32917380.

Bori L, Dominguez F, Fernandez EI, Del Gallego R, Alegre L, Hickman C, Quiñonero A, Nogueira MFG, Rocha JC, Meseguer M. An artificial intelligence model based on the proteomic profile of euploid embryos and blastocyst morphology: a preliminary study. Reprod Biomed Online. 2021 Feb;42(2):340-350. doi: 10.1016/j.rbmo.2020.09.031. Epub 2020 Oct 8. PMID: 33279421.

Bori L, Meseguer F, Valera MA, Galan A, Remohi J, Meseguer M. The higher the score, the better the clinical outcome: retrospective evaluation of automatic embryo grading as a support tool for embryo selection in IVF laboratories. Hum Reprod. 2022 May 30;37(6):1148-1160. doi: 10.1093/humrep/deac066. PMID: 35435210.

ARTÍCULO I

Artículo I: Novel and conventional embryo parameters as input data for artificial neural networks: an artificial intelligence model applied for prediction of the implantation potential.

Bori L, Paya E, Alegre L, Viloria TA, Remohi JA, Naranjo V, Meseguer M.

Fertil Steril. 2020 Dec;114(6):1232-1241. doi: 10.1016/j.fertnstert.2020.08.023.

Epub 2020 Sep 8. PMID: 32917380.

Factor de impacto 2021: 7,490
5-años factor de impacto: 8,109

Novel and conventional embryo parameters as input data for artificial neural networks: an artificial intelligence model applied for prediction of the implantation potential

Lorena Bori, M.Sc.,[a] Elena Paya, M.Sc.,[a,b] Lucia Alegre, M.Sc.,[a] Thamara Alexandra Viloria, Ph.D.,[a] Jose Alejandro Remohi, M.D., Ph.D.,[a] Valery Naranjo, Ph.D.,[b] and Marcos Meseguer, Ph.D.[a,c]

[a] IVI-RMA Valencia; [b] Instituto de Investigación e Innovación en Bioingeniería, Universitat Politécnica de Valencia; and [c] Health Research Institute la Fe, Valencia, Spain

Objective: To describe novel embryo features capable of predicting implantation potential as input data for an artificial neural network (ANN) model.
Design: Retrospective cohort study.
Setting: University-affiliated private IVF center.
Patient(s): This study included 637 patients from the oocyte donation program who underwent single-blastocyst transfer during two consecutive years.
Intervention(s): None.
Main Outcome Measure(s): The research was divided into two phases. Phase 1 consisted of the description and analysis of the following embryo features in implanted and nonimplanted embryos: distance and speed of pronuclear migration, blastocyst expanded diameter, inner cell mass area, and trophectoderm cell cycle length. Phase 2 consisted of the development of an ANN algorithm for implantation prediction. Results were obtained for four models fed with different input data. The predictive power was measured with the use of the area under the receiver operating characteristic curve (AUC).
Result(s): Out of the five novel described parameters, blastocyst expanded diameter and trophectoderm cell cycle length had statistically different values in implanted and nonimplanted embryos. After the ANN models were trained and validated using fivefold cross-validation, they were capable of predicting implantation on testing data with AUCs of 0.64 for ANN1 (conventional morphokinetics), 0.73 for ANN2 (novel morphodynamics), 0.77 for ANN3 (conventional morphokinetics + novel morphodynamics), and 0.68 for ANN4 (discriminatory variables from statistical test).
Conclusion(s): The novel proposed embryo features affect the implantation potential, and their combination with conventional morphokinetic parameters is effective as input data for a predictive model based on artificial intelligence. (Fertil Steril® 2020;114:1232–41. ©2020 by American Society for Reproductive Medicine.)
El resumen está disponible en Español al final del artículo.

Key Words: Embryo parameters, implantation, artificial intelligence, time-lapse, artificial neural network

Received May 4, 2020; revised August 14, 2020; accepted August 19, 2020; published online September 8, 2020.
L.B. has nothing to disclose. E.P. has nothing to disclose. L.A. has nothing to disclose. T.A.V. has nothing to disclose. J.A.R. has nothing to disclose. V.N. has nothing to disclose. M.M. has nothing to disclose.
Supported by the Ministry of Science, Innovation, and Universities CDTI (IDI-20191102), an Industrial Ph.D. grant (DIN2018-009911), and Agencia Valenciana de Innovació (INNCAD00-18-009) to E.P. and M.M.
Reprint requests address: Lorena Bori, M.Sc., IVI Valencia, Pl. Policía Local, 3, Valencia, Spain (E-mail: lorena.bori@ivirma.com).

Fertility and Sterility® Vol. 114, No. 6, December 2020 0015-0282/$36.00

https://doi.org/10.1016/j.fertnstert.2020.08.023

The European In Vitro Fertilization (IVF)–Monitoring Consortium (EIM) for the European Society of Human Reproduction and Embryology reported, in its 18th annual report, more than 8 million treatments with the use of assisted reproductive technology and nearly 1.5 million newborn children (1). Most treatments reported to EIM were performed through intracytoplasmic sperm injection (ICSI) and subsequent in vitro embryo culture. The selection of the most appropriate embryo of an entire cohort is a relevant factor for the successful outcome of an infertility treatment.

From the very beginning of IVF practice, morphology has been the criterion par excellence to evaluate the development of the embryo (2). The assessment is usually performed under an optical microscope at ×400 magnification to count the number of cells, fragmentation level, or multinucleation, among other parameters. Limitations of this method are not only associated with the subjectivity of the embryologist (3), but also with the evaluation per se. Even though the incubator has optimal culture conditions, gas concentrations and temperature are altered by removing the embryos from the incubator to allow a static observation (4). Therefore, embryos are evaluated at limited time points and a lot of information is missing from the observations (5). It is well reported that the embryo stage and classification can vary in a few hours (6, 7), resulting in nonsuccessful embryo selection.

The introduction of time-lapse (TL) systems in IVF laboratories allows the continuous monitoring of embryo development in real time. This technology has become a useful tool to study the dynamic embryo development without disturbing the culture conditions and offers objective and precise information in a qualitative and quantitative way (8). It has been used to create predictive algorithms by applying morphologic and morphokinetic parameters to choose the best embryo to transfer (9).

Abnormal division patterns, multinucleation, fragmentation, or collapse are some of the deselecting parameters used to categorize embryo quality (10). These parameters have been associated with inadequate blastocyst formation (11), low euploidy rate (12) and poor implantation and live birth rates (12–20).

Over time, the final goal of the algorithms has changed from appropriate embryo development to healthy live birth. The most used morphokinetic parameters to predict blastulation were the duration of the second cell cycle (cc2), the time period to complete synchronous divisions (s2 and s3), the division time to two cells (t2), and the division time to five cells (t5) (13, 21–28). The events more frequently used to predict implantation were cc2, t5, and s2 (13, 28–32). Even though morphokinetic parameters are not enough to predict ploidy (33), most of the embryos with abnormal cell division times have chromosomal alterations (5, 29, 34). It is also reported that aneuploid embryos are delayed compared with euploid ones in different morphokinetic parameters, such as the timing of morula and blastocyst formation (35–37). Therefore, TL technology could reduce the risk of transferring aneuploid embryos in treatments with no preimplantation genetic testing (PGT) (38).

Nevertheless, there has been very little improvement in live birth rate over the past few years (1, 39), raising the need to investigate new approaches. The continuous recording of the embryo development provides high-quality images that allow the embryologists to find precise markers to determine embryo quality. The problem of existing algorithms is the incapacity for using the large amount of data provided by time-lapse systems. Innovative artificial intelligence (AI) techniques are capable of changing the subject of study from limited independent variables to big data. AI could be defined as the development of algorithms with the capacity of creating learned models and exercising an intelligent behavior (40). Supervised machine learning is the AI methodology that uses mathematical techniques to give computer systems the ability to learn from labeled data and make a prediction. The techniques most used in this field are artificial neural networks (ANNs), such as a convolutional neural network (41) and multilayer perceptron (MLP) (42). Recently, the introduction of ANNs in assisted reproduction investigations has increased sevenfold (43) with promising results (44, 45).

The main aim of the present study was to predict embryo implantation potential using novel noninvasive parameters observed by TL monitoring systems. To achieve this objective, we proposed new embryo morphodynamic parameters, which had not been evaluated so far by TL, and analyzed their association with the implantation probability. Finally, we developed a model using an ANN to predict the implantation success.

MATERIALS AND METHODS

Study Population

This research was a single-center retrospective study carried out at IVI Valencia (Spain). We included recipients from the oocyte donation program who underwent ICSI cycles without PGT from the past two consecutive years. The exclusion criteria for recipients were: uterine pathologies, endometriosis, polycystic ovary syndrome, and body mass index >30 kg/m^2. Out of the 8,832 treatments with these characteristics, 845 were included in the EmbryoScope Plus TL system (Vitrolife). Single fresh embryo transfers were performed in 637 of them, whose embryos were assessed in this project.

Ovarian Stimulation and Uterine Receptivity

Donors were stimulated by means of the conventional controlled ovarian stimulation protocol with GnRH agonist treatment. GnRH agonist (Decapeptyl 1; Ipsen Pharma) was administered by intramuscular injection until more than eight follicles had reached a mean diameter of ≥18 mm. Transvaginal oocyte retrieval was scheduled 36 hours later. The endometrial preparation of patients was undertaken with the use of the hormone replacement therapy described by Cerrillo et al. (46). After embryo transfer, oocyte recipients received a daily dose of 400 mg vaginal micronized progesterone (Progeffik; Laboratorios Effik) every 12 hours as luteal-phase support.

Oocyte Retrieval and ICSI

Transvaginal oocyte retrieval was performed through follicular aspiration, and oocytes were washed in gamete medium

FIGURE 1

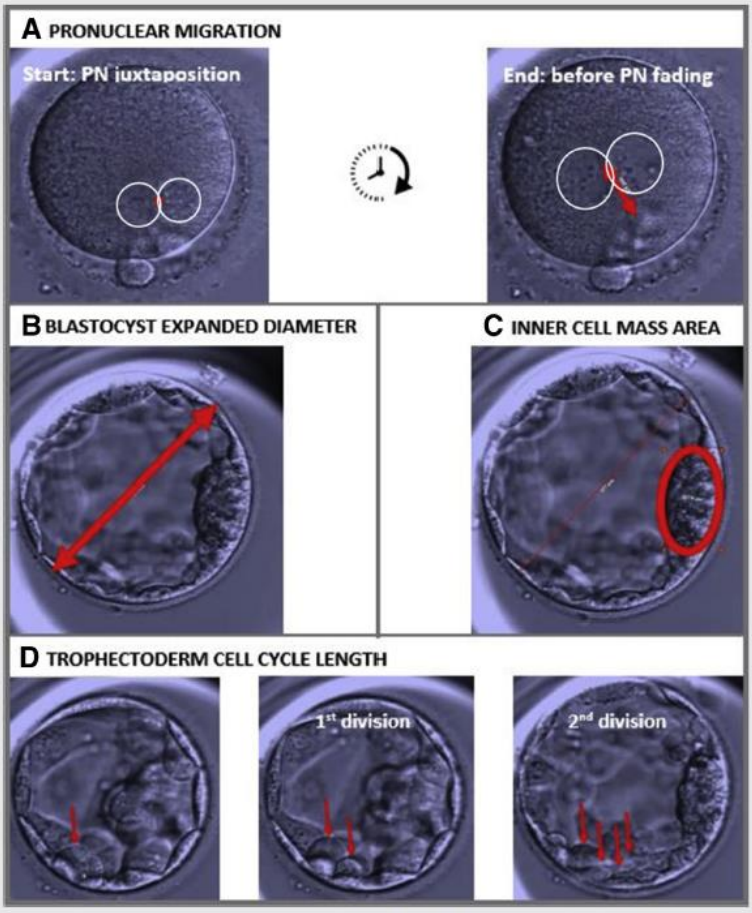

Measurement methodology carried out with the use of the drawing tools provided by the EmbryoViewer (Vitrolife). (**A**) Measurement of pronuclear (PN) migration; the image on the right represents the initial migration point and the image on the left represents the distance traveled by the pronuclei at the migration end point. (**B**) Measurement of blastocyst expanded diameter. (**C**) Measurement of inner cell mass area. (**D**) Measurement of trophectoderm cell cycle length; the image on the left represents the selected trophectoderm cell, the center image represents the two daughter cells from the selected cell, and the image on the right represents the four daughter cells from the two cells of the previous image.

Bori. Novel markers of embryo implantation. Fertil Steril 2020.

(Cook Medical). Then, oocytes were cultured in fertilization medium (Origio; Cooper Surgical) at 5% CO_2, 5% O_2, and 37°C. Denudation was carried out just before ICSI, 4 hours after oocyte retrieval, with the use of mechanical and chemical procedures (pipetting in 40 IU/mL hyaluronidase). ICSI was performed at ×400 magnification with the use of an Olympus IX7 microscope. Finally, oocytes were placed in preequilibrated EmbryoSlides (Vitrolife) with 16 microwells divided into two groups, with 90 μL single-step medium (Gems; Genea Biomedx) per group and 1.6 mL mineral oil per dish.

Embryo Incubation, Scoring, and Selection

Embryos were cultured in the EmbryoScope Plus TL system up to the blastocyst stage. Images were taken automatically every 10–20 minutes and in up to 11 focal planes. Embryo development was assessed on an external computer with software for the analysis (EmbryoViewer workstation; Vitrolife). Fertilization was evaluated at 16–19 hours after ICSI and confirmed by the presence of two pronuclei and two polar bodies. The number of cells, fragmentation level, symmetry among blastomeres, and compaction degree were annotated

on days 2 and 3 of development. Later, blastocysts were assessed and selected by applying a hierarchic classification procedure based on a combination of standard Asociación para el Estudio de la Biología de la Reproducción (ASEBIR) morphologic grading (Supplemental Tables 1–3, available online at www.fertstert.org) and KIDScore D5 algorithm (EmbryoViewer software; Vitrolife). Embryos were graded from A (high morphologic quality) to D (low morphologic quality) by senior embryologists and scored from 1 (low likelihood of implantation) to 9.9 (high likelihood of implantation) by KIDScore D5. The embryo with the highest score among those with good-quality morphology was selected to transfer in each treatment. Implantation of transferred embryos was confirmed by ultrasound scanning for gestational sacs with fetal heart beat after 8 weeks of pregnancy.

Experimental Design

The project was divided into two phases.

Phase 1 consisted of analysis of novel morphokinetic parameters: distance and speed of pronuclear migration (PNm), blastocyst expanded diameter (BEd), inner cell mass area (ICMa), and cell cycle length in the trophectoderm (ccTroph). Not all of the parameters could be analyzed on all of the transferred embryos, owing to image failures such as darkness, presence of bubbles, or out-of-focus images. The measurements were carried out by a designated embryologist, who was responsible for the annotation of morphokinetic variables (to avoid interoperator variations), using the drawing tools provided by EmbryoViewer. The distance of PNm was assessed 505 embryos by drawing a line from the point of PN juxtaposition up to the position where PNs faded in (Fig. 1A). The speed of PNm was calculated from the distance and the duration of this movement. The BEd was measured in 451 embryos in their maximum expansion and always before the embryo started hatching (Fig. 1B). The ICMa was evaluated with a circle surrounding its perimeter when the ICM was compacted, in 477 embryos (Fig. 1C). To normalize data of BEd and ICMa in early and delayed embryos, we calculated a ratio with the time when the annotations were performed: BEd/tBEd and ICMa/tICMa. The ccTroph length was measured in 360 embryos. We selected one cell and made two marks, the first one when this cell divided into two daughter cells and the second one when one of the daughter cells divided again (Fig. 1D). Subtracting these two division times, we obtained ccTroph.

Phase 2 consisted of development of the predictive model based on ANNs. Novel morphodynamic parameters (distance and speed of PNm, BEd, ICMa, and ccTroph) and conventional morphokinetic parameters (the time of the second polar body emission, tPB2; the time of appearance of the two pronuclei, tPNa; the time of their fade-out, tPNf; the division time to two cells, t2; the division time to three cells, t3; the division time to four cells, t4; the division time to five cells, t5; the division time to six cells, t6; the division time to seven cells, t7; the division time to eight cells, t8; the time from ICSI to early compaction, tSC; the time of morula formation, tM; the time to early blastulation, tSB; the time to full blastocyst, tB; the time to expanded blastocyst, tEB; and the time to early hatching blastocyst, tHiB) were considered to develop the model.

The ANN that we designed was an MLP and involved the selection of several hyperparameters. The number of hidden layers and the number of hidden neurons were chosen empirically but starting from rule-of-thumb methods. First, one or two hidden layers should be enough to solve any nonlinear complex problem (47). In the present work, the selection of two hidden layers improved model performance. Second, the number of hidden layers neurons should be two-thirds the size of the input layer (48, 49). The best model was designed with 15 neurons in each hidden layer (Supplemental Fig. 1, available online at www.fertstert.org). Too many neurons can result in overfitting problems and not lead to correct generalization.

Initially, the data was preprocessed by cleaning the database (removing samples with more than five missing values) and then filling missing values with the use of different techniques and standardizing the variables by means of Z score. Conventional variables were time dependent. Therefore, we could approximate missing values by means of interpolation. Novel variables were filled by using their corresponding means. In this way, 451 embryos were considered to feed the ANNs. Afterward, the parameters were randomized and split into two groups: 85% for the learning process (training and validation) and 15% for the blind test. In the learning process, the ANN was fed with the input data, the prediction was calculated, and the error was obtained by comparing the output value with the target value. Then, the backward propagation of the error allowed for the model parameter updates. A fivefold cross-validation approach was performed to guarantee robustness in the model (50). In this way, the learning data was divided into five sets and the network trained and validated with different sets of data in each iteration. Finally, the model was tested with the 15% of embryos, which were unknown for the model. It took the embryo parameters as input data and generated a confidence score in the range from 0 to 1. According to the probability of belonging to each class, the sample was assigned to the majority class.

The ANN was trained and tested by using distinct groups of variables, resulting in four models with the same architecture and different input data: conventional morphokinetic parameters for ANN1, novel morphodynamical parameters for ANN2, conventional and novel parameters for ANN3, and those parameters which had significant differences between implanted and nonimplanted embryos for ANN4.

Statistical Analysis

The discriminatory capacity of each variable and the correlation among them was analyzed. Statistical tests were applied to probe significant differences in the values of each variable between implanted and nonimplanted embryos. A t test was used for parameters with normal distribution and Wilcoxon rank sum test for those with nonnormal distribution. The subsequent results were expressed in terms of the 95% confidence interval and significance. Also, a study of the correlation for each pairwise variable combination was performed. The Pearson correlation coefficients and their respective P values were

obtained to test the null hypothesis and if they were independent.

Finally, receiver operator characteristic curves were used to analyze the predictive power of the ANN. The resulting graph represents the ratio of true test positives to total positive (sensitivity) per the proportion of false positives (1 − specificity). The higher the area under the curve (AUC), the more balanced the compensation between sensitivity and specificity. As a measure of the model performance, we also used the combined metric *F* score, which considered predictive positive values and sensitivity.

Ethical Approval

The procedure and protocol were approved by an institutional review board (IRB reference: 1709-VLC-094-MM) that regulates and approves database analysis and clinical IVF procedures for research at IVI Valencia. In addition, the project complies with the Spanish law governing assisted reproductive technologies (14/2006).

RESULTS

Phase 1: Analysis of Novel Morphokinetic Parameters

The means and standard deviations for novel morphodynamic parameters from implanted and nonimplanted embryos are presented in Table 1.

Pronuclei from the analyzed embryos traveled distances of 2–38 μm. We found nonsignificant differences between implanted and nonimplanted embryos regarding distance and speed.

BEd reached 114–225 μm. Implanted embryos had significantly higher diameters than nonimplanted ones. The implantation rate also improved as the ratio BEd/tBEd was higher: 46.2% for $\leq$1.37, 45.3% for 1.38–1.52, 66.7% for 1.53–1.64, and 70.7% for >1.64.

ICMa was 1,051–4,847 μm^2. Nonsignificant differences were found related to implantation rate. The tendency was that embryos with larger ICM areas had better implantation rates. Similar results were found for the ratio ICMa/tICMa: 52.1% for $\leq$19.07, 61.00% for 19.08–23.87, 63.8% for 23.88–28.90, and 57.4% for >28.90.

ccTroph was shorter than blastomeric cell cycle. In addition, we found significant differences between implanted and nonimplanted embryos.

Phase 2: Development of the Predictive Model Based on ANN

The means and standard deviations for conventional morphokinetic parameters from implanted and nonimplanted embryos are presented in Table 1.

TABLE 1

Mean and standard deviation for each embryo parameter analyzed.

		Implanted embryos		Nonimplanted embryos		
Variable	**Unit (SI)**	**Mean**	**SD**	**Mean**	**SD**	***P* value**
tPB2	h	3.763	1.425	3.858	1.585	.907
tPNa	h	8.559	2.187	8.735	2.283	.926
tPNf	h	23.192	2.559	23.508	2.745	.194
t2	h	25.654	2.956	25.951	2.973	.383
t3	h	36.219	3.361	36.500	3.817	.356
t4	h	37.403	3.663	38.154	3.975	.031[a]
t5	h	48.801	5.109	49.104	5.812	.526
t6	h	50.386	5.006	51.519	5.779	.023[a]
t7	h	52.777	5.464	54.468	7.031	.009[a]
t8	h	56.607	7.817	59.840	10.137	.003[a]
t9	h	69.889	8.209	72.800	8.635	<.001[a]
tSC	h	80.891	8.757	83.139	9.163	.012[a]
tM	h	86.925	8.265	88.689	8.591	.017[a]
tSB	h	96.843	6.712	98.978	6.979	.001[a]
tB	h	102.436	6.740	104.326	7.216	.005[a]
tEB	h	107.940	6.452	110.274	6.592	.001[a]
tHiB	h	110.638	7.694	114.796	9.790	.418
PNm distance	μm	13.649	7.234	13.648	6.898	.936
PNm speed	μm/h	1.377	1.989	1.174	0.995	.079
BEd	μm	177.090	21.374	170.830	18.575	<.001[a]
ICMa	μm^2	2763.036	707.134	2716.188	830.591	.069
ccTroph	h	9.945	2.706	9.758	2.702	<.001[a]
tICMa	h	113.369	5.419	114.252	9.046	.184
tBEd	h	113.527	3.787	113.637	2.915	.461

Note: BEd = blastocyst expanded diameter; ccTroph = trophectoderm cell cycle; ICMa = inner cell mass area; PNm = pronuclear migration; t2, the division time to two cells; t3 = division time to three cells; t4 = the division time to four cells; t5, the division time to five cells; t6 = division time to six cells; t7 = division time to seven cells; t8 = division time to eight cells; tB = time from intracytoplasmic sperm injection (ICSI) to full blastocyst; tPB2 = the time of the second polar body emission; tEB = time from ICSI to expanded blastocyst; tHiB = time from ICSI to early hatching blastocyst; tM = time from ICSI to morula formation; tPNa = time of appearance of the two pronuclei; tPNf = time of their fade out; tSB = time from ICSI to early blastulation;. tSC = time from ICSI to early compaction.

[a] *P*< .05, statistically significant difference between implanted and nonimplanted embryos.

Boi. Novel markers of embryo implantation. Fertil Steril 2020.

FIGURE 2

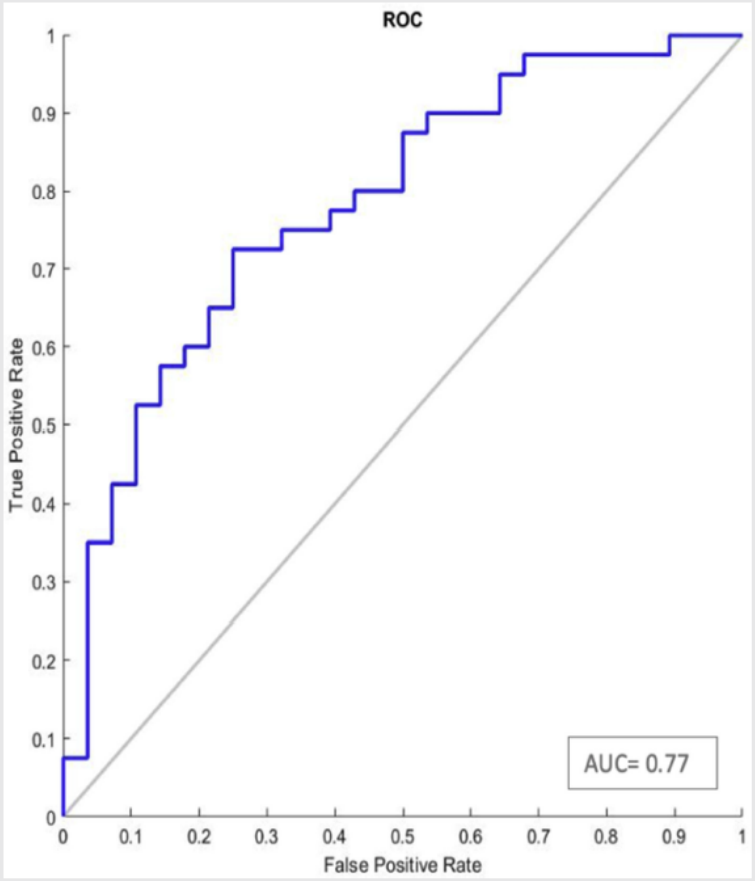

Receiver operating characteristic curve for prediction of implantation on the testing dataset by artificial neural network 3 (all conventional morphokinetic and novel parameters as input data). AUC = area under the receiver operating characteristic curve.

Bori. Novel markers of embryo implantation. Fertil Steril 2020.

Independent variables capable of discriminating between implanted and nonimplanted embryos were: t4, t6, t7, t8, t9, tSC, tM, tSB, tB, tEB, VEd, and ccTroph.

After the preprocessing of the dataset, 451 embryos were considered to develop the ANN architecture. The highest predictive power was achieved by ANN3, with an AUC of 0.77 (Fig. 2). The results in terms of sensitivity, specificity, accuracy, *F* score, and AUC for the four models in the testing data set are presented in Table 2.

DISCUSSION

Novel embryo morphodynamic parameters described in this research could play an important role in implantation potential prediction. Their combination with conventional morphokinetic parameters in ANNs has resulted in an effective tool to predict the success of an IVF treatment.

Since the introduction of time-lapse systems in IVF laboratories, several algorithms have been developed using morphokinetic parameters to improve embryo evaluation and selection (24, 29). The efficacy of six time-lapse imaging embryo selection algorithms to predict implantation (5, 25, 32, 35, 51, 52) showed AUCs ranging from 0.543 to 0.629 (53). The insertion of new embryo features and new methodologies of data analysis could improve the predictive power.

The appearance, movement, and fading of PNs has been previously studied (54–56). Whereas the female PN appears near the second polar body, in the cortex of the oocyte, the

TABLE 2

Results obtained in terms of sensitivity, specificity, accuracy, *F* score, and area under the curve for each artificial neural network model on the testing data set.

Artificial neural network	Input data	Sensitivity	Specificity	Accuracy	*F* score	AUC
ANN1	tPB2, tPNa, tPNf, t2, t3, t4, t5, t6, t7, t8, tSC, tM, tSB, tB, tEB, tHiB	0.88	0.46	0.71	0.78	0.64
ANN2	Distance of PNm, speed of PNm, BEd, ICMa, ccTroph	0.86	0.58	0.75	0.80	0.73
ANN3	tPB2, tPNa, tPNf, t2, t3, t4, t5, t6, t7, t8, tSC, tM, tSB, tB, tEB, tHiB, distance of PNm, speed of PNm, BEd, ICMa, ccTroph length	0.82	0.67	0.76	0.80	0.77
ANN4	t4, t6, t7, t8, t9, tSC, tM, tSB, tB, tEB, BEd, ccTroph length	0.85	0.57	0.74	0.79	0.68

Note: ANN = artificial neural network; AUC = area under the curve; BEd = blastocyst expanded diameter; ccTroph = trophectoderm cell cycle; ICMa = inner cell mass area; PNm = pronuclear migration; t2 = division time to two cells; t3 = division time to three cells; t4 = division time to four cells; t5 = division time to five cells; t6 = the division time to six cells; t7 = the division time to seven cells; t8, the division time to eight cells; tB = the time from intracytoplasmic sperm injection (ICSI) to full blastocyst; tEB = the time from ICSI to expanded blastocyst; tHiB = the time from ICSI to early hatching blastocyst; tM = time from ICSI to morula formation; tPB2 = time of the second polar body emission; tPNa = time of appearance of the two pronuclei; tPNf = time of their fade out; tSB = the time from ICSI to early blastulation; tSC = the time from (ICSI) to early compaction.

Boni. Novel markers of embryo implantation. Fertil Steril 2020.

male PN can emerge in the center (53.6%), the cortex (15.2%), or an intermediate point (31.2%) (55). The central position of PN juxtaposition and the presence of multinucleated blastomeres at the two-cell stage have been associated with the likelihood of live birth when transferring embryos on day 2 or 3 (56). As a general rule, both PNs move together, merge, and fade (55). The distance and speed of PN migration before fading were added as input data in our AI model. We did not find an association between implantation rate and multinucleation at the two-cell stage. However, we found that the intermediate PN position at juxtaposition was associated with higher clinical pregnancy rates, but the inclusion of this parameter as input variable for ANN did not improve its performance (unpublished data).

According to the ASEBIR criteria and Gardner grading, ICM, blastocyst expansion, and trophectoderm are the best criteria for evaluating and selecting embryos on day 5 of development (Supplemental Tables 1–4, available online at www.fertstert.org). Therefore, we wanted to analyze these parameters in an objective and quantitative way by using measurements of BEd, ICMa, and ccTroph. Two decades ago, Richter et al. were the first group to demonstrate that embryos with larger ICMa had higher implantation rates (57). Although we did not find statistical difference regarding the impact of ICMs over the implantation potential as an independent variable (Table 1), the most predictive ANNs included this parameter (Table 2). The relationship between BEd and clinical outcome was first described with the use of an ocular micrometer in 2008 (58). Although the bBEd and the ICMa had already been assessed with the tools of the Embryo Viewer (59), this is the largest retrospective cohort study in a TL system including these blastocyst features. In agreement with our results, the transfer of fully expanded blastocysts yielded greater implantation rates in fresh (60, 61) and frozen-thawed (62) embryo transfers. Blastocyst expansion has been also associated with embryo ploidy, as euploid blastocysts usually expand earlier than aneuploid ones (63). To our knowledge, this is the first time that the ccTroph has been measured, although rapid expansion has been associated with integrative cellular mitosis in trophectoderm cells (63). To ensure that ccTroph was representative of each embryo, we performed the measurement on two different cells for 100 embryos without obtaining significant variations (unpublished data).

The development of AI algorithms has become a common practice in embryologic investigations (43). Most of them are focused on image analysis through computer vision. Although, computer vision is a promising tool to use all the data hidden in TL images, it is still improving in the field of human embryology. There is one tool, called STORK, proposed to predict blastocyst quality with high predictive value (AUC = 0.98), based on TL images (45). Nevertheless, in their classification, good- and bad-quality embryos had little difference in the probability to lead to a birth: 61.4% and 50.9%, respectively. Complete videos of the whole embryo development have also been tested in software called IVY, with a high capacity of predicting fetal heart beat (AUC = 0.93) (44). However, the predictive power was calculated with the use of all kind of embryos, even nonviable (7,063 discarded embryos out of 10,683). The main goal should be to distinguish among viable embryos with similar appearance, among those that have the possibility of being transferred.

Currently, there is no doubt that AI techniques such as ANNs are more powerful than conventional statistical methodologies for data analysis. Among the models of ANN performed in this research, the third one was the most successful: All of the characteristics together were more predictive than individually. In addition, we found that the new parameters analyzed were responsible for the increase in the predictive power for implantation: The AUC for conventional

morphokinetics was 0.64, and for their combination with the novel parameters it was 0.77. Also, the accuracy for implantation prediction was higher with the new parameters than with the conventional ones: 0.75 and 0.71, respectively. Digging deeper into the predictive results, the highest sensitivity was found with those parameters that were significantly different in implanted and nonimplanted embryos (Table 2). They had higher capacity for discriminating the implanted embryos, but not the nonimplanted ones, because the specificity was too low. Thus, the most balanced model was the ANN3, which had the highest specificity and an excellent sensitivity (0.67 and 0.82, respectively).

The predictive value of implantation would be likely higher with the addition of parameters related to the patients. We recognize that implantation is not dependent only on the embryo quality; the characteristics of the endometrium and reproductive history also play important roles in IVF treatments. Regardless of the patient demographics, our further aim is to apply this ANN tool to improve the embryo selection in the laboratory before transfer.

We used morphodynamic annotations, which are more consistent, robust, and objective than morphologic ones (64). However, the interobserver variability of TL annotations limit the generalizability of our findings, especially with the newly described parameters. In addition, although we used a high-quality TL system supplied with different focal planes, the embryonic three-dimensional morphology made the evaluation of some events difficult, mainly those related to the PNs. In the near future, these annotations could be performed automatically with the use of computer vision to reduce subjectivity. This study is also limited by its retrospective nature, which is necessary before using a new embryo selection model in the IVF laboratory.

CONCLUSION

From this study, we can underscore the identification of nonconventional embryo parameters involved in the implantation potential. The use of AI to analyze big data provided by TL systems showed that the most predictive model was made up of all of the variables described and not just those that were individually discriminatory. The further step will be to compare our model prospectively against standard selection methodologies. We expect that the imminent introduction of new technologies and the resulting use of these morphodynamic parameters may increase objectivity in embryo evaluation.

Acknowledgments: The authors acknowledge the embryologists and technicians of the IVF laboratory from IVI-RMA Global Valencia for their clinical support.

REFERENCES

1. de Geyter C, Calhaz-Jorge C, Kupka MS, Wyns C, Mocanu E, Motrenko T, et al. ART in Europe, 2014: results generated from European registries by ESHRE. Hum Reprod 2018;33:1586–601.
2. Edwards RG, Fishel SB, Cohen J, Fehilly CB, Purdy JM, Slater JM, et al. Factors influencing the success of in vitro fertilization for alleviating human infertility. J In Vitro Fert Embryo Transf 1984;1:3–23.
3. Ferraretti AP, Goossens V, de Mouzon J, Bhattacharya S, Castilla JA, Korsak V, et al. Assisted reproductive technology in Europe, 2008: results generated from European registers by ESHRE. Hum Reprod 2012;27:2571–84.
4. Zhang JQ, Li XL, Peng Y, Guo X, Heng BC, Tong GQ. Reduction in exposure of human embryos outside the incubator enhances embryo quality and blastulation rate. Reprod Biomed Online 2010;20:510–5.
5. Cruz M, Garrido N, Herrero J, Pérez-Cano I, Muñoz M, Meseguer M. Timing of cell division in human cleavage-stage embryos is linked with blastocyst formation and quality. Reprod Biomed Online 2012;25:371–81.
6. Kirkegaard K, Agerholm IE, Ingerslev HJ. Time-lapse monitoring as a tool for clinical embryo assessment. Hum Reprod 2012;27:1277–85.
7. Montag M, Liebenthron J, Köster M. Which morphological scoring system is relevant in human embryo development? Placenta 2011;32:252–6.
8. Aparicio B, Cruz M, Meseguer M. Is morphokinetic analysis the answer? Reprod Biomed Online 2013;27:654–63.
9. del Gallego R, Remohí J, Meseguer M, Affiliations A, Valencia IG. Time-lapse imaging: the state of the art. Biol Repod 2019;101:1146–54.
10. Zaninovic N, Irani M, Meseguer M. Assessment of embryo morphology and developmental dynamics by time-lapse microscopy: is there a relation to implantation and ploidy? Fertil Steril 2017;108:722–9.
11. Wirka KA, Chen AA, Conaghan J, Ivani K. Atypical embryo phenotypes identi fi ed by time-lapse microscopy: high prevalence and association with embryo development. Fertil Steril 2014;101:1637–48.e5.
12. Zhan Q, Ye Z, Clarke R, Rosenwaks Z, Zaninovic N. Direct unequal cleavages: embryo developmental competence, genetic constitution and clinical outcome. PLoS One 2016;11:1–19.
13. Goodman LR, Goldberg J, Falcone T, Austin C, Desai N. Does the addition of time-lapse morphokinetics in the selection of embryos for transfer improve pregnancy rates? A randomized controlled trial. Fertil Steril 2016;105:275–85.
14. Desai N, Ploskonka S, Goodman L, Attaran M, Goldberg JM, Austin C, et al. Delayed blastulation, multinucleation, and expansion grade are independently associated with live-birth rates in frozen blastocyst transfer cycles. Fertil Steril 2016;106:1370–8.
15. Aguilar J, Rubio I, Muñoz E, Pellicer A, Meseguer M. Study of nucleation status in the second cell cycle of human embryo and its impact on implantation rate. Fertil Steril 2016;106:291–9.
16. Rubio I, Kuhlmann R, Agerholm I, Kirk J, Herrero J. Limited implantation success of direct-cleaved human zygotes: a time-lapse study. Fertil Steril 2012;98:11–5.
17. Desai N, Ploskonka S, Goodman LR, Austin C, Goldberg J, Falcone T. Analysis of embryo morphokinetics, multinucleation and cleavage anomalies using continuous time-lapse monitoring in blastocyst transfer cycles. Reprod Biol Endocrinol 2014;12:54.
18. Ebner T, Höggerl A, Oppelt P, Radler E, Enzelsberger SH, Mayer RB, et al. Time-lapse imaging provides further evidence that planar arrangement of blastomeres is highly abnormal. Arch Gynecol Obstet 2017;296:1199–205.
19. Azzarello A, Hoest T, Hay-Schmidt A, Mikkelsen AL. Live birth potential of good morphology and vitrified blastocysts presenting abnormal cell divisions. Reprod Biol 2017;17:144–50.
20. Desch L, Bruno C, Luu M, Barberet J, Choux C, Lamotte M, et al. Embryo multinucleation at the two-cell stage is an independent predictor of intracytoplasmic sperm injection outcomes. Fertil Steril 2017;107:97–103.e4.
21. Kirkegaard K, Hindkjaer JJ, Grøndahl ML, Kesmodel US, Ingerslev HJ. A randomized clinical trial comparing embryo culture in a conventional incubator with a time-lapse incubator. J Assist Reprod Genet 2012;29:565–72.
22. Wong CC, Loewke KE, Bossert NL, Behr B, de Jonge CJ, Baer TM, et al. Non-invasive imaging of human embryos before embryonic genome activation predicts development to the blastocyst stage. Nat Biotechnol 2010;28:1115–21.
23. Conaghan J, Chen AA, Willman SP, Ivani K, Chenette PE, Boostanfar R, et al. Improving embryo selection using a computer-automated time-lapse image analysis test plus day 3 morphology: Results from a prospective multicenter trial. Fertil Steril 2013;100:412–9.
24. Milewski R, Kuć P, Kuczyńska A, Stankiewicz B, Łukaszuk K, Kuczyński W. A predictive model for blastocyst formation based on morphokinetic parameters in time-lapse monitoring of embryo development. J Assist Reprod Genet 2015;32:571–9.

25. Chamayou S, Patrizio P, Storaci G, Tomaselli V, Alecci C, Ragolia C, et al. The use of morphokinetic parameters to select all embryos with full capacity to implant. J Assist Reprod Genet 2013;30:703–10.
26. Milewski R, Czerniecki J, Kuczyńska A, Stankiewicz B, Kuczyński W. Morphokinetic parameters as a source of information concerning embryo developmental and implantation potential. Ginekol Pol 2016;87:677–84.
27. Motato Y, de los Santos MJ, Escriba MJ, Ruiz BA, Remohí J, Meseguer M. Morphokinetic analysis and embryonic prediction for blastocyst formation through an integrated time-lapse system. Fertil Steril 2016;105:376–84.
28. Petersen BM, Boel M, Montag M, Gardner DK. Development of a generally applicable morphokinetic algorithm capable of predicting the implantation potential of embryos transferred on day 3. Hum Reprod 2016;31:2231–44.
29. Meseguer M, Herrero J, Tejera A, Hilligsøe KM, Ramsing NB, Remoh J. The use of morphokinetics as a predictor of embryo implantation. Hum Reprod 2011;26:2658–71.
30. Liu Y, Chapple V, Feenan K, Roberts P, Matson P. Time-lapse deselection model for human day 3 in vitro fertilization embryos: the combination of qualitative and quantitative measures of embryo growth. Fertil Steril 2016;105:656–62.
31. Vermilyea MD, Tan L, Anthony JT, Conaghan J, Ivani K, Gvakharia M, et al. Computer-automated time-lapse analysis results correlate with embryo implantation and clinical pregnancy: a blinded, multi-centre study. Reprod Biomed Online 2014;29:729–36.
32. Basile N, Vime P, Florensa M, Aparicio Ruiz B, García Velasco JA, Remohí J, et al. The use of morphokinetics as a predictor of implantation: a multicentric study to define and validate an algorithmfor embryo selection. Hum Reprod 2015;30:276–83.
33. Aparicio-Ruiz B, Romany L, Meseguer M. Selection of preimplantation embryos using time-lapse microscopy in in vitro fertilization: state of the technology and future directions. Birth Defects Res 2018;110:648–53.
34. Barrie A, Homburg R, McDowell G, Brown J, Kingsland C, Troup S. Preliminary investigation of the prevalence and implantation potential of abnormal embryonic phenotypes assessed using time-lapse imaging. Reprod Biomed Online 2017;34:455–62.
35. Campbell A, Fishel S, Bowman N, Duffy S, Sedler M, Hickman CFL. Modelling a risk classification of aneuploidy in human embryos using non-invasive morphokinetics. Reprod Biomed Online 2013;26:477–85.
36. Desai N, Goldberg JM, Austin C, Falcone T. Are cleavage anomalies, multinucleation, or specific cell cycle kinetics observed with time-lapse imaging predictive of embryo developmental capacity or ploidy? Fertil Steril 2018;109:665–74.
37. Amir H, Barbash-Hazan S, Kalma Y, Frumkin T, Malcov M, Samara N, et al. Time-lapse imaging reveals delayed development of embryos carrying unbalanced chromosomal translocations. J Assist Reprod Genet 2019;36:315–24.
38. del Carmen Nogales M, Bronet F, Basile N, Martínez EM, Liñán A, et al. Type of chromosome abnormality affects embryo morphology dynamics. Fertil Steril 2017;107:229–35.
39. Dyer S, Chambers GM, de Mouzon J, Nygren KG, Mansour R, Ishihara O, et al. International Committee for Monitoring Assisted Reproductive Technologies world report: assisted reproductive technology 2008, 2009 and 2010. Hum Reprod 2016;31:1588–609.
40. Simopoulou M, Sfakianoudis K, Maziotis E, Antoniou N, Rapani A, Anifandis G, et al. Are computational applications the "crystal ball" in the IVF laboratory? The evolution from mathematics to artificial intelligence. J Assist Reprod Genet 2018;35:1545–57.
41. Matusevičius A, Dirvanauskas D, Maskeliūnas R, Raudonis V. Embryo cell detection using regions with convolutional neural networks. CEUR Workshop Proc 2017;1856:89–93.
42. Milewski R, Kuczyńskabc A, Stankiewiczb B, Kuczyński W. How much information about embryo implantation potential is included in morphokinetic data? A prediction model based on artificial neural networks and principal component analysis. Adv Med Sci 2017;62:202–6.
43. Curchoe CL, Bormann CL. Artificial intelligence and machine learning for human reproduction and embryology presented at ASRM and ESHRE 2018. J Assist Reprod Genet 2019;36:591–600.
44. Tran D, Cooke S, Illingworth PJ, Gardner DK. Deep learning as a predictive tool for fetal heart pregnancy following time-lapse incubation and blastocyst transfer. Hum Reprod 2019;34:1011–8.
45. Khosravi P, Kazemi E, Zhan Q, Malmsten JE, Toschi M, Zisimopoulos P, et al. Deep learning enables robust assessment and selection of human blastocysts after in vitro fertilization. NPJ Digit Med 2019;2:1–9.
46. Cerrillo M, Herrero L, Guillén A, Mayoral M, García-Velasco JA. Impact of endometrial preparation protocols for frozen embryo transfer on live birth rates. Rambam Maimonides Med J 2017;8:e0020.
47. Karsoliya S. Approximating number of hidden layer neurons in multiple hidden layer BPNN architecture. Int J Eng Trends Technol 2012;3:714–7.
48. Boger Z, Guterman H. Knowledge extraction from artificial neural network models. In 1997 IEEE International Conference on Systems, Man, and Cybernetics. Comput Cybern Simul 1997;4:3030–5.
49. Panchal G, Ganatra A, Kosta Y, Panchal D. Behaviour analysis of multilayer perceptrons with multiple hidden neurons and hidden layers. Int J Comput Theory Eng 2011;3:332–7.
50. Kuhn M, Johnson K. Applied Predictive Modeling. New York: Springer; 2013.
51. Azzarello A, Hoest T, Mikkelsen AL. The impact of pronuclei morphology and dynamicity on live birth outcome after time-lapse culture. Hum Reprod 2012;27:2649–57.
52. dal Canto M, Coticchio G, Mignini Renzini M, de Ponti E, Novara PV, Brambillasca F, et al. Cleavage kinetics analysis of human embryos predicts development to blastocyst and implantation. Reprod Biomed Online 2012;25:474–80.
53. Barrie A, Homburg R, McDowell G, Brown J, Kingsland C, Troup S. Examining the efficacy of six published time-lapse imaging embryo selection algorithms to predict implantation to demonstrate the need for the development of specific, in-house morphokinetic selection algorithms. Fertil Steril 2017;107:613–21.
54. Coticchio G, Renzini MM, Novara PV, Lain M, de Ponti E, Turchi D, et al. Focused time-lapse analysis reveals novel aspects of human fertilization and suggests new parameters of embryo viability. Hum Reprod 2018;33:23–31.
55. Aguilar J, Motato Y, Escribá MJ, Ojeda M, Muñoz E, Meseguer M. The human first cell cycle: impact on implantation. Reprod Biomed Online 2014;28:475–84.
56. Barberet J, Bruno C, Valot E, Jonval L, Chammas J, Choux C, et al. Can novel early non-invasive biomarkers of embryo quality be identified with time-lapse imaging to predict live birth? Hum Reprod Update 2019;34:1439–49.
57. Richter KS, Harris DC, Daneshmand ST, Shapiro BS. Quantitative grading of a human blastocyst: optimal inner cell mass size and shape. Fertil Steril 2001;76:1157–67.
58. Shapiro BS, Daneshmand ST, Garner FC, Sc M. Large blastocyst diameter , early blastulation , and low preovulatory serum progesterone are dominant predictors of clinical pregnancy in fresh autologous cycles. Fertil Steril 2008;90:302–9.
59. Almagor M, Harir Y, Fieldust S, Or Y, Shoham Z. Ratio between inner cell mass diameter and blastocyst diameter is correlated with successful pregnancy outcomes of single blastocyst transfers. Fertil Steril 2016;106:1386–91.
60. della Ragione T, Verheyen G, Papanikolaou EG, van Landuyt L, Devroey P, van Steirteghem A. Developmental stage on day-5 and fragmentation rate on day-3 can influence the implantation potential of top-quality blastocysts in IVF cycles with single embryo transfer. Reprod Biol Endocrinol 2007;8:1–8.
61. Shapiro BS, Harris DC, Richter KS. Ph D. Predictive value of 72-hour blastomere cell number on blastocyst development and success of subsequent transfer based on the degree of blastocyst development. Fertil Steril 2000;73:10–3.
62. Coello A, Meseguer M, Galán A, Alegre L, Remohí J, Cobo A. Analysis of the morphological dynamics of blastocysts after vitrification/warming: defining new predictive variables of implantation. Fertil Steril 2017;108:659–66.e4.
63. Huang TT, Huang DH, Ahn HJ, Arnett C, Huang CT. Early blastocyst expansion in euploid and aneuploid human embryos: evidence for a non-invasive and quantitative marker for embryo selection. Reprod Biomed Online 2019;39:27–39.
64. Sundvall L, Ingerslev HJ, Breth Knudsen U, Kirkegaard K. Inter- and intra-observer variability of time-lapse annotations. Hum Reprod 2013;28:3215–21.

Nuevos y convencionales parámetros embrionarios como datos de entrada para redes neuronales artificiales: un modelo de inteligencia artificial aplicado para la predicción del potencial de implantación.

Objetivo: Describir nuevas características de embriones capaces de predecir el potencial de implantación como datos de entrada para un modelo de red neuronal artificial (ANN).

Diseño: Estudio de cohorte retrospectivo.

Entorno: Centro de FIV privado afiliado a la universidad.

Paciente (s): Este estudio incluyó a 637 pacientes del programa de donación de ovocitos que se sometieron a transferencia de un solo blastocisto durante dos años consecutivos.

Intervención (es): Ninguna.

Principales medidas de resultado: La investigación se dividió en dos fases. La fase 1 consistió en la descripción y análisis de las siguientes características embrionarias en embriones implantados y no implantados: distancia y velocidad de migración pronuclear, diámetro del blastocisto expandido, área de masa celular interna y duración del ciclo celular del trofoectodermo. La fase 2 consistió en el desarrollo de un algoritmo ANN para la predicción de la implantación. Se obtuvieron resultados para cuatro modelos alimentados con diferentes datos de entrada. El poder predictivo se midió con el uso del área bajo la curva característica operativa del receptor (AUC).

Resultado (s): De los cinco nuevos parámetros descritos, el diámetro expandido del blastocisto y la duración del ciclo celular del trofoectodermo tenían valores estadísticamente diferentes en los embriones implantados y no implantados. Después de que los modelos ANN fueron entrenados y validados mediante validación cruzada cinco veces, estos fueron capaces de predecir la implantación en los datos de prueba con AUC de 0,64 para ANN1 (morfocinética convencional), 0,73 para ANN2 (morfodinámica novedosa), 0,77 para ANN3 (morfocinética convencional morfodinámica novedosa) y 0,68 para ANN4 (variables discriminatorias de prueba estadística).

Conclusión (es): Las nuevas características embrionarias propuestas afectan al potencial de implantación y su combinación con parámetros morfocinéticos convencionales es eficaz como datos de entrada para un modelo predictivo basado en inteligencia artificial.

Supplemental Figure 1

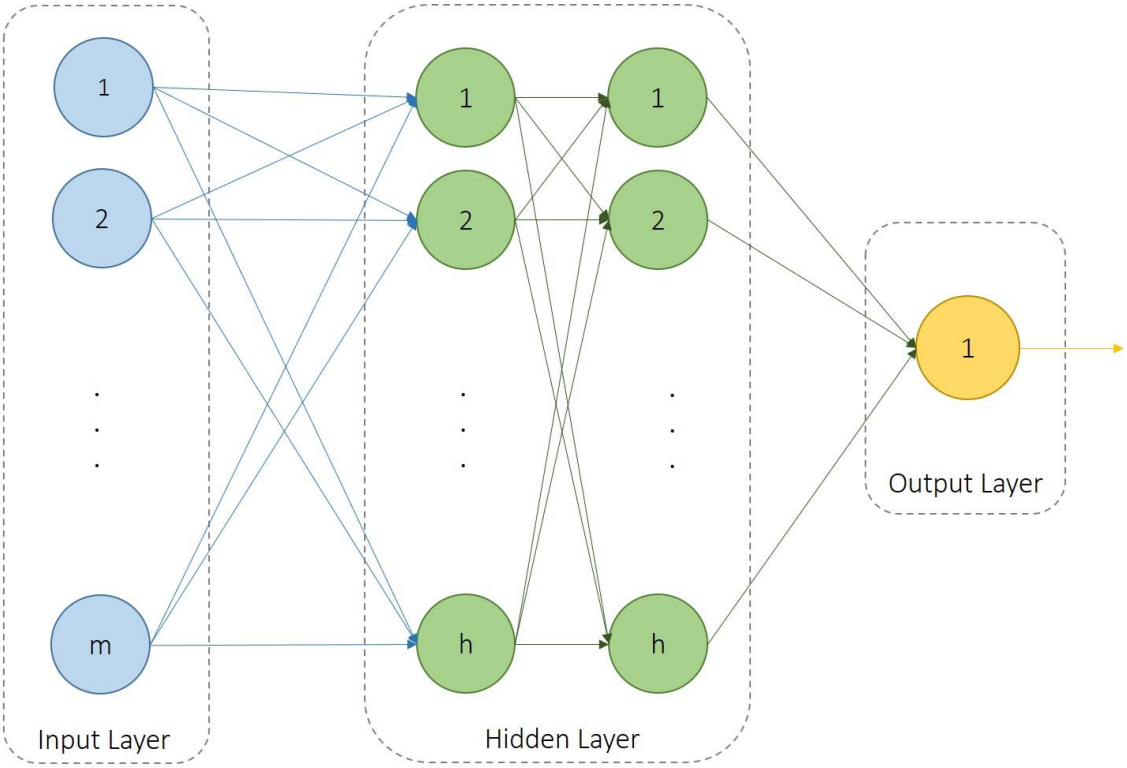

Scheme of the designed architecture of Artificial Neural Network, where m is the number of input variables and h is the number of neurons in the hidden layers.

Supplemental Tables

Supplemental table 1.

Category	Inner Cell Mass size (µm2)	Cohesion
A	3800-1900	Compact
B	3800-1900	Non compact
C	<1900	Indifferent
D	Degeneration signs	
Excluded	Degenerated	

Supplemental table 2.

Category	Trophectoderm description
A	Homogeneous, united and full of cells
B	homogeneous, less cells
C	Few cells
D	Degeneration signs
Excluded	Degenerated

Supplemental table 3.

Blastocyst stage	Grade	Characteristics
Early blastocyst	1	The blastocoele is less than half the volume of the embryo
Blastocyst	2	The blastocoele is greater than or equal to half of the volume of the embryo
Full blastocyst	3	The blastocoele completely fills the embryo
Expanded blastocyst	4	The blastocoele volume is larger than that of the early embryo and the zona pellucida is thinning
Hatching blastocyst	5	The trophectoderm has started to herniate through zona pellucida
Hatched blastocyst	6	The blastocyst has completely escaped from the zona pellucida
Inner Cell Mass	A	Tightly packed, many cells
	B	Loosely grouped, several cells
	C	Very few cells
Trophectoderm	A	Many cells forming a tightly knit epithelium
	B	Few cells
	C	Very few cells forming a loose epithelium

Supplemental table 4.

<table>
<tr><th colspan="4">D+5</th></tr>
<tr><th>Expansion grade</th><th>ICM</th><th>Trophectoderm</th><th>ASEBIR</th></tr>
<tr><td rowspan="13">Since “starting expansion”

Up to “hatched”</td><td rowspan="4">A</td><td>A</td><td>A</td></tr>
<tr><td>B</td><td>B</td></tr>
<tr><td>C</td><td>C</td></tr>
<tr><td>D</td><td>D</td></tr>
<tr><td rowspan="4">B</td><td>A</td><td>A</td></tr>
<tr><td>B</td><td>B</td></tr>
<tr><td>C</td><td>C</td></tr>
<tr><td>D</td><td>D</td></tr>
<tr><td rowspan="4">C</td><td>A</td><td>A</td></tr>
<tr><td>B</td><td>B</td></tr>
<tr><td>C</td><td>C</td></tr>
<tr><td>D</td><td>D</td></tr>
<tr><td>D</td><td>A, B, C or D</td><td>D</td></tr>
<tr><td colspan="3">Early blastocyst (Thick pellucid zone)</td><td>C</td></tr>
<tr><td colspan="2">Morula</td><td colspan="2">Excluded</td></tr>
</table>

ARTÍCULO II

Artículo II: An artificial intelligence model based on the proteomic profile of euploid embryos and blastocyst morphology: a preliminary study.

Bori L, Dominguez F, Fernandez EI, Del Gallego R, Alegre L, Hickman C, Quiñonero A, Nogueira MFG, Rocha JC, Meseguer M.

Reprod Biomed Online. 2021 Feb;42(2):340-350. doi: 10.1016/j.rbmo.2020.09.031

Epub 2020 Oct 8. PMID: 33279421.

Factor de impacto 2021: 4,567

5-años factor de impacto: 4,603

RBMO

ELSEVIER

ARTICLE

An artificial intelligence model based on the proteomic profile of euploid embryos and blastocyst morphology: a preliminary study

BIOGRAPHY

Lorena Bori is doctoral researcher at IVIRMA Valencia, Spain. She received her biology degree in 2016 and her Master's degree in the biotechnology of human assisted reproduction in 2018 from the University of Valencia. Her primary field of research is embryo evaluation and selection using non-invasive methodologies, especially artificial intelligence.

Lorena Bori[1], Francisco Dominguez[2,3,*], Eleonora Inacio Fernandez[4], Raquel Del Gallego[2], Lucia Alegre[1], Cristina Hickman[5], Alicia Quiñonero[2], Marcelo Fabio Gouveia Nogueira[4], Jose Celso Rocha[4], Marcos Meseguer[1,3]

KEY MESSAGE

An artificial intelligence model was designed using proteomic and morphological data from blastocysts. The algorithm, based on artificial neural networks, is capable of discriminating with high accuracy between euploid embryos that lead to a live birth and those which do not.

ABSTRACT

Research question: The study aimed to develop an artificial intelligence model based on artificial neural networks (ANNs) to predict the likelihood of achieving a live birth using the proteomic profile of spent culture media and blastocyst morphology.

Design: This retrospective cohort study included 212 patients who underwent single blastocyst transfer at IVI Valencia. A single image of each of 186 embryos was studied, and the protein profile was analysed in 81 samples of spent embryo culture medium from patients included in the preimplantation genetic testing programme. The information extracted from the analyses was used as input data for the ANN. The multilayer perceptron and the back-propagation learning method were used to train the ANN. Finally, predictive power was measured using the area under the curve (AUC) of the receiver operating characteristic curve.

Results: Three ANN architectures classified most of the embryos correctly as leading (LB+) or not leading (LB–) to a live birth: 100.0% for ANN1 (morphological variables and two proteins), 85.7% for ANN2 (morphological variables and seven proteins), and 83.3% for ANN3 (morphological variables and 25 proteins). The artificial intelligence model using information extracted from blastocyst image analysis and concentrations of interleukin-6 and matrix metalloproteinase-1 was able to predict live birth with an AUC of 1.0.

Conclusions: The model proposed in this preliminary report may provide a promising tool to select the embryo most likely to lead to a live birth in a euploid cohort. The accuracy of prediction demonstrated by this software may improve the efficacy of an assisted reproduction treatment by reducing the number of transfers per patient. Prospective studies are, however, needed.

[1] IVF laboratory, IVI Valencia, Valencia, Spain
[2] IVI Foundation, Valencia, Instituto Universitario IVI (IUIVI), Valencia, Spain
[3] Health Research Institute la Fe, Valencia, Spain
[4] Universidade Estadual Paulista (Unesp), Faculdade de Ciências e Letras, Câmpus de Assis SP, Brazil
[5] Institute of Reproduction and Developmental Biology, Hammersmith Campus, Imperial College, London, UK

*Corresponding author. E-mail address: Francisco.dominguez@ivirma.com (F. Dominguez). https://doi.org/10.1016/j.rbmo.2020.09.031 1472-6483/
Declaration: The authors report no financial or commercial conflicts of interest

KEY WORDS
Artificial intelligence
Artificial neural network
Blastocyst morphology
Live birth
Proteomics

INTRODUCTION

The two main factors responsible for the success of an IVF treatment are the endometrium and the embryo (*Edwards et al., 1984*). Non-invasive methods (morphological and morphokinetic) as well as invasive methods (genetic testing) are currently used in IVF laboratories in embryo selection. However, new approaches to select embryos are still being investigated due to the limited improvement in live birth rate over the last few years (*Dyer et al., 2016*; *De Geyter et al., 2018*).

New non-invasive methods based on "-omic" sciences, such as metabolomics and proteomics, have emerged to assess embryo viability and improve clinical outcomes (*Krisher et al., 2015*). There is evidence for the importance of soluble ligands and receptors in both the embryo and the female reproductive tract during the embryonic preimplantation stage (*Thouas et al., 2015*). The group of proteins secreted or metabolized by the embryo is known as the secretome (*Hathout, 2007*); by analysing the culture medium, this is a promising source of information about the protein and metabolic state of the embryo (*Hollywood et al., 2006*).

Thirty years ago, platelet-activating factor in spent embryo culture media was reported as the first evidence of the embryo secretome (*Punjabi et al., 1990*). Since then, several proteins have been identified during the preimplantation stage, for example IFN-α2 (interferon-α2; *Jones et al., 1992*), SP1 (pregnancy-specific P-I glycoprotein; *Saith et al., 1994*), HLA-G (human leukocyte antigen G ; *Noci et al., 2005*), Apo-A1 (apolipoprotein A1; *Mains et al., 2011*), HCG (human chorionic gonadotrophin; *Butler et al., 2013*) and GM-CSF (granulocyte-macrophage colony-stimulating factor; *Ziebe et al., 2013*). Methods for protein analysis have improved in terms of sensitivity, leading to the simultaneous study of multiple proteins (e.g. using mass spectrometry techniques or microarray technology). This has made it possible to observe associations among protein expression patterns, developmental stages and embryo morphology (*Katz-Jaffe and Gardner, 2007*; *Katz-JAFFE and McReynolds, 2013*).

Analysis of the embryo culture medium has revealed the secretion and consumption of several proteins by the embryo. The increase in the culture medium of TNF (tumour necrosis factor) R1, IL (interleukin) 10, IL-6, VEGFA (vascular endothelial growth factor A), EMMPRIN (extracellular matrix metalloproteinase inducer), PLGF (placental growth factor), EpCAM (epithelial cell adhesion molecule), caspase-3, HE-4 (Human epididymis protein 4) and IL-6 meant that the embryo had secreted those proteins (*Dominguez et al., 2008*, *2015*; *Lindgren et al., 2018*). Similarly, a decrease in CXCL (C-X-C motif chemokine ligand) 13, SCF (stem cell factor), TRAIL-R3 (receptor for the cytotoxic ligand TRAIL), MIP-1β (macrophage inflammatory protein-1β) and MSP-α (macrophage stimulating protein-α) in the culture medium indicated that the embryo had consumed or metabolized those proteins (*Dominguez et al., 2008*). Furthermore, different protein patterns were observed according to implantation potential and embryo quality. Embryos that implanted consumed more CXCL13 and GM-CSF than non-implanted ones (*Dominguez et al., 2010*; *Robertson, 2007*;). In addition, culture medium from blastocysts showed higher concentrations of EMMPRIN than samples from arrested embryos. Higher concentrations of caspase-3 were found in culture medium from good quality blastocysts (*Lindgren et al., 2018*).

Artificial intelligence, in terms of the machine capacity to learn and exercise intelligent behaviour (*Simopoulou et al., 2018*), is making headway in human embryology. Publications increased seven-fold in 1 year (*Curchoe and Bormann, 2019*), which shows the potential of using artificial intelligence to improve the efficiency of assisted reproductive treatments.

It has recently been shown that artificial intelligence is a non-invasive tool with a high potential for predicting a live birth due to its capacity for recognizing patterns (*Miyagi, 2019*; *Qiu et al., 2019*). Among artificial intelligence techniques, the most outstanding are the following: deep learning, which requires large databases (*Chen et al., 2019*; *Miyagi, 2019*) and hard computational efforts (*Najafabadi et al., 2015*); convolutional neural networks, which are a subset of deep learning widely used in image analysis (*Matusevičius et al., 2017*); the multilayer perceptron, whose artificial neural network (ANN) architecture contains intermediate layers between input and output data (*Abiodun et al., 2018*; *Milewski et al., 2017*; *Zador, 2019*); and Bayesian networks, which are probabilistic models (*Hernández-González et al., 2018*; *Uyar et al., 2015*). All these techniques use artificial neural networks as the basis of the model.

ANNs are computational techniques inspired by the functioning of the human brain whose main objective is to learn tasks that seek to solve complex problems (*Vanneschi and Castelli, 2018*). This technique simulates a biological neuron and imitates its ability to learn through trial and error. The characterization of an ANN is achieved via its self-learning through training. A commonly used algorithm for supervised learning is back-propagation (*Gupta and Sexton, 1999*).

Nowadays, the potential of ANNs is being increasingly explored mainly by associating other techniques, such as genetic algorithms, to optimize the results. The latter are evolutionary algorithms based on both Darwin's theory of evolution and Gregor Mendel's laws of genetics. This methodology generates a random population of individuals that is evaluated during the evolutionary process. In this process, the most qualified individuals are maintained in the next generations. After the creation of a new population, the process is repeated until a satisfactory solution is found (*Ghaheri, 2015*; *Rigla et al., 2018*; *Rosa and Luz, 2009*). In this case, the individuals are the ANNs (*Takahashi et al., 2016*).

The introduction of artificial intelligence to IVF laboratories would allow the analysis of raw embryo images without previous manual annotations. Even though the incorporation of continuous monitoring increases the objectivity of embryo assessment, manual annotations are subject to disparity among embryologists (*Martínez-Granados et al., 2017*; *Storr et al., 2017*; *Sundvall et al., 2013*). The introduction of systems with computer vision capable of extracting objective and standardized image information (*Danuser, 2011*) and performing automatic annotations could reduce the subjectivity of embryo selection (*Manna et al., 2013*). Macroscopic characteristics such as the number of cells, texture or movement

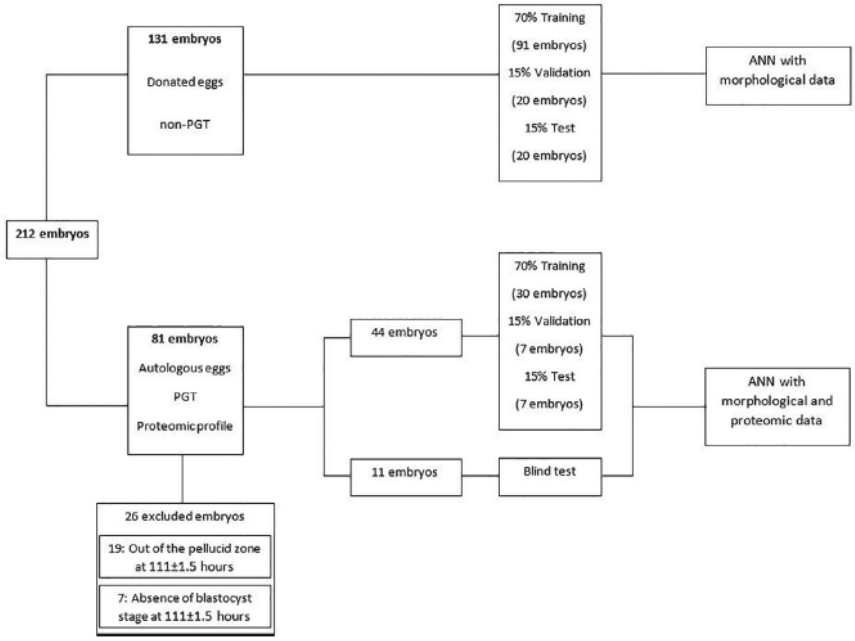

FIGURE 1 The study design shown as a flow diagram representing the distribution of embryos in the project. ANN, artificial neural network; PGT, preimplantation genetic testing.

patterns could be learned through training data.

Methods to fully automatize the evaluation of mammalian embryos have been already proven to work (*Rocha et al., 2017*), and the next step is to transfer this knowledge to human embryology (*Blank et al., 2019*). Recently, several approaches using artificial intelligence techniques for embryo classification and prediction of clinical outcomes have been published (see, for example, *Bormann et al., 2020*; *Chavez-Badiola et al., 2020*; *Dirvanauskas et al., 2019*; *Khosravi et al., 2019*; *Rad et al., 2018*; *Rocha et al., 2018*; *Tran et al., 2019*; *Zaninovic et al., 2018*).

The objective of the current study was to develop a combinative predictive model based on artificial intelligence. First, morphological data from several embryos were used to create an ANN capable of predicting live birth. Donated oocytes were used, assuming that, as they were obtained from young women, they would result in mostly euploid embryos (*Dang et al., 2019*; *Rubio et al., 2003*;). Second, information from blastocyst images and proteomic information was used to predict the potential of a euploid embryo to lead to a live birth. To the authors' knowledge, this is the first approach to predict the likelihood of achieving a live birth by relying on machine learning and proteomic data.

MATERIALS AND METHODS

Study design and participants

In this single-centre project, two populations were enrolled (FIGURE 1): 131 recipients of the oocyte donation programme of IVI Valencia (no preimplantation genetic testing [PGT]) and 81 women using autologous eggs in the PGT for aneuploidies (PGT-A) programme. The resulting embryos were individually cultured up to blastocyst stage in a continuous monitoring system (EmbryoScope; Vitrolife, Denmark).

A single time-lapse image from each embryo acquired at 111.5 ± 1.5 h of development was analysed using computational vision to extract information (as described below). Additionally, 20 µl of culture medium (Gems; Genea Biomedx, Australia) was collected for the proteomic analysis from the biopsied embryos and eight control samples (medium in which no embryos had been cultured). Samples were obtained on day 5 of development and were stored at –80°C until the proteomic analysis. Only the medium from euploid embryos was analysed after single-embryo transfer.

A total of 212 embryos was selected for application of the artificial intelligence technique: the first group consisted of 131 embryos obtained from the oocyte donation programme, and the second group included 81 embryos from autologous treatments with proteomic information. After the image analysis, 26 embryos were excluded from the second group: 19 blastocysts were outside the zona pellucida at 111 ± 1.5 h of development, which made image analysis difficult and not comparable with the 186 images finally remaining, and seven embryos did not reach the blastocyst stage at the proposed time and were discarded due to their early developmental stage. Therefore, the second group included 55 embryos for analysis, of which 11 were used for the

blind test. Thus, the database totalled 186 embryos to undergo application of the artificial intelligence technique.

Ovarian stimulation in treatments with donated oocytes

Donors received stimulatory treatment using the conventional ovarian stimulation protocol with gonadotrophin-releasing hormone (GnRH) agonist treatment. GnRH agonist (Decapeptyl; Ipsen Pharma, Spain) was administered by intramuscular injection until more than eight follicles had reached a mean diameter of 18 mm or more. Transvaginal oocyte retrieval was scheduled for 36 h later. Endometrial preparation was undertaken using hormone replacement therapy as described by Cerrillo and colleagues (*Cerrillo et al., 2017*). After embryo transfer, oocyte recipients received a daily dose of 400 mg of vaginal micronized progesterone (Progeffik; Lab. Effik, Spain) every 12 h as luteal phase support.

Ovarian stimulation in treatments with autologous oocytes

GnRH-antagonist treatments were applied, the GnRH-agonist being administered when at least three leading follicles had reached a mean diameter of 18 mm. Transvaginal oocyte retrieval was scheduled for 36 h later through follicular aspiration, and oocytes were washed in gamete medium (Cook Medical, Australia).

Oocyte retrieval and embryo incubation

Oocytes were cultured in fertilization medium (Origio; CooperSurgical, Denmark) in 5% CO_2 and 5% O_2 at 37°C. Denudation was carried out just before intracytoplasmic sperm injection (ICSI), 4 h after oocyte retrieval, using mechanical and chemical procedures (pipetting in 40 IU/ml hyaluronidase). ICSI was performed in a HEPES-buffered gamete medium at × 400 magnification using an Olympus IX7 microscope (Olympus Corporation, Japan). Finally, oocytes were placed in EmbryoSlides (Vitrolife, Denmark) pre-equilibrated to blastocyst stage with 28 µl of single-step medium (Gems; Genea Biomedx, Australia) and 1.6 ml of mineral oil.

Embryos were cultured individually up to the fifth or sixth day of development in the time-lapse system EmbryoScope (Vitrolife, Denmark). Successful fertilization was assessed at 16–19 h after ICSI.

Embryo morphology was evaluated on day 3 (62–72 h after ICSI) based on digital images, taking into consideration the number, the symmetry of the blastomeres, the percentage of fragmentation and the degree of compaction. Blastocysts were scored on day 5 (120 h after ICSI) based on the Association for the Study of Biology of Reproduction (ASEBIR) criteria (Supplementary Tables 1, 2 and 3) and the KIDScore Day 5 (with EmbryoViewer software; Vitrolife, Denmark). Embryologists annotated the morphokinetic parameters: the timings of cell divisions to the 2-cell (t2), 3-cell (t3), 4-cell (t4), 5-cell (t5), 8-cell (t8), 9-cell (t9), compaction (CP), morula (tM), start of blastulation (tSB), blastocyst (tB) and expanding blastocyst (tEB) were calculated, with the start of ICSI being used as t0. The durations of the cell cycle intervals t3–t2 (cc2), t4–t3 (s2), t5–t2, t5–t3 (cc3) and t8–t5 (s3) were also calculated. If there was more than one embryo of the same morphological quality, the score provided by the KIDScore Day 5 decided which would be transferred.

PGT-A

Embryos were taken out of the incubator on day 3 of development to undergo a small laser incision traversing the zona pellucida (assisted hatching) using a Lykos laser (Hamilton Thorne, USA). This procedure made the trophectoderm biopsy on day 5 of culture easier, when a biopsy pipette was used to remove approximately 5 cells. Chromosome analysis was performed using next-generation sequence technology (Thermo Fisher Scientific, USA).

Embryo transfer and clinical outcome

A single-embryo transfer of one blastocyst was performed for all patients; for those in the PGT-A programme, the blastocyst had previously been vitrified and warmed using the Cryotop method (Kitazato Biopharma, Japan). Embryo selection for transfer was based on chromosomal status, morphology and morphokinetics. The β-HCG concentration was determined 10 days after embryo transfer, and clinical pregnancy was confirmed by the presence of gestational sac at the fifth week of pregnancy. Finally, patients inform about live birth after the delivery.

Protein analysis in spent culture media

The relative concentrations of 92 proteins from 81 samples of spent embryo culture medium and eight control samples (medium in which no embryos had been cultured) were analysed using Proseek Multiplex Assays (Olink Bioscience, Sweden) based on proximity extension assay (PEA) technology.

Proteins were measured using the Olink Inflammation panel (Olink Proteomics, Sweden) according to the manufacturer's instructions. The PEA technology used for the Olink protocol has been well described (*Assarsson et al., 2014*); it enables 92 proteins to be analysed simultaneously, using 1 µl of each sample. In brief, pairs of oligonucleotide-labelled antibody probes bind to their target protein. If the two probes are closely located, the oligonucleotides will hybridize in a pairwise manner. The addition of a DNA polymerase leads to a proximity-dependent DNA polymerization event, generating a unique polymerase chain reaction (PCR) target sequence. The resulting DNA sequence is subsequently detected and quantified using a microfluidic real-time PCR instrument (Biomark HD; Fluidigm, USA). Data are then quality controlled and normalized using an internal extension control and an inter-plate control, to adjust for intra- and inter-run variation. The final assay readout is presented as Normalized Protein eXpression (NPX) values, which are arbitrary units on a $\log_2$ scale, where a high value corresponds to a higher protein expression. Hence, a 1 NPX difference means a doubling of protein concentration. All assay validation data (detection limits, intra- and inter-assay precision data, reproducibility and specificity) are available on manufacturer's website (www.olink.com).

Artificial intelligence model: image analysis, collinearity analysis, ANN and genetic algorithms

Standardization of the 186 blastocyst images was necessary before applying the artificial intelligence technique. The methodology used was as described by Rocha and colleagues (*Rocha et al., 2017*). The images were initially imported automatically into Matlab software (MathWorks, USA) and a standardization algorithm was run to normalize them in terms of contrast and resolution (*Russ, 2016*). Afterwards, blastocyst images were segmented into regions of interest. Using the Hough transform, the algorithm analysed three regions separately (*Hassanein et al., 2015*; *Mukhopadhyay and Chaudhuri, 2014*): the area of the

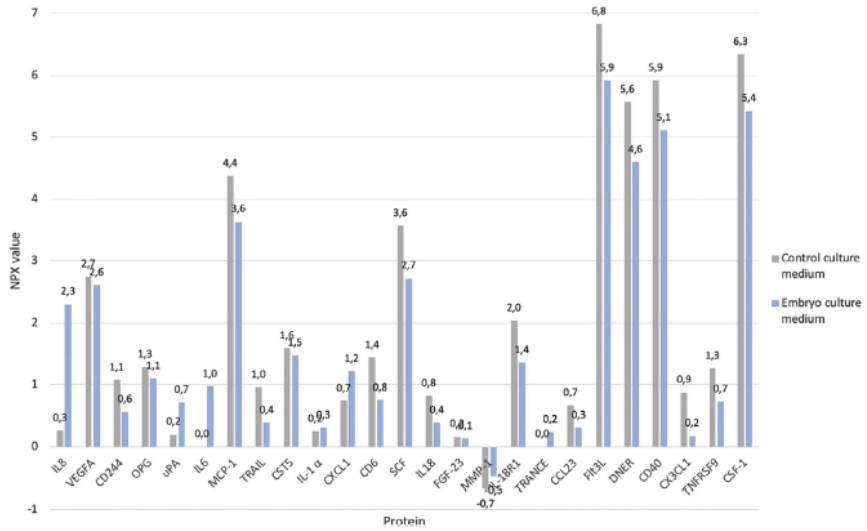

FIGURE 2 The grouped column chart represents the average of the Normalized Protein eXpression (NPX) value obtained using the proximity extension assay technique for the 25 useful proteins analysed in culture medium from 81 embryos generated from autologous eggs. Grey columns represent control media (n = 8), and blue columns represent conditioned media collected on day 5 of embryo culture.

expanded blastocyst, the inner cell mass and the trophectoderm. Finally, the algorithm obtained 33 mathematical variables by using the measurement of the area, the number of pixels present in each segmented portion of the blastocyst image, the binary patterns (*Huang et al., 2011*) and the texture analysis (*Bino et al., 2012*). These variables were chosen seeking to represent all the relevant characteristics of the blastocyst for embryo quality assessment and live birth prediction through artificial intelligence.

After the embryo images had been standardized and isolated, and the mathematical variables had been extracted, a collinearity analysis was used to check if the variables were correlated with one another based on the variance inflation factor (VIF). The VIF represents the degree of independence or non-redundancy between a variable and another independent variable. According to previous studies, collinear variables were considered to be those with VIF values higher than 10 (*O'Brien, 2007*; *Walczak and Cerpa, 1999*); removal of collinear variables reduced the number of variables representing the human embryo to 20 (Supplementary Table 4).

Likewise, a collinearity analysis was performed to discriminate the independent and non-redundant proteins. As it is shown in detail in 'Collinearity analysis for proteins', below, seven proteins were suitable for using as input to the ANN, in conjunction with the 20 morphological variables. The artificial intelligence technique associated ANNs (multilayer perceptron) with the genetic algorithm by using the back-propagation learning algorithm (*Gupta and Sexton, 1999*) for the training phase. The genetic algorithm used the ANNs as individuals in a population, which, over generations, end up selecting the best ANN (i.e. the one with the highest accuracy for live birth prediction).

The dataset of 131 embryos was randomly divided into 70% for training, 15% for validation and 15% for testing the ANN. Of the dataset of 55 embryos, 20% were used for the blind test, and the remaining 44 embryos were randomly divided into 68% for training, 16% for validation and 16% for testing the ANN (*Kalpana et al., 2015*).

Statistical analysis

Statistical tests were applied to probe significant differences in the values of each protein in conditioned compared with control media and in conditioned media from implanted compared with non-implanted embryos. A t-test was used for parameters with a normal distribution, and a Wilcoxon rank sum test for those with a non-normal distribution. Values of P that were <0.05 were considered statistically significant.

The image analysis and the final model were tested using two techniques. First, receiver operating characteristic (ROC) curves were used to analyse the artificial intelligence results for pattern recognition. The resulting graph represents the ratio of true test positives to total positives (the sensitivity) per the false positive fraction, i.e. the ratio of false test positives to total negatives (1 – specificity). An area under the ROC curve (AUC) of greater than 0.5 might indicate a predictive power to identify embryos that lead (LB+) or do not lead (LB–) to a live birth. The greater the AUC, the more favourable the compensation between sensitivity and specificity. It tells how much the model is capable of distinguishing among LB+ and LB– embryos. Second, confusion matrix methodology was used to analyse the intersection between the data provided by the model (the artificial intelligence system) and the real results. The authors considered as true positive the number of embryos that achieved a live birth, the model classifying them as positive,

TABLE 1 NPX VALUES OBTAINED USING THE PEA TECHNIQUE FOR THE SEVEN INDEPENDENT PROTEINS RESULTING FROM THE COLLINEARITY ANALYSIS

Protein	NPX value (mean ± SD)		
	LB+ (*n* = 38)	LB– (*n* = 43)	*P*-value
MMP-1	–0.39 ± 0.83	–0.49 ± 0.53	0.579
IL-6	0.94 ± 0.53	0.75 ± 0.67	0.261
VEGFA	2.40 ± 0.37	2.59 ± 0.53	0.137
uPA	0.67 ± 0.42	0.61 ± 0.52	0.634
TRANCE	0.19 ± 0.51	–0.05 ± 0.15	0.023
Flt3L	5.87 ± 0.20	6.00 ± 0.27	0.051
DNER	4.57 ± 0.29	4.71 ± 0.27	0.077

LB+, positive for live birth; LB–, negative for live birth; NPX, Normalized Protein eXpression; PEA, proximity extension assay; SD, standard deviation.

and as true negatives those embryos that did not achieve a live birth, the model classifying them as negative. The embryos wrongly classified as leading to a positive or negative live birth were described as false positive and false negative, respectively.

Ethical approval

An Institutional Review Board (IRB reference 1802-VLC-012-MM), which regulates and approves database analysis and clinical IVF procedures for research at IVI, approved the procedure and protocol on 10 April 2018. Additionally, the project complies with the Spanish law governing assisted reproductive technologies (14/2006).

RESULTS

The mean age of the patients included in the study was 41.6 years, with a mean body mass index (BMI) of 23.2 kg/m^3 for the women receiving autologous oocytes. Regarding the clinical outcome, this group showed a positive β-HCG of 63.0%, an implantation rate of 56.8% and a live birth rate of 47.0%. The patients included in the oocyte donation programme had a mean age of 37.9 years with a mean BMI of 22.9 kg/m^3 and their treatments achieved a positive β-HCG of 68.7%, an implantation rate of 54.20% and a live birth rate of 40.5%.

Proteomic profile of preimplantation embryos

Of the total of 92 proteins, 67 had identical NPX values in all the samples analysed (conditioned and control media). The lack of variation in the signal for each sample was decisive for not including these proteins in the following analyses. Only 25 of the total protein samples analysed had different NPX values. The means of the NPX values for these 25 proteins in control and conditioned medium are shown in FIGURE 2. Higher concentrations of three proteins were detected in the spent embryo culture media compared with background concentrations in control media. These proteins were IL-8 ($P = 0.025$), IL-6 ($P = 0.001$) and uPA (urokinase-type plasminogen activator; $P = 0.006$). Furthermore, lower concentrations of 14 proteins were detected in spent embryo culture media compared with background concentrations. These proteins were DNER (Delta/Notch-like EGF-related receptor; $P < 0.001$), CSF-1 (macrophage colony-stimulating factor 1; $P < 0.001$), Flt3L (FMS-like tyrosine kinase 3 ligand; $P < 0.001$), SCF ($P < 0.001$), CD40 ($P < 0.001$), MCP-1 (methyl-accepting chemotaxis protein; $P < 0.001$), CX3CL1 ($P < 0.001$), CD6 ($P < 0.001$), TRAIL ($P = 0.002$), TNFRSF9 (tumour necrosis factor receptor superfamily member 9; $P < 0.001$), CD244 ($P < 0.001$), IL-18 ($P < 0.001$), CCL23 ($P < 0.001$) and IL-18R1 ($P < 0.001$).

The only protein with a different NPX value in implanted (NPX value 2.44) and non-implanted embryos (NPX value 2.76) was VEGFA ($P = 0.017$).

Collinearity analysis for proteins

The collinearity analysis of the 25 proteins demonstrated that most of them were highly correlated with one another (data not shown). Thus, after correcting the collinearity, seven independent and non-redundant proteins remained for use in the ANN: matrix metalloproteinase-1 (MMP-1), IL-6, VEGFA, uPA, TNF-related activation-induced cytokine (TRANCE), Flt3L and DNER. The relative NPX values for each protein are shown in TABLE 1.

Artificial intelligence model

An extraction of relevant variables from the 131 blastocyst images included in the first population was required to design the ANN using morphological data. The training performed with 70% of the images was capable of correctly classifying 89% of the embryos as either LB+ or LB– (true positive, 33; true negative, 48; false positive, 6; false negative, 4), with 95% correctly classified in the test (true positive, 6; true negative, 13; false positive, 1; false negative, 0).

Regarding the validation of the ANN with the second embryo population and the additional proteomic data, the three most efficient architectures obtained using the genetic algorithm technique are shown in TABLE 2. Considering only the test data, the ANN was successful in predicting positive and negative live birth (mean of total success 89.67%).

Regarding the test dataset, the ROC curves for the three architectures are shown in FIGURE 3. The architecture developed using IL-6 and MMP-1 achieved a correct classification of all the embryos as a positive or negative live birth in the training, validation and test phases (total success 100%). The resulting AUC to predict the positive and negative live birth reached the highest value, 1.0.

The blind test for architecture 1 was performed with 11 embryos that had not previously been used, and reached an accuracy of prediction of 72.7% (FIGURE 4). It correctly classified eight embryos out of the total number (true positive 4, true negative 4, false positive 1 and false negative 2).

DISCUSSION

Information from the blastocyst images and proteomic information gained from the analysis of the embryonic secretome were used to predict the potential of a euploid embryo to lead to a live birth.

The proteomic analysis of the culture media showed that, out of 92 proteins measured, only IL-6, uPA and IL-8 were differentially secreted by the developing human embryos. Previous studies revealed that the concentration of IL-6 in the culture medium could be useful in selecting the

TABLE 2 TEST ACCURACIES OF THE THREE MOST EFFICIENT ANN ARCHITECTURES IN LIVE BIRTH PREDICTION

ANN architecture	Morphology from image analysis[a]	Proteomic data	Testing data (n = 7)		
			Success for LB+ (%) (n = 4)	Success for LB– (%) (n = 3)	Total success (%)
1	20 variables	MMP-1, IL-6	100 (AUC = 1)	100 (AUC = 1)	100
2	20 variables	MMP-1, IL-6, VEGFA, uPA, TRANCE, Flt3L and DNER	100 (AUC = 0.9)	80 (AUC = 0.9)	85.7
3	20 variables	25 proteins[b]	87.5 (AUC = 0.83)	80 (AUC = 0.84)	83.3

[a] The variables are described in Supplementary Table 4.
[b] IL-8, VEGFA, CD244, OPG, uPA, IL-6, MCP-1, TRAIL, CST5, IL-1α, CXCL1, CD6, SCF, IL-18, FGF-23, MMP-1, IL-18R1, TRANCE, CCL23, Flt3L, DNER, CD40, CX3CL1, TNFRSF9, CSF-1.
ANN, Artificial Neural Network; LB+, positive for live birth; LB–, negative for live birth.

embryo for implantation (*Dominguez et al., 2015*). Another research group has demonstrated higher concentrations of IL-6 in embryos that reach blastocyst stage than in arrested ones (*Lindgren et al., 2018*). In addition, there is evidence about the secretion of IL-6 by the endometrial epithelial cells that emphasizes the importance of this cytokine in embryo development (*Dominguez et al., 2010*). The other prominent proteins found in the current work to be differentially secreted have also previously been detected. Whereas the first evidence of uPA in embryo culture media was in 1996 (*Khamsi et al., 1996*), the presence of IL-8 was not identified in the embryo secretome until 2018 (*Lindgren et al., 2018*), using PEA technology.

At the end of the collinearity analysis, seven proteins remained for use in the artificial intelligence model. According to the current study's results, two of these proteins (IL-6 and uPA) were secreted by the embryos, two others (DNER and Flt3L) were the ones consumed, and one protein (VEGFA) was related to poor implantation. Regarding the other two proteins, the authors consider that they have passed the collinearity analysis due to their exclusive characteristics: MMP-1 was the only one with a negative mean value in both control medium and medium from the embryos; and TRANCE was not found in control media, but was present in all media that had contained an embryo (see FIGURE 2). Furthermore, TRANCE was the only one out of the seven proteins with significant difference in relative concentration between LB+ and LB– samples (TABLE 1).

The image analysis performed in the present research on the blastocyst pictures has been proven in a previous study that showed good results in classifying the quality of bovine blastocysts (*Rocha et al., 2017*). This software considered that 20 morphological variables (Supplementary Table 4) of human embryos were enough to predict the likelihood of achieving a live birth. These parameters were combined with the data from the proteomic analysis to develop the current artificial intelligence model of prediction.

The current results demonstrated that the accuracy of prediction was higher as the ANN architecture improved. First, the model created using 25 proteins correctly classified 83.3% of the embryos used in the test. Second, the collinearity analysis was shown to be efficient as the predictive power improved to 85.7% when only the resulting seven independent proteins were used. Finally, the artificial intelligence model achieved the highest accuracy in predicting live birth (AUC = 1) when considering IL-6, MMP-1 and the 20 morphological variables. It is reported that these proteins play an important role in reproductive function. IL-6 is relevant for embryonic development (*Dominguez et al., 2010*, *2015*; *Iles, 2019*), and MMP-1 has been detected in mammalian ovaries (*Hulboy, 1997*) and human follicular fluid (*Lee et al., 2005*).

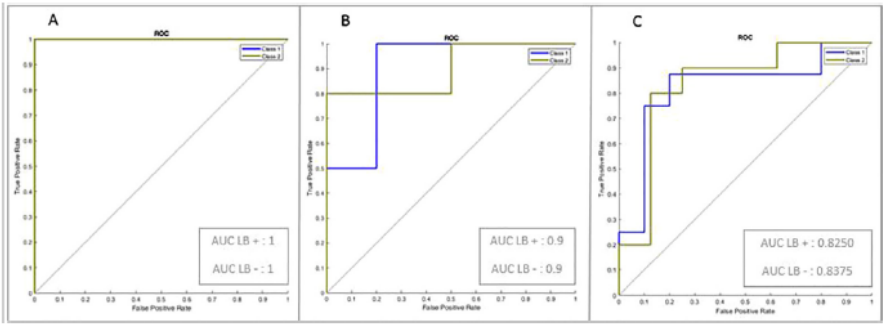

FIGURE 3 Receiver operating characteristic (ROC) curves for live birth (LB) prediction using the testing dataset (n = 7) and the artificial neural network with architecture 1 (A), architecture 2 (B) and architecture 3 (C) (see *Table 2* for information on the architectures). The y-axis represents the sensitivity, and the x-axis refers to 1 – Specificity. Class 1, positive live birth; Class 2, negative live birth.

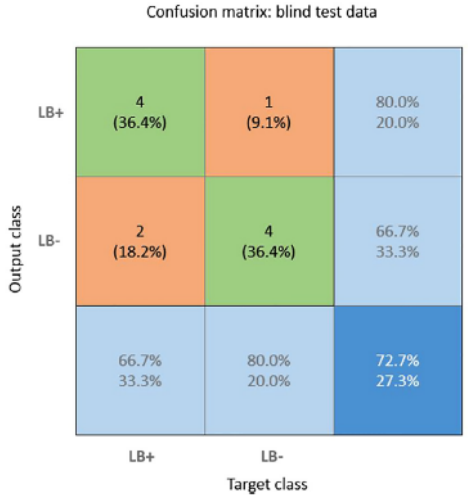

FIGURE 4 Confusion matrix for the blind testing dataset using the artificial neural network (ANN) with architecture 1. The *y*-axis refers to the output value predicted by the ANN, and the *x*-axis to the real value. Green areas represent the embryos classified correctly, and orange ones the embryos classified incorrectly. Dark blue areas represent the total hits (72.7%) and total mistakes (27.3%), and light blue areas provide the right:wrong ratio for each column. LB+, positive for live birth; LB–, negative for live birth.

A recent publication demonstrated that, for embryo selection an objective time-lapse imaging algorithm is superior to the subjective blastocyst morphological scoring system (*Fishel et al., 2019*). The algorithm used had previously been published (*Fishel et al., 2017*) and obtained an AUC of 67.43% for live birth prediction, compared with 61.74% using the blastocysts' morphological grade. The accuracy of embryo selection using the current proposed model is higher than using standard morphological selection alone, as well as using algorithms developed with time-lapse images.

This study differs from previously published approaches to artificial intelligence in terms of the experimental design, including the proteomic analysis, and the outcome. The first application of ANN to predict the outcome of an IVF treatment achieved an accuracy of 59% (*Kaufmann et al., 1997*). Since then, several predictive models have been developed based on different populations of patients, such as in cycles associated with male factor infertility (*Wald, 2005*) or women with endometriosis (*Ballester et al., 2012*). In addition, embryo morphokinetic parameters were exclusively used as input data for an ANN that predicted 70% of pregnancies (*Milewski et al., 2017*).

Machine learning methods have been used to combine morphokinetic algorithms and factors of infertility such as sperm motility, anti-Müllerian hormone (AMH) concentration and blastomere size on day 3 (*Blank et al., 2019*).

Embryo images provided by time-lapse systems have now become the subject of studies based on artificial intelligence. Deep learning techniques have been used to predict blastocyst quality and select the most appropriate embryo to transfer (*Khosravi et al., 2019*). Embryos classified as good quality by these authors' deep neural network, called STORK, showed higher probabilities of leading to a live birth than those classified as bad quality (61.4% and 50.9%, respectively). Nevertheless, STORK cannot estimate the pregnancy rate, although it showed a very high AUC (0.98) in predicting blastocyst quality. Another deep learning model was recently developed by Tran and colleagues (*Tran et al., 2019*) that used the complete video of embryo development to predict the likelihood of pregnancy, with an AUC of 0.93 in 5-fold stratified cross-validation. The likelihood of an IVF treatment ending up with a live birth has recently been analysed considering patient and treatment characteristics (*Vogiatzi et al., 2019*).

Limitations of the current study that should be considered are reflected in the design of the research. This model was trained with proteomic data and morphological variables from the image analysis of one time-lapse system. The total population of embryos was distributed into two groups with different phases (training, validation and testing), resulting in a small number of embryos in each. Additionally, only one laboratory and a unique culture medium were involved in this study. This could be considered as an advantage in the proteomic analysis, but applicability to other laboratories remains unclear. In addition, there is evidence of inter-batch protein and pH variability with the same medium (*Dyrlund et al., 2014*; *Leonard et al., 2013*; *Tarahomi et al., 2018*). In general, the models developed with ANNs could also be affected by the overfitting phenomenon. The current study tried to avoid this by defining the input and output variables. The overall success on the blind test may be considered as evidence (72.7% for the blind test versus 100% for training, validation and testing). It is also necessary to highlight that the model with autologous oocytes was built using only euploid embryos, so the clinical value lies in distinguishing the most viable embryo among those that test as euploid. Further studies should have a large sample size and multicentric nature, and should include data from different time-lapse systems to standardize the artificial intelligence model and globalize its use.

In conclusion, the introduction of artificial intelligence to IVF laboratories would help embryologists to predict the success of an embryo for achieving a live birth. The combination of proteomic analysis of the embryo culture medium and morphological information from the blastocyst images has never previously been assessed using artificial intelligence techniques. The present preliminary research has shown the predictive power of this combination. The ANN achieved excellent accuracy for detecting euploid embryos capable of resulting in a live birth, especially in terms of IL-6 and MMP-1. In fact, the model proposed in this manuscript is a promising tool to select the most successful embryo of a euploid cohort. In further studies, the ANN should be retrospectively tested with an appropriately sized study to confirm the effectiveness of this innovative method before its prospective application.

ACKNOWLEDGEMENTS

The authors acknowledge the embryologists and technicians of the IVF laboratory at IVI-RMA Global Valencia for their clinical support. The authors also thank the contribution of the IVI Foundation and the State University of São Paolo in this project. This work was supported by the Ministry of Science and Universities CDTI (IDI-20191102) awarded to M.M.; grants # 2017/19323-5, 2018/19371-2 and 2018/24252-2 from the São Paulo Research Foundation (FAPESP); and from the Spanish Ministry of Economy and Competitiveness through the Miguel Servet programme [CPII018/00002] awarded to F.D.

SUPPLEMENTARY MATERIALS

Supplementary material associated with this article can be found, in the online version, at doi:10.1016/j.rbmo.2020.09.031.

REFERENCES

Abiodun, O., Jantan, A., Omolara, A., Dada, K., Mohamed, N., Arshad, H. **State-of-the-art in artificial neural network applications : A survey.** Heliyon 2018; 4: e00938

Assarsson, E., Lundberg, M., Holmquist, G., Björkesten, J., Thorsen, S.B., Ekman, D., Eriksson, A., Dickens, E.R., Ohlsson, S., Edfeldt, G. **Homogenous 96-Plex PEA Immunoassay Exhibiting High Sensitivity, Specificity, and Excellent Scalability.** PLoS One 2014; 9: e95192

Ballester, M., Oppenheimer, A., Mathieu, E., Touboul, C., Antoine, J., Coutant, C., Darai, E. **Nomogram to predict pregnancy rate after ICSI – IVF cycle in patients with endometriosis.** Hum. Reprod. 2012; 27: 451–456

Bino, V.S., Unnikrishnan, A., Balakrishnan, K. **Gray Level Co - Occurence Matrices: Generalisation and some new features.** Int. J. Comput. Sci. Eng. Inf. Technol. 2012; 2: 151–157

Blank, C., Wildeboer, R., Decroo, I., Tilleman, K., Weyers, B., Sutter, P., Mischi, M., Schoot, B. **Prediction of implantation after blastocyst transfer in in vitro fertilization : a machine-learning perspective.** Fertil. Steril. 2019; 111: 318–326

Bormann, C., Thirumalaraju, P., Kanakasabapathy, M., Kandula, H., Souter, I., Dimitriadis, I., Gupta, R., Pooniwala, R., Shafiee, H. **Consistency and objectivity of automated embryo assessments using deep neural networks.** Fertil. Sterility Sci. Congr. Suppl. Oral Poster Sess. Abstr. 2020; 113: 781–787

Butler, S.A., Luttoo, J., Freire, M.O.T., Abban, T.K., Borrelli, P.T.A., Iles, R.K. **Human chorionic gonadotropin (hCG) in the secretome of cultured embryos: Hyperglycosylated hCG and hCG-free beta subunit are potential markers for infertility management and treatment.** Reprod. Sci. 2013; 20: 1038–1045

Cerrillo, M., Herrero, L., Guillén, A., Mayoral, M., García-Velasco, J.A. **Impact of Endometrial Preparation Protocols for Frozen Embryo Transfer on Live Birth Rates.** Rambam Maimonides Med. J 2017; 8: e0020

Chavez-Badiola, A., Flores-Saiz, A., Mendizabal-Ruiz, G. **Predicting pregnancy test results after embryo transfer by image feature extraction and analysis using machine learning.** Sci. Rep. 2020; 10: 4394

Chen, T., Zheng, W., Liu, C., Huang, I., Lai, H., Liu, M. **Using Deep Learning with Large Dataset of Microscope Images to Develop an Automated Embryo Grading System.** Fertil. Reprod. 2019; 1: 51–56

Curchoe, C.L., Bormann, C.L. **Artificial intelligence and machine learning for human reproduction and embryology presented at ASRM and ESHRE 2018.** J. Assist. Reprod. Genet. 2019; 36: 591–600

Dang, T., Phung, T., Le, H., Nguyen, T., Nguyen, T., Nguyen, T. **Preimplantation Genetic Testing of Aneuploidy by Next Generation Sequencing : Association of Maternal Age and Chromosomal Abnormalities of Blastocyst.** Open Access Maced J. Med. Sci. 2019; 7: 4427–4431

Danuser, G. **Essay Computer Vision in Cell Biology.** Cell 2011; 147: 973–978

Dirvanauskas, D., Maskeliunas, R., Raudonis, V., Damasevicius, R. **Embryo development stage prediction algorithm for automated time lapse incubators.** Comput. Methods Programs Biomed. 2019; 177: 161–174

Dominguez, F., Gadea, B., Esteban, F.J., Horcajadas, J.A., Pellicer, A., Simon, C. **Comparative protein-profile analysis of implanted versus non-implanted human blastocysts.** Hum. Reprod. 2008; 23: 1993–2000

Dominguez, F., Gadea, B., Mercader, A., Esteban, F., Pellicer, A., Simón, C. **Embryologic outcome and secretome profile of implanted blastocysts obtained after coculture in human endometrial epithelial cells versus the sequential system.** Fertil. Steril. 2010; 93: 774–782e1

Dominguez, F., Ph, D., Meseguer, M., Ph, D., Aparicio-ruiz, B., Ph, D. **New strategy for diagnosing embryo implantation potential by combining proteomics and time-lapse technologies.** Fertil. Steril. 2015; 104: 908–914

Dyer, S., Chambers, G.M., De Mouzon, J., Nygren, K.G., Mansour, R., Ishihara, O., Banker, M., Adamson, G.D. **International Committee for Monitoring Assisted Reproductive Technologies world report : Assisted Reproductive Technology 2008, 2009 and 2010.** Hum. Reprod. 2016; 31: 1588–1609

Dyrlund, T.F., Kirkegaard, K., Poulsen, E.T., Sanggaard, K.W., Hindkjær, J.J., Kjems, J., Enghild, J.J., Ingerslev, H.J. **Unconditioned commercial embryo culture media contain a large variety of non-declared proteins : a comprehensive proteomics analysis.** Hum. Reprod. 2014; 29: 2421–2430

Edwards, R.G., Fishel, S.B., Cohen, J., Fehilly, C.B., Purdy, J.M., Slater, J.M., Steptoe, P.C., Webster, J.M. **Factors influencing the success of in vitro fertilization for alleviating human infertility.** J. Vitr. Fertil. Embryo. Transf. 1984; 1: 3–23

Fishel, S., Campbell, A., Foad, F., Davies, L., Best, L., Davis, N., Smith, R., Duffy, S., Wheat, S., Montgomery, S. **Evolution of Embryo Selection for IVF from Subjective Morphology Assessment to Objective Time-Lapse Algorithms Improves Chance of Live Birth.** Reprod. Biomed. Online 2019; 40: 61–70

Fishel, S., Campbell, A., Montgomery, S., Smith, R., Nice, L., Duffy, S., Jenner, L., Berrisford, K., Kellam, L., Smith, R. **Live births after embryo selection using morphokinetics versus conventional morphology: a retrospective analysis.** Reprod. Biomed. Online 2017; 35: 407–416

De Geyter, C., Calhaz-Jorge, C., Kupka, M.S., Wyns, C., Mocanu, E., Motrenko, T., Scaravelli, G., Smeenk, J., Vidakovic, S., Goossens, V. **ART in Europe, 2014: Results generated from European registries by ESHRE.** Hum. Reprod. 2018; 33: 1586–1601

Ghaheri, A. **The Applications of Genetic Algorithms in Medicine.** Oman Med. J. 2015; 30: 406–416

Gupta, J.N.D., Sexton, R.S. **Comparing backpropagation with a genetic algorithm for neural network training.** Omega 1999; 27: 679–684

Hassanein, A.S., Mohammad, S., Sameer, M., Ragab, M.E. **A Survey on Hough Transform, Theory, Techniques and Applications.** Int. J. Comput. Sci. Issues 2015; 12: 139–156

Hathout, Y. **Approaches to the study of the cell secretome.** Expert Rev. Proteomics 2007; 4: 239–248

Hernández-González, J., Inza, I., Crisol-Ortíz, L., Guembe, M.A., Iñarra, M.J., Lozano, J.A.

Fitting the data from embryo implantation prediction: Learning from label proportions. Stat Methods Med. Res. 2018; 27: 1056–1066
Hollywood, K., Brison, D.R., Goodacre, R. **Metabolomics : Current technologies and future trends.** Proteomics 2006; 6: 4716–4723
Huang, D., Shan, C., Ardabilian, M., Wang, Y., Liming, C. **Local Binary Patterns and Its Application to Facial Image Analysis: A Survey.** EEE Trans Syst. Man., Cybern 2011; 4: 1–17
Hulboy, D. **Matrix metalloproteinases as mediators of reproductive function.** Mol. Hum. Reprod. 1997; 3: 27–45
Iles, R.K. **Secretome profile selection of optimal IVF embryos by matrix-assisted laser desorption ionization time-of-flight mass spectrometry.** J. Assist. Reprod. Genet. 2019; 36: 1153–1160
Jones, K., Warnock, S., Urry, R., Edwin, S., Mitchell, M. **Immunosuppressive activity and alpha interferon concentrations in human embryo culture media as an index of potential for SUC- cessfal implantation.** Fertil. Steril. 1992; 57: 637–640
Kalpana, R., Chitra, M., Vijayakalashmi, K. **Pattern classification of EEG signals on different states of cognition using linear and nonlinear classifiers.** Res. J. Appl. Sci. Eng. Technol. 2015; 11: 623–629
Katz-Jaffe, M., Gardner, D.K. **Embryology in the era of proteomics.** Theriogenology 2007; 1: S125–S130
Katz-jaffe, M.G., McReynolds, S. **Embryology in the era of proteomics.** Fertil. Steril. 2013; 99: 1073–1077
Kaufmann, S.J., Eastaugh, J.L., Snowden, S., Smye, S.W., Sharma, V. **The application of neural networks in predicting the outcome of in-vitro fertilization.** Hum. Reprod. 1997; 12: 1454–1457
Khamsi, F., Armstrong, D.T., Zhang, X. **Expression of urokinase-type plasminogen activator in human preimplantation embryos.** Mol. Hum. Reprod. 1996; 2: 273–276
Khosravi, P., Kazemi, E., Zhan, Q., Malmsten, J.E., Toschi, M., Zisimopoulos, P., Sigaras, A., Lavery, S., Cooper, L.A.D., Hickman, C. **Deep learning enables robust assessment and selection of human blastocysts after in vitro fertilization.** npj Digit. Med. 2019; 2: 1–9
Krisher, R.L., Schoolcraft, W.B., Katz-jaffe, M.G. **Omics as a window to view embryo viability.** Fertil. Steril. 2015; 103: 333–341
Lee, D.M., Lee, T.K., Song, H.B., Kim, C.H. **The expression of matrix metalloproteinase-9 in human follicular fluid is associated with in vitro fertilisation pregnancy.** BJOG An. Int. J. Obstet. Gynaecol. 2005; 112: 946–951
Leonard, P.H., Charlesworth, M.C., Benson, L., Walker, D.L., Fredrickson, J.R., Morbeck, D.E. **Variability in protein quality used for embryo culture: Embryotoxicity of the stabilizer octanoic acid.** Fertil. Steril. 2013; 100: 544–549
Lindgren, K.E., Yaldir, F.G., Hreinsson, J., Holte, J., Sundström-poromaa, I., Kaihola, H., Åkerud, H., Lindgren, K.E., Yaldir, F.G., Hreinsson, J. **Differences in secretome in culture media when comparing blastocysts and arrested embryos using multiplex proximity assay.** Ups J. Med. Sci. 2018; 123: 143–152
Mains, L.M., Christenson, L., Yang, B., Sparks, A.E.T., Mathur, S., Van Voorhis, B.J. **Identification of apolipoprotein A1 in the human embryonic secretome.** Fertil. Steril. 2011; 96: 422–427
Manna, C., Nanni, L., Lumini, A. **Artificial intelligence techniques for embryo and oocyte classification.** Reprod. Biomed. Online 2013; 26: 42–49
Martínez-Granados, L., Serrano, M., González-Utor, A., Ortiz, N., Badajoz, V., Olaya, E., Prados, N., Boada, M., Castilla, J.A. **Inter-laboratory agreement on embryo classification and clinical decision: Conventional morphological assessment vs. time lapse.** PLoS One 2017; 12: 1–13
Matusevičius, A., Dirvanauskas, D., Maskeliūnas, R., Raudonis, V. **Embryo cell detection using regions with convolutional neural networks.** CEUR Workshop Proc. 2017; 1856: 89–93
Milewski, R., Kuczyńska, A., Stankiewicz, B., Kuczyński, W. **How much information about embryo implantation potential is included in morphokinetic data? A prediction model based on artificial neural networks and principal component analysis.** Adv. Med. Sci. 2017; 62: 202–206
Miyagi, Y. **Feasibility of deep learning for predicting live birth from a blastocyst image in patients classified by age.** Reprod. Med. Biol. 2019; 18: 190–203
Mukhopadhyay, P., Chaudhuri, B.B. **A survey of Hough Transform.** Pattern Recognit. 2014; 48: 993–1010
Najafabadi, M.M., Villanustre, F., Khoshgoftaar, T.M., Seliya, N., Wald, R., Muharemagic, E. **Deep learning applications and challenges in big data analytics.** J. Big Data 2015; 2: 1–21
Noci, I., Fuzzi, B., Rizzo, R., Melchiorri, L., Criscuoli, L., Dabizzi, S., Biagiotti, R., Pellegrini, S., Menicucci, A., Baricordi, O. **Embryonic soluble HLA-G as a marker of developmental potential in embryos.** Hum. Reprod. 2005; 20: 138–146
O'Brien, R.M. **A caution regarding rules of thumb for variance inflation factors.** Qual. Quant. 2007; 41: 673–690
Punjabi, U., Vereecken, A., Delbeke, L., Angle, M., Gielis, M., Gerris, J., Johnston, J., Buytaert, P. **Embryo-Derived Platelet Activating Factor, a Marker of Embryo Quality and Viability Following Ovarian Stimulation for in Vitro Fertilization.** J. Vitr. Fertil. Embryo. Transf. 1990; 7: 3–8
Qiu, J., Li, P., Dong, M., Xin, X., Tan, J. **Personalized prediction of live birth prior to the first in vitro fertilization treatment : a machine learning method.** J. Transl. Med. 2019; 18: 1–8
Rad, R., Saeedi, P., Au, J., Havelock, J. **Blastomere cell counting and centroid localization in microscopic images of human embryo.** IEEE 20th Int. Work Multimed Signal Process MMSP 2018 2018: 1–6
Rigla, M., García-Sáez, G., Pons, B., Hernando, M. **Artificial Intelligence Methodologies and Their Application to Diabetes.** J. Diabetes Sci. Technol. 2018; 12: 303–310
Robertson, S.A. **GM-CSF regulation of embryo development and pregnancy.** Cytokine Growth Factor Rev. 2007; 18: 287–298
Rocha, J., Nogueira, M., Zaninovic, N., Hickman, C. **Is AI assessment of morphokinetic data and digital image analysis from time-lapse culture predictive of implantation potential of human embryos?** Fertil Sterility Sci. Congr. Suppl. Oral. Poster Sess. Abstr. 2018; 110: E373
Rocha, J.C., Passalia, F.J., Matos, F.D., Takahashi, M.B., Ciniciato, D.D.S., Maserati, M.P., Alves, M.F., De, T.G. **A Method Based on Artificial Intelligence To Fully Automatize The Evaluation of Bovine Blastocyst Images.** npj Digit. Med. 2017; 7: 1–10
Rosa, T.D., Luz, H. **Conceitos Básicos de Algoritmos Genéticos: Teoria e Práctica.** Ulbra-ToBr 2009: 27–37
Rubio, C., Simon, C., Vidal, F., Rodrigo, L., Pehlivan, T., Remohí, J., Pellicer, A. **Chromosomal abnormalities and embryo development in recurrent miscarriage couples.** Hum. Reprod. 2003; 18
Russ, J. 2016 **The image processing handbook.** CRC press
Saith, R.R., Bersinger, N.A., Barlow, D.H. **The role of pregnancy-specific P-l glycoprotein (SP1) in assessing human blastocyst quality in vitro.** Hum. Reprod. 1994; 11: 1038–1042
Simopoulou, M., Sfakianoudis, K., Maziotis, E., Antoniou, N., Rapani, A., Anifandis, G., Bakas, P., Bolaris, S., Pantou, A., Pantos, K. **Are computational applications the "crystal ball" in the IVF laboratory? The evolution from mathematics to artificial intelligence.** J. Assist. Reprod. Genet. 2018; 35: 1545–1557
Storr, A., Venetis, C.A., Cooke, S., Kilani, S., Ledger, W. **Inter-observer and intra-observer agreement between embryologists during selection of a single Day 5 embryo for transfer: A multicenter study.** Hum. Reprod. 2017; 32: 307–314
Sundvall, L., Ingerslev, H.J., Breth Knudsen, U., Kirkegaard, K. **Inter- and intra-observer variability of time-lapse annotations.** Hum. Reprod. 2013; 28: 3215–3221
Takahashi, M.B., Rocha, J.C., Núñez, E.G.F. **Optimization of artificial neural network by genetic algorithm for describing viral production from uniform design data.** Process Biochem. 2016; 51: 422–430
Tarahomi, M., de Melker, A., van Wely, M., Hamer, G., Repping, S., Mastenbroek, S. **pH stability of human preimplantation embryo culture media: effects of culture and batches.** RBMO 2018; 37: 409–414
Thouas, G.A., Dominguez, F., Green, M.P., Vilella, F., Simon, C., Gardner, D.K. **Soluble ligands and their receptors in human embryo development and implantation.** Endocr. Rev. 2015; 36: 92–130
Tran, D., Cooke, S., Illingworth, P.J., Gardner, D.K. **Deep learning as a predictive tool for fetal heart pregnancy following time-lapse incubation and blastocyst transfer.** Hum. Reprod. 2019; 34: 1011–1018
Uyar, A., Bener, A., Ciray, H. **Predictive modeling of implantation outcome in an in vitro fertilization setting: an application of machine learning methods.** Med. Decis. Mak. 2015; 35: 714–725
Vanneschi, L., Castelli, M. **Multilayer Perceptrons.** Encycl Bioinforma Comput Biol 2018; 1: 1–9
Vogiatzi, P., Pouliakis, A., Siristatidis, C. **An artificial neural network for the prediction of assisted reproduction outcome.** J. Assist. Reprod. Genet. 2019; 36: 1441–1448
Walczak, S., Cerpa, N. **Heuristic principles for the design of artificial neural networks.** Inf. Softw. Technol. 1999; 41: 107–117
Wald, M. **Computational models for prediction of IVF / ICSI outcomes with surgically retrieved spermatozoa.** Reprod. Biomed. Online 2005; 11: 325–331
Zador, A. **A critique of pure learning and what artificial neural networks can learn from animal brains.** Nat. Commun. 2019; 10

Zaninovic, N., Rocha, J.C., Zhan, Q., Toschi, M., Malmsten, J., Nogueira, M., Meseguer, M., Rosenwaks, Z., Hickman, C. **Application of artificial intelligence technology to increase the efficacy of embryo selection and prediction of live birth using human blastocysts cultured in a time-lapse incubator.** Fertil. Sterility Sci. Congr. Suppl. Oral. Poster Sess. Abstr. 2018; 110: e372

Ziebe, S., Loft, A., Povlsen, B.B., Erb, K., Agerholm, I., Aasted, M., Gabrielsen, A., Hnida, C., Zobel, D., Mundig, B. **A randomized clinical trial to evaluate the effect of granulocyte-macrophage embryo culture medium for in vitro fertilization.** Fertil. Steril. 2013; 99: 1600–1609

Received 11 May 2020; received in revised form 17 September 2020; accepted 30 September 2020.

Supplemental Table. Morphological variables extracted from time-lapse human blastocyst images after collinearity analysis and used as input data for the Artificial Neural Network.

VARIABLES	DESCRIPTION
correlationMinus	Demonstrate the correlation between the image pixels in determined neighbor across the entire image. Values -1 or 1 shows a perfect correlated image, negative or positive respectively.
energyMinus	Square of sum of the GLCM elements. An energy value equals to 1 correspond to a constant image.
contrastIntersect	GLCM determined variable. Contrast is the measurement of the intensity difference between a pixel and its neighbors across the entire image with a constant image of zero contrast.
correlationIntersect	Demonstrate the correlation between the image pixels in determined neighbor across the entire image. Values -1 or 1 shows a perfect correlated image, negative or positive respectively.
homogeneityIntersect	Proximity measurement of the distribution of GLCM elements with the GLCM diagonal. The homogeneity value is 1 for a diagonal GLCM.
correlationICM	Same of correlationMinus, but only for ICM isolate image.

energyICM	Same of energyMinus, but only for ICM isolate image.
Soma	A binary ER image is calculated, using the Otsu algorithm for the threshold detection. Next, the sum of all values from the binary image is calculated. Finally, this value is divided by the total area of the blastocyst.
mediaMinus	Grey mean intensity of the pixels.
modaMinus	The total value of luminous intensity more frequently.
darkMinus	Initially, pixels with luminous intensity less or equal to 25, which is 10% of the limit allowed (remembering as it uses 8-bit values, the luminous intensity varies between 0 and 255). Then, this value is divided by the total area of the embryo.
meanCountMinus	All the pixels with luminous intensity between 10 pixels below and 10 pixels above than the mean intensity were counted. Then, this value is divided by the embryo total area.
brightMinus	Same as darkMinus, but using the pixels counting of intensity higher or equal to 230 (10% lighter of the image).
modaIntersect	Same of modaMinus, but only for TE isolate image.
darkIntersect	Same of darkMinus, but only for TE isolate image.

meanCountIntersect	Same of meanCountMinus, but only for TE isolate image.
brightIntersect	Same of brightMinus, but only for TE isolate image.
LBPmeanEx	Extract local binary pattern (LBP) features – LBP: Texture operator, which labels the pixels of an image by thresholding the neighborhood of each pixel and considers the result as a binary number.
LBPmeanTE	Same of LBPmeanEx, but only for TE isolate image.
LBPmeanICM	Same of LBPmeanEx, but only for ICM isolate image.

ARTÍCULO III

Artículo III: The higher the score, the better the clinical outcome: retrospective evaluation of automatic embryo grading as a support tool for embryo selection in IVF laboratories.

Bori L, Meseguer F, Valera MA, Galan A, Remohi J, Meseguer M.

Hum Reprod. 2022 May 30;37(6):1148-1160. doi: 10.1093/humrep/deac066. PMID: 35435210.

Factor de impacto 2021: 6,353

5-años factor de impacto: 7,736

Human Reproduction, Vol.37, No.6, pp. 1148–1160, 2022
Advance Access Publication on April 18, 2022 https://doi.org/10.1093/humrep/deac066

human reproduction

ORIGINAL ARTICLE ***Embryology***

The higher the score, the better the clinical outcome: retrospective evaluation of automatic embryo grading as a support tool for embryo selection in IVF laboratories

Lorena Bori [1,2,*], Fernando Meseguer[1,2], M. Angeles Valera [1,2], Arancha Galan[1], Jose Remohi[1,2], and Marcos Meseguer[1,2]

[1]IVIRMA, Valencia, Spain [2]Fundación IVI, Instituto de Investigación Sanitaria La Fe, Medicina Reproductiva, Valencia, Spain

*Correspondence address. IVI Valencia, Pl. Policia Local, 3, Valencia, Spain. Tel: +34-610-55-37-99; E-mail: lorena.bori@ivirma.com
https://orcid.org/0000-0003-1495-2646

Submitted on December 7, 2021; resubmitted on March 22, 2022; editorial decision on March 28, 2022

STUDY QUESTION: Is the automatic embryo grading function of specific time-lapse systems clinically useful as a decision support tool for IVF laboratories?

SUMMARY ANSWER: Blastocyst grading according to the automatic scoring system is directly associated with the likelihood of implantation and live birth, at least in treatments without preimplantation genetic testing for aneuploidy (PGT-A).

WHAT IS KNOWN ALREADY: Several embryo selection algorithms have been described since the introduction of time-lapse technology in IVF laboratories, but no one algorithm has yet been sufficiently consolidated for universal use. Multicentric models based on automated grading systems offer promise for standardization of embryo selection.

STUDY DESIGN, SIZE, DURATION: A retrospective cohort study was performed including 1678 patients who underwent IVF treatments between 2018 and 2020 and whose embryos (n = 12 468) were cultured in time-lapse systems.

PARTICIPANTS/MATERIALS, SETTING, METHODS: After obtaining the required parameters (division time to 2, 3, 4 and 5 cells; time of blastocyst formation; inner cell mass quality; and trophectoderm quality), the automatic embryo score was calculated using the software included in the appropriate workstation. First, embryo score was compared with conventional morphological quality and the subsequent clinical outcomes of 1952 single blastocyst transfers. Second, we quantified the contribution of the automatic embryo score and conventional morphological grade to implantation and live birth outcome with multivariate logistic regression analysis in different patient populations.

MAIN RESULTS AND THE ROLE OF CHANCE: A higher embryo score was associated with a better clinical outcome of IVF treatment. The mean of the automatic embryo score varied significantly ($P < 0.001$) among embryos with different morphological categories, between euploid and aneuploid embryos, between embryos resulting in positive versus negative pregnancy, between implanted and non-implanted embryos, and between embryos resulting in positive and negative live birth. Embryo score was related to the odds of implantation and live birth in the oocyte donation program (odds ratio (OR)=1.29; 95% CI [1.19–1.39]; $P < 0.001$ for implantation and OR = 1.26; 95% CI [1.16–1.36]; $P < 0.001$ for live birth) and in conventional treatments with autologous oocytes (OR = 1.38; 95% CI [1.24–1.54]; $P < 0.001$ for implantation and OR = 1.47; 95% CI [1.30–1.65]; $P < 0.001$ for live birth). There was no significant association of embryo score with implantation or live birth in treatments involving PGT-A.

LIMITATIONS, REASONS FOR CAUTION: This study is limited by its retrospective nature. Further prospective randomized trials are required to confirm the clinical impact of these findings. The single-center design should be taken into account when considering the universal application of the model.

WIDER IMPLICATIONS OF THE FINDINGS: Evidence of the clinical efficiency of automated embryo scoring for ranking embryos with different morphological grade and potential in order to achieve higher implantation and live birth rates may make it a decision support tool for embryologists when selecting blastocysts for embryo transfer.

STUDY FUNDING/COMPETING INTEREST(S): This research has been funded by a grant from the Ministry of Science, Innovation and Universities FIS (PI21/00283) awarded to M.M. There are no competing interests to declare.

TRIAL REGISTRATION NUMBER: N/A.

Key words: KIDScore D5™ / automatic embryo scoring / implantation / live birth / time-lapse / preimplantation genetic testing for aneuploidy / embryo morphology / automatism

Introduction

Embryo assessment and selection are defining factors in the successful outcome of IVF treatment. Evaluation *in vitro* has been based on embryo morphology since the beginning of assisted reproduction. Prior to the introduction of time-lapse technologies, morphological features were assessed at specific time points during embryo development. However, this method of evaluation has often involved a loss of information, and an inability to observe embryo developmental events related to treatment outcome, such as the existence of multinucleated blastomeres (Meseguer *et al.*, 2011), direct cleavage (Rubio *et al.*, 2012; Desai *et al.*, 2018) or reverse cleavage (Liu *et al.*, 2014).

Characterizing the morphokinetic parameters of embryo development went hand-in-hand with the introduction of time-lapse technology in IVF laboratories, and several algorithms have been created in an attempt to find out relevant variables that can improve embryo selection (Meseguer *et al.*, 2011; Cruz *et al.*, 2012; Dal Canto *et al.*, 2012; Motato *et al.*, 2016). Manual annotations of quantitative and qualitative parameters have been used to predict blastocyst formation, implantation potential or even live birth. Early cleavage (Milewski *et al.*, 2015) and time of morula formation (Motato *et al.*, 2016) have been used to predict blastocyst formation. The length of the second cell cycle, the division time to five cells, the second synchrony (the time interval between division from three to four cells) and the time of pronuclei fading are the most influential parameters of embryo implantation potential, according to the review of time-lapse technology by Del Gallego *et al.* (2019; Meseguer *et al.*, 2011; VerMilyea *et al.*, 2014; Goodman *et al.*, 2016; Petersen *et al.*, 2016). Late embryo developmental events (e.g. initiation of blastulation, morula formation time, or trophectoderm quality) have been identified as the most reliable predictors of live birth (Fishel *et al.*, 2017, 2018; Rienzi *et al.*, 2019). The lack of reproducibility is the main obstacle to a universal use of existing algorithms (Fréour *et al.*, 2015; Barrie *et al.*, 2017). Confounding factors that can affect the reliability of time-lapse technology algorithms include the environment and the techniques used in each laboratory, patient characteristics and the subjectivity of manual annotations (Sundvall *et al.*, 2013; Martínez-Granados *et al.*, 2017; ESHRE Working Group on Time-Lapse Technology *et al.*, 2020).

Currently, there are three main options for embryo evaluation and selection with time-lapse systems. The conventional approach is for embryologists to manually annotate a number of morphological and/or morphokinetic parameters to evaluate the quality of the embryo. These values are then used in models of clinical outcome prediction (Meseguer *et al.*, 2011; Basile *et al.*, 2015; Motato *et al.*, 2016). Embryo selection can be automated by using artificial intelligence (AI) to predict morphokinetic and morphology parameters (Kragh *et al.*, 2019). In this case, AI is employed in an indirect way to optimize the daily workflow based on existing traditional parameters. Finally, the most innovative approach is the use of AI to directly predict pregnancy, implantation or even live birth by using only time-lapse images (Khosravi *et al.*, 2019; Tran *et al.*, 2019; Bori *et al.*, 2020a). Nowadays, there are few time-lapse incubators that include specific computer software capable of detecting division time points and embryo morphological features (Kragh *et al.*, 2019). In addition, the time-lapse systems from Vitrolife contain a decision support tool, the KIDScore D5™ (EmbryoViewer software; Vitrolife), which increases the objectivity and consistency of embryo evaluation by ranking embryos according to probability of implantation. The first version of the algorithm (KIDScore D5™ v1) was based on the number of pronuclei (PN), blastocyst morphology and eight morphokinetic parameters: time of PN fade-out (tPNf); time of division into two cells (t2), three cells (t3), four cells (t4), five cells (t5) and eight cells (t8); time to early blastulation (tSB); and time to full blastocyst formation (tB). For the second version of the algorithm (KIDScore D5™ v2) the input variables were reduced to five morphokinetic parameters (t2, t3, t4, t5 and tB). Both versions have recently been retrospectively validated as a decision-making tool to help embryologists (Reignier *et al.*, 2019; Gazzo *et al.*, 2020).

The KIDScore™ D5 algorithm version 3 (KIDScore D5™ v3, or automatic embryo scoring), which is inbuilt into the EmbryoScope and EmbryoScope Plus devices, classifies embryos based on their cleavage regularity, developmental pace and blastocyst quality. It was designed using a multicenter dataset of more than 5000 embryos with known implantation data (KID embryos). According to the developers, the latest version of this model takes into consideration the number of PN, t2, t3, t4, t5, tB, inner cell mass and trophectoderm quality. A final linear score ranging between 1 and 9.9 is generated for each embryo, corresponding with low to high implantation probability. Automatic embryo scoring is recommended for embryos originating through conventional IVF or ICSI treatments and cultured under reduced oxygen conditions (4–6%). Contrary to algorithm versions 1 and 2, the latest version has never been evaluated externally with a large dataset. Therefore, the main aim of the present study was to evaluate the reliability of its automatic embryo scoring as a decision support tool for IVF laboratories. First, we analyzed the association between embryo score and a series of clinical outcomes, such as embryo ploidy, pregnancy, implantation and live birth. Second, we quantified the embryo score's contribution to implantation and live birth outcomes in different scenarios in an individualized context.

Materials and methods

Study design and population

The procedure and protocol for analyzing embryos were approved by the Institutional Review Board (IRB reference 1709-VLC-094-MM), which monitors and approves database analyses and clinical IVF procedures for research at IVIRMA Global. This retrospective analysis included 12 468 embryos cultured at IVI Valencia (Spain) over 3 years (from 2018 to 2020). We considered patients and recipients who had undergone ICSI cycles and whose embryos were grown until the fifth/sixth day of development in the time-lapse systems EmbryoScope and EmbryoScope Plus (Vitrolife, Copenhagen, Denmark). Embryos that were not scored by the KIDScore D5 v3 algorithm owing to technical problems (e.g. bubble formation or loss of embryo development recording) or because fertilization (presence of two polar bodies and two PN) was not successfully achieved were excluded from the analysis.

The flow chart of the study population is represented in Fig. 1. Out of the total population, 2321 embryos were graded as non-viable prior to the fifth day of development, 10 147 embryos were assessed at the blastocyst stage, and 1574 embryos were included in the preimplantation genetic testing for aneuploidy (PGT-A) program. Single blastocyst transfer was eventually performed in 1952 patients.

Ovarian stimulation and uterine receptivity

Donors were stimulated with a GnRH agonist, following the conventional controlled ovarian stimulation protocol. The GnRH agonist (Decapeptyl 1, Ipsen Pharma, Spain) was administered by i.m. injection until at least eight follicles had reached a mean diameter of ≥18 mm. Transvaginal oocyte retrieval was scheduled 36 h later. Endometrial preparation of recipients was undertaken using the hormone replacement therapy described by Cerrillo et al. (2017). After embryo transfer, all patients received a daily dose of 400 mg of vaginal micronized progesterone (Progeffik, Lab. Effik, Madrid, Spain) every 12 h, as luteal-phase support.

GnRH antagonist protocols were used for ovarian stimulation. In a few cases, long GnRH agonist (GnRHa) protocols were administered or LH surge suppression was omitted. The protocols followed have been described elsewhere (Cozzolino et al., 2020). In brief, the initial dose of gonadotrophins was selected based on patient characteristics (age, antral follicle count, anti-Müllerian hormone, BMI and previous ovarian responses, if any); recombinant FSH ranged from 150 to 300 IU/day (Gonal-F®, Merck Serono; Puregon®, MSD; or Bemfola®, Gedeon Richter), commonly in combination with 75 IU highly purified HMG (Menopur®, Ferring Pharmaceuticals). Gonadotrophins were initiated during the first 3 days of menstruation, or 5 days after discontinuation of the contraceptive pill. As part of the GnRH antagonist protocols, estrogens were generally administered from the midluteal phase of the previous cycle, for programming purposes. In the long GnRH agonist cycles, 0.1 mg/day of GnRHa (Decapeptyl®; IpsenPharma) was administered from Day 21 of the previous cycle.

The first transvaginal ultrasound was performed on stimulation Day 5 and every 2 days thereafter, as were serum estradiol (E2) and progesterone (P) determinations. A daily dose of 0.25 mg GnRH antagonist (Orgalutran®, MSD; or Cetrotide®, Merck Serono, Istanbul, Turkey) was introduced when at least one follicle reached a mean diameter of 14 mm. In the GnRH antagonist cycles, final oocyte maturation was triggered with 0.2 mg GnRHa (Decapeptyl®; IpsenPharma) and/or with a single dose of recombinant hCG (rhCG 250 mcg, Ovitrelle®; Merck Serono) when at least three follicles reached a mean diameter of 17–18 mm; in the case of long GnRHa cycles, only rhCG was administered.

Oocyte retrieval and ICSI

Transvaginal ovarian puncture was carried out by follicular aspiration. Oocytes were washed with Gamete medium (Cook Medical®, Australia) and cultured with fertilization medium (Origio, Cooper Surgical®, Denmark) in 6% CO_2, 5% O_2 at 37 °C. Denudation was performed just before ICSI, 4 h after oocyte retrieval, by means of mechanical and chemical procedures (pipetting in 40 IU/ml of hyaluronidase). ICSI was carried out in fertilization medium (Origio, Cooper Surgical®, Denmark) at ×400 magnification with the aid of an Olympus IX7 microscope. Finally, oocytes were placed in pre-equilibrated EmbryoSlides (EmbryoSlide®, Vitrolife) until the blastocyst stage with 28 µl (for conventional EmbryoScope) or 180 µl (for EmbryoScope Plus) single-step medium (Gems, Genea Biomedx®, Sydney, Australia) and 1.6 ml mineral oil.

Embryo incubation and selection

Embryos were cultured individually (conventional EmbryoScope) or in groups of up to eight (EmbryoScope Plus) until the fifth/sixth day of development. Images of up to 11 multiple focal planes were taken automatically every 10–20 minutes. Embryo development was assessed on an external computer with analysis software (EmbryoViewer™ workstation, Vitrolife). Fertilization was evaluated between 16 and 19 h after ICSI and confirmed by the presence of two pronuclei and two polar bodies. Division times to 2 cells (t2), 3 cells (t3), 4 cells (t4), 5 cells (t5) and tB, and ICM and trophectoderm quality were automatically annotated by the guided annotations tool inbuilt into Embryoviewer. If an error occurred, it was manually modified. In the meantime, blastocysts were evaluated (at 114–118 h post-insemination/Day 5 and 136–140 h post-insemination/Day 6) by senior embryologists, who monitored the expansion of the blastocele cavity, the inner cell mass and trophectoderm quality based on the Asociación para el Estudio de la Biología de la Reproducción (ASEBIR) criteria (Supplementary Tables SI, SII, SIII and SIV). Embryo selection was performed according to a hierarchical classification procedure based on a combination of standard (ASEBIR) morphological grading and the KIDScore D5 v3 algorithm (EmbryoViewer software; Vitrolife). Embryos were graded from A (high morphologic quality) to D (low morphologic quality) by senior embryologists and scored from 1 (low likelihood of implantation) to 9.9 (high likelihood of implantation) by KIDScore D5™ v3. The first criterion for embryo selection was the ASEBIR category. If two or more embryos were assigned the same category, the one with the highest score was selected.

PGT-A

Embryos included in the PGT-A program (n = 1574) were removed from the incubator on the third day of development and a small laser incision traversing the zona pellucida (assisted hatching) was performed with the Hamilton-Thorne Lykos® laser. Biopsy was performed on

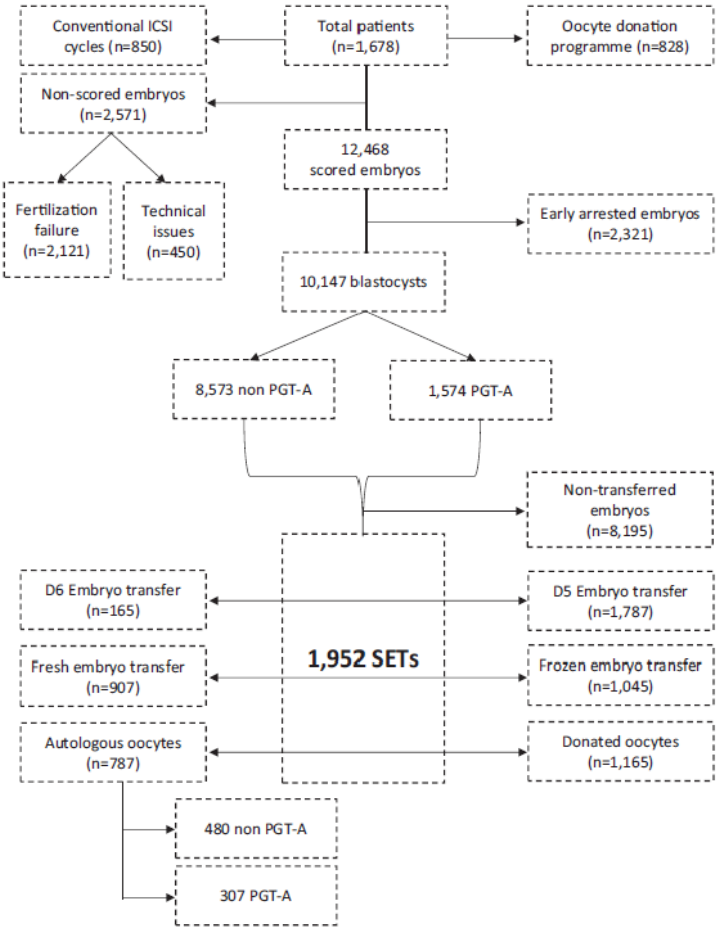

Figure 1. Distribution of patients included in the project, represented as a flow diagram. PGT-A, preimplantation genetic testing for aneuploidy.

Day 5 of culture by removing approximately five trophectoderm cells with a biopsy pipette. Chromosome analysis was performed using next generation sequencing technology (Thermo Fisher Scientific, Waltham, MA, USA).

Embryo transfer and clinical outcome

Single embryo transfer of one blastocyst was performed in 1952 patients. The β-hCG value was determined 10 days after embryo transfer and implantation was confirmed when a gestational sac was observed by ultrasound in the eighth week of pregnancy. The patients confirmed live birth after the delivery by e-mail or telephone.

In the case of deferred embryo transfers, embryos were vitrified and warmed by the Cryotop method prior to transfer (Kitazato Biopharma, Japan).

Statistical analysis

Differences in embryo score within each group of embryos (morphological grade, euploid versus aneuploid, positive and negative β-hCG, implanted and non-implanted embryos, positive and negative live birth) were calculated and compared by ANOVA and a chi-squared test.

Next, we quantified the correlation of the automatic embryo scoring and the conventional morphological category with both implantation

and live birth outcome. A stepwise multivariate logistic regression model was employed to consider possible confounding factors: oocyte origin (donated versus autologous); type of embryo transfer (fresh versus frozen); oocyte age; patient BMI; PGT-A (tested versus non-tested embryos); day of embryo transfer (fifth versus sixth day of embryo development); culture strategy (group versus single); blastocyst morphology (embryos graded as A versus C and embryos graded as B versus C); and indication for infertility treatment, that includes female etiology (low ovarian reserve, ovulatory dysfunction, endometriosis, genetic disease, advanced maternal age, uterine etiology, tubal etiology, vaginismus and oncologic preservation), male etiology (seminal pathology, karyotype alteration, genetic disease, impotence and oncologic preservation), mixed etiology, social or unknown factor. A forward procedure was used and variables were included if the corresponding *P*-value for the Wald test was higher than 0.05. The probability values between 0 (non-implantation) and 1 (implantation) obtained by the logistic regression models were used to create ROC curves and calculate areas under the ROC curve (AUC). The AUC provides an aggregated metric to evaluate the performance of the models. It represents the ratio of true test positives to total positives (sensitivity) per false positive fraction; i.e. the ratio of false positives to total negatives (1−specificity). AUC values between 0.9 and 1.0 denote excellent performance, good for 0.8–0.9, fair for 0.7–0.8, poor for 0.6–0.7 and failed for AUC values between 0.5 and 0.6.

All analyses were performed using IBM SPSS statistics software (New York, USA). $P < 0.05$ was considered significant for all tests, and odds ratios (OR) were provided with 95% CI.

Results

A general description of the study population, including treatment type and patient characteristics, is presented in Table I.

A total of 12 468 embryos from 1678 patients were automatically scored by the KIDScore D5^{TM} v3 model. This does not represent the number of metaphase II oocytes aspired from the follicular punction, but rather the number that were correctly fertilized and scored by the model. The average number of scored embryos per patient was 7.0 ± 3.7. The maximum score among the study population was 9.8, and the minimum score was 1.3. The difference between the maximum (8.5 points) and minimum (0 points) score was considerable for all patients. The mean of this difference (maximum score−minimum score) was 4.5 ± 2.0.

Of the total population of 12 468 embryos, 1952 resulted in single embryo transfers (SETs; including fresh and frozen). Subsequent overall clinical outcome was as follows: 63.1% biochemical pregnancy rate; 55.3% implantation rate; and 46.6% live birth rate.

Association between automatic embryo scoring and clinical outcomes

The mean score was significantly different ($P < 0.001$) among embryos graded with different morphological categories according to the ASEBIR criteria (8.3 ± 1.1 for embryos graded as A, n = 640; 5.9 ± 1.3 for B, n = 4560; 3.7 ± 1.2 for C, n = 2822; and 2.2 ± 0.9 for D, n = 2125) and between euploid (5.4 ± 1.7, n = 674) and aneuploid embryos (4.7 ± 1.8, n = 900). The mean of the embryo score for the SET population was 6.6 ± 1.6 for positive β-hCG and 5.9 ± 1.7 for negative β-hCG ($P < 0.001$); 6.6 ± 1.6 for positive implantation and 5.9 ± 1.7 for negative implantation ($P < 0.001$); and 6.7 ± 1.6 for positive live birth and 5.9 ± 1.7 for negative live birth ($P < 0.001$).

After the embryos were divided into quartiles of similar sample size by the SPSS software, a significant tendency ($P < 0.001$) toward better clinical outcomes was observed as the embryo score rose (Fig. 2).

Relevance of automatic embryo scoring to implantation rate and live birth outcome

The distribution of automatically scored embryos according to treatment success (implantation and live birth) can be visualized in Supplementary Fig. S1. A further logistic regression analysis of KIDScore D5^{TM} v3 grading took into account possible confounding factors: oocyte origin (donated versus autologous); type of embryo transfer (fresh versus frozen); oocyte age; patient BMI; PGT-A (tested versus non-tested embryos); day of embryo transfer (fifth versus sixth

Table I Characteristics of the study population and treatment type.

	Conventional ICSI cycles (n = 850)			Oocyte donation program (n = 828)	Total patients (n = 1678)
	Non PGT-A (n = 591)	PGT-A (n = 259)	General (n = 850)		
Oocyte age* (patient age, years)	35.9 ± 3.9	38.4 ± 3.2	36.6 ± 3.9	25.0 ± 4.8	30.9 ± 7.3
BMI of patients* (kg/m^2)	23.6 ± 4.1	23.1 ± 3.4	23.4 ± 3.9	23.7 ± 4.5	23.6 ± 4.2
Number of retrieved/donated oocytes*	12.1 ± 6.0	11.3 ± 5.9	11.9 ± 6.0	12.6 ± 3.2	12.2 ± 4.9
Number of MII oocytes*	9.4 ± 5.3	8.3 ± 5.6	9.0 ± 5.4	11.7 ± 3.1	10.3 ± 4.6
Number of fertilized oocytes (2PN)*	7.0 ± 4.3	6.0 ± 4.5	6.7 ± 4.4	9.2 ± 2.8	7.9 ± 3.9
Mean of KIDScore D5^{TM} v3**	3.4 ± 2.1 (n = 3748)	5.0 ± 1.8 (n = 1574)	3.9 ± 2.2 (n = 5322)	4.2 ± 2.3 (n = 7146)	4.1 ± 2.2 (n = 12 468)

2PN, 2 pronuclei; MII, metaphase II; PGT-A, preimplantation genetic testing for aneuploidy.
*Mean and SD are represented by cycles.
**Mean and SD are represented by total embryos, including non-viable embryos.

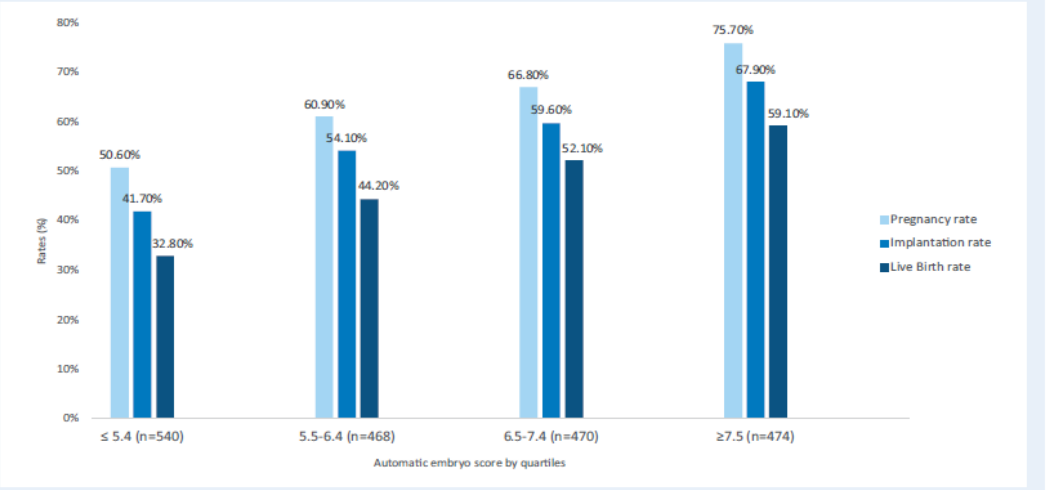

Figure 2. Pregnancy rate, implantation rate and live birth rate according to automatic embryo score by quartiles.

day of embryo development); culture strategy (group versus single); blastocyst morphology (embryos graded as A versus C and embryos graded as B versus C); and indication for infertility treatment (female, male, mixed, social or unknown factor).

The stepwise multivariate analysis for the different patient subpopulations was performed by analyzing implantation and live birth outcome. The contribution of embryo score to both outcomes was statistically significant for all treatments in general, for patients from the oocyte donation program and for conventional ICSI cycles with autologous oocytes and non-PGT-A (Table II). However, the automatic embryo score was not related to implantation or live birth outcome in embryos that had been genetically analyzed ($n = 307$, $P = 0.226$ for implantation and $P = 0.731$ for live birth).

In addition, we performed a logistic regression analysis using SART (Society for Assisted Reproductive Technology) age groups as a categorical variable instead of oocyte age as a continuous numerical variable. In this case, the embryo score was also related to the odds of implantation and live birth in the oocyte donation program (OR = 1.285; 95% CI [1.189–1.390]; $P < 0.001$ for implantation and OR = 1.260; 95% CI [1.166–1.362]; $P < 0.001$ for live birth) and in conventional treatments with autologous oocytes (OR = 1.381; 95% CI [1.236–1.543]; $P < 0.001$ for implantation and OR = 1.495; 95% CI [1.326–1.685]; $P < 0.001$ for live birth).

We also quantified the effect of KIDScore D5^{TM} consecutive quartiles on implantation and live birth potential by performing a logistic regression analysis (Supplementary Table SV).

Comparison between automatic embryo scoring and conventional morphology

We performed a logistic regression model that was identical to the previous one except for one difference; namely, the conventional morphological category replaced the automatic embryo scoring. In this case, the correlation of the ASEBIR category with implantation and live birth rates was also statistically significant for all treatments; for patients from the oocyte donation program and for conventional ICSI cycles with autologous oocytes and non-PGT-A (Table III). A further stepwise multivariate analysis was performed taking into account both grading methodologies (automatic embryo scoring and conventional morphology), in addition to the confounding factors discussed above. The resulting model correlated automatic scoring, but not ASEBIR category, with clinical outcome in the oocyte donation program and in conventional treatments (Supplementary Table SVI). The AUCs for each model are represented in Fig. 3.

Discussion

Our data reveal that embryos with the potential for pregnancy, implantation and live birth achieve a higher automatic embryo score than unsuccessful embryos. We also demonstrate that embryo score is significantly correlated with clinical outcomes in patients whose embryos are not genetically tested.

According to the developers, KIDScore models are tools designed to support embryologists in selecting embryos for transfer. The variant of the model for embryo transfer on Day 3 of development uses the time of pronuclei fading (tPNf) and division to t2, t3, t4, t5 and t8 to rank embryos into five classes (1–5) according to implantation potential. This selection algorithm was externally correlated with both implantation and live birth rates (Adolfsson *et al.*, 2018). Since then, three different KIDScore^{TM} versions have been created to help to choose which embryos to transfer on Day 5 of development. The first version (KIDScore D5^{TM} v1) was evaluated in euploid embryos and non-genetically tested embryos. Two studies evaluated the clinical

Table II Results from the multivariate logistic regression analysis including automatic embryo score for implantation and live birth outcome in different patient populations.

	Implantation			Live birth		
	ORa	95% CI	P-value	OR[a]	95% CI	P-value
All treatments (n = 1952 SETs)						
Automatic embryo score	1.285	[1.214–1.360]	<0.001	1.288	[1.215–1.364]	<0.001
PGT-A Tested (15.7%) versus non-tested (84.3%)	1.401	[1.080–1.817]	0.011	1.544	[1.189–2.006]	0.001
Embryo transfer fresh (46.5%) versus frozen (53.5%)	1.389	[1.131–1.705]	0.002	1.510	[1.228–1.857]	<0.001
BMI	–	–	–	0.968	[0.947–0.990]	0.005
Oocyte donation program (n = 1165 SETs)						
Automatic embryo score	1.285	[1.189–1.390]	<0.001	1.260	[1.166–1.362]	<0.001
Embryo transfer Fresh (54.7%) versus frozen (45.3%)	1.451	[1.139–1.848]	0.003	1.642	[1.291–2.088]	<0.001
BMI	0.970	[0.944–0.997]	0.029	0.966	[0.940–0.993]	0.014
Autologous oocytes, non-PGT-A (n = 480 SETs)						
Automatic embryo score	1.381	[1.236–1.543]	<0.001	1.465	[1.298–1.653]	<0.001
Oocyte age	–	–	–	0.909	[0.853–0.969]	0.003

OR, odds ratio; PGT-A, preimplantation genetic testing for aneuploidy; SET, single embryo transfer.
[a]ORs computed from stepwise multivariate logistic regression.
– Variables not considered by the model.

efficiency of this version for selecting euploid blastocysts in 107 and 184 SETs (27,30, respectively). The results suggested that this initial version was capable of identifying euploid embryos with high implantation potential and the authors concluded that the KIDScore D5™ v1 had the potential to improve clinical outcomes in PGT-A cycles. Conversely, our results, obtained in nearly twice as many embryos, reveal that the new version does not contribute significantly to an effective dassification of genetically tested embryos with different implantation potential. With regard to non-PGT-A cycles, both KIDScore D5 v1 and v2 have been significantly associated with probability of implantation and live birth after single blastocyst transfer (Reignier *et al.*, 2019), and our results confirm this for v3 (Table II). Additionally, the second version has been shown to positively correlate blastocyst metabolism with glucose consumption (Ferrick *et al.*, 2020). Our research group performed a preliminary validation of version 2 and version 3 of the KIDScore D5 and we obtained more consistent results using the new version (v3) of the algorithm for both implantation and live birth outcome (Bori *et al.*, 2020b). In regard to other commercially available automatic models, only one diagnostic test—Eeva™ system—has been correlated with blastocyst formation, quality and implantation potential and ongoing pregnancy (Aparicio-Ruiz *et al.*, 2016). This classification is based on the study by Wong *et al.* (2010), in which the time between the first and second cytokinesis (P2 = t3−t2) and the time between the second and third cytokinesis (P3 = t4−t3) were found to be the most relevant parameters in the prediction model. The Eeva system classifies embryos into three different categories (high, medium, and low) that are related to ASEBIR morphology categories (blastocyst formation and quality) (Aparicio-Ruiz *et al.*, 2016). However, in a prospective study, Kaser *et al.* (2017) showed that manual annotations were superior to the automated annotations provided by Eeva version 2.2.

The automatic embryo scoring evaluated in the present study and several embryo selection algorithms employ some common embryo developmental parameters (Meseguer *et al.*, 2011; Basile *et al.*, 2015; Desai *et al.*, 2016; Mizobe *et al.*, 2016; Wu *et al.*, 2016). However, the algorithms in question are based on relatively small numbers of embryos from single centers and, although they fit the original set of data well, they have failed independent validation by other external evaluations (Barrie *et al.*, 2017; Zaninovic *et al.*, 2017; Liu *et al.*, 2020). In contrast, the KIDScore D5™ v3 model was developed using datasets from multiple clinics and should, therefore, be applicable to any IVF laboratory. We are aware that embryo selection models need to be validated in-house prior to implementation, since there is evidence of the ineffectiveness of time-lapse algorithms (Meseguer *et al.*, 2011; Conaghan *et al.*, 2013) when applied to independent data sets (Kirkegaard *et al.*, 2014; Fréour *et al.*, 2015). Nonetheless, our study suggests a similar performance of this algorithm for automatic embryo scoring to the conventional embryo selection method in our local setting. To our knowledge, this is the first study to externally evaluate the clinical efficiency of this model.

According to our results, a one-unit increase in embryo score, independent of the other clinical variables included in the analysis, increases the OR of implantation by 1.29 in the case of the oocyte donation program and by 1.38 in the case of conventional cycles with

Table III Multivariate logistic regression analysis including conventional morphological categories for implantation and live birth outcome in different patient populations.

	Implantation			Live birth		
	OR[a]	95% CI	P-value	OR[a]	95% CI	P-value
All treatments (n = 1952 SETs)						
Conventional morphology A-embryos (19.6%) versus C-embryos (14.3%)	4.131	[2.953–5.779]	<0.001	3.605	[2.559–5.080]	<0.001
Conventional morphology B-embryos (66.0%) versus C-embryos (14.3%)	2.184	[1.668–2.861]	<0.001	2.120	[1.592–2.823]	<0.001
PGT-A TESTED (15.7%) versus non-tested (84.3%)	1.526	[1.175–1.984]	0.002	1.863	[1.400–2.479]	<0.001
Embryo transfer fresh (46.5%) versus Frozen (53.5%)	1.419	[1.157–1.741]	0.001	1.547	[1.259–1.900]	<0.001
BMI	–	–	–	0.968	[0.947–0.990]	0.004
Oocyte age	–	–	–	0.983	[0.968–0.999]	0.033
Oocyte donation program (n = 1165 SETs)						
Conventional morphology A-embryos (24.6%) versus C-embryos (9.0%)	3.575	[2.182–5.856]	<0.001	3.792	[2.281–6.305]	<0.001
Conventional morphology B-embryos (39.6%) versus C-embryos (9.0%)	2.038	[1.313–3.163]	0.001	2.557	[1.598–4.091]	<0.001
Embryo transfer fresh (54.7%) versus Frozen (45.3%)	1.456	[1.143–1.855]	0.002	1.704	[1.342–2.163]	<0.001
BMI	0.973	[0.946–0.999]	0.044	0.970	[0.944–0.997]	0.027
Day of embryo transfer 5 (56.1%) versus 6 (43.9%)	1.760	[1.033–2.998]	0.038	–	–	–
Autologous oocytes, non-PGT-A (n = 480 SETs)						
Conventional morphology A-embryos (18.3%) versus C-embryos (20.8%)	6.430	[3.403–12.150]	<0.001	6.835	[3.503–13.337]	<0.001
Conventional morphology B-embryos (60.8%) versus C-embryos (20.8%)	3.176	[1.922–5.249]	<0.001	2.758	[1.580–4.815]	<0.001
Oocyte age	–	–	–	0.902	[0.846–0.961]	0.001

OR, odds ratio; PGT-A, preimplantation genetic testing for aneuploidy; SET, single embryo transfer.
[a]ORs computed from stepwise multivariate logistic regression.
– Variables not considered by the model.

autologous oocytes. According to the external validation of the EEVA™ system (Aparicio-Ruiz *et al.*, 2016), the OR for implantation obtained by the logistic regression analysis was not statistically significant for medium versus low embryo category. However, the implantation rate increased by 2.24 for high versus low embryo classification. We should stress that these results are not comparable to ours, since EEVA classifies embryos according to three simple categories, while the KIDScore D5™ v3 provides a continuous numerical classification from 1 to 9.9. Indeed, when dividing the automatic embryo scoring by quartiles, we obtained higher ORs than those reported for EEVA.

In addition, we analyzed the contribution of embryo score to live birth rate, even though the scoring was designed to predict fetal heartbeat. In the case of all the treatments involving single blastocyst transfer, a significant correlation between the automatic embryo scoring and live birth outcome was observed (OR = 1.26 for the oocyte donation program and OR = 1.47 for conventional treatments with autologous oocytes). Although some authors have proposed different parameters as markers to predict live birth (Azzarello *et al.*, 2012; Barberet *et al.*, 2019; Coticchio *et al.*, 2021; Dal Canto *et al.*, 2021; Inoue *et al.*, 2021), only one model based on morphokinetics has been externally validated (Azzarello *et al.*, 2012), and was subsequently studied as one of six embryo selection algorithms (Barrie *et al.*, 2017). According to the results of this latter analysis, the AUCs were 0.584 for the model of Azzarello *et al.* (2012) to predict live birth, 0.558 for the model of Cruz *et al.* (2012) to predict blastocyst formation and quality, 0.573 for the model of Campbell *et al.* (2013) to predict aneuploidy, 0.612 for the model of Chamayou *et al.* (2013) to predict implantation, 0.543 for the model of Dal Canto *et al.* (2012) to predict development to blastocyst and implantation; and 0.629 for the model of Basile *et al.* (2015) to predict implantation. Our models using automatic embryo scoring applied to treatments administered within the oocyte donation program achieved AUCs of 0.63 for implantation and 0.64 for live birth, and the AUCs were higher for conventional treatments with autologous oocytes (0.65 for implantation and 0.69 for live birth).

The higher correlation of the automatic embryo scoring with implantation and live birth in treatments with autologous oocytes versus the oocyte donation program could be related to aneuploidy rates. It has been shown that cycles with young oocytes have higher rates of euploid embryos than cycles with older oocytes (Irani *et al.*, 2019). According to several studies, the most important reason for IVF failure is embryo aneuploidy (Dahdouh *et al.*, 2015), with many finding an association between embryo morphology and/or morphokinetics and chromosome status (Magli *et al.*, 2007; Campbell *et al.*, 2013; Minasi *et al.*, 2016; Majumdar *et al.*, 2017; Amir *et al.*, 2019; Zhan *et al.*, 2020), although no single or combined morphokinetic parameter was

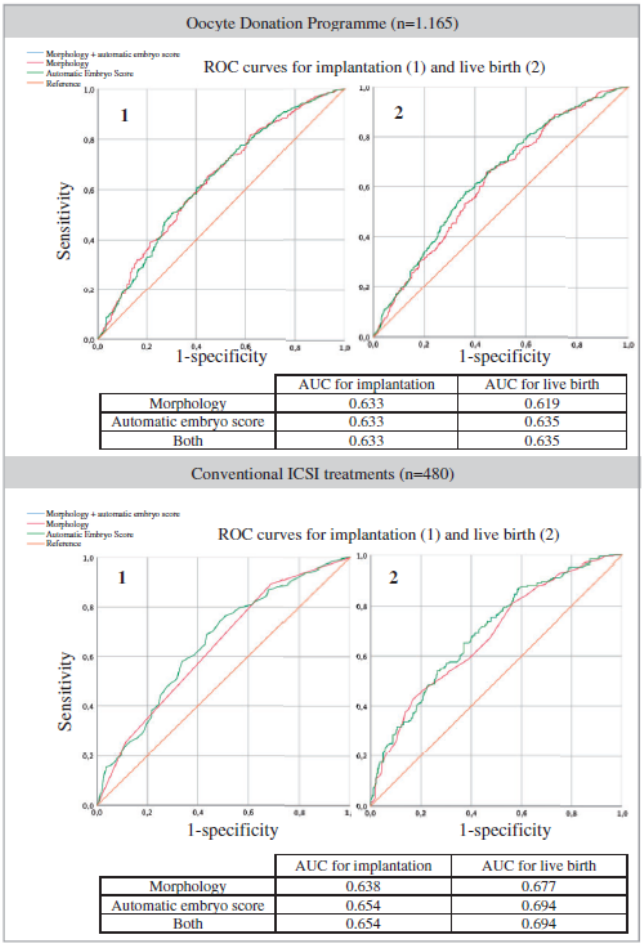

	AUC for implantation	AUC for live birth
Morphology	0.633	0.619
Automatic embryo score	0.633	0.635
Both	0.633	0.635

	AUC for implantation	AUC for live birth
Morphology	0.638	0.677
Automatic embryo score	0.654	0.694
Both	0.654	0.694

Figure 3. Receiver operating characteristic curves for implantation and live birth prediction. Analysis using the probability value for each embryo generated by the multivariate analysis, including automatic embryo score, conventional morphological categories or both. ROC, receiver operating characteristic.

consistently identified as being predictive of embryo ploidy (Reignier *et al.*, 2018; Kimelman *et al.*, 2019). Although morphologically normal blastocysts still run a significant risk of aneuploidy, the mean of the KIDScore D5^{TM} v3 values for euploid and aneuploid embryos was statistically different in our analysis. Nonetheless, the euploid embryo score did not contribute to implantation or live birth outcome. In this sense, our results demonstrate that the score tends to be higher for euploid embryos, which suggests that automatic embryo grading is more relevant for embryos that are not genetically tested and are prone to high rates of aneuploidy (i.e. those in conventional treatments with autologous oocytes). In fact, we found no relationship between embryo score and clinical outcomes in PGT-A treatments.

On the one hand, this fact could be related to the methodology used in the laboratory that involves assisted hatching of embryos on Day 3 of development. Therefore, the automatic annotations may be altered for blastulation time and for blastocyst morphology. On the other hand, the unsuccessful outcome after euploid embryo transfer may be more related to the stimulation protocol, the uterus or the patient herself, than to the embryo itself.

According to our results, the KIDScore D5™ algorithm offers advantages over conventional morphology assessment for embryo selection. Although the ORs obtained for the ASEBIR category were evidently higher than those for the automatic embryo score, this does not imply that the magnitude of the effect was superior, as the number of grades was different. In fact, the areas under the ROC curve were equal to or higher for models with automatic scoring than for models with conventional morphology in all the patient subpopulations (Fig. 3). We found that the automatic score was strongly associated with the ASEBIR category; however, when we combined the two variables only the automatic score remained in the final model for oocyte donation program and for conventional ICSI cycles. We believe that this was due to the added effect of the morphokinetic parameters considered in the KIDScore D5™ algorithm, in addition to the variables in common with conventional embryo evaluation (inner cell mass and trophectoderm quality). Nevertheless, when the data is combined under all treatments, there appears to be a weak correlation between ASEBIR category and implantation (Supplementary Table SVI): the lack of data contributing towards C grade embryos could be the reason. Although, when dividing the populations, the automatic embryo score was related to clinical outcomes in both donated oocytes (low percentage of C embryos, 9.0%) and conventional treatments (higher percentage of C embryos, 20.8%). In addition, conventional morphology was manually annotated by senior embryologists, which implies additional value of the automatic morphology. However, the correlation is so weak that when the sample size is reduced, it is no longer significant. Although the effect of morphology remains, as it is included in the KIDScore D5 variable. Recently, Ahlström *et al.* (2022), published an article concluding that time-lapse selection with this commercially available time-lapse model did not improve ongoing pregnancy when compared with selection by morphology alone. However, they considered three versions of the KIDScore D5 model together (i.e. three different algorithms whose variables are not identical) versus Gardner's morphological criterion. Being aware that the latest version (v3) of the KIDScore D5 considers blastulation time, ICM and trophectoderm quality, along with regularity and speed of cell divisions; the main power of improvement against the morphological criterion would be morphokinetics, which not surprisingly may have the least weight in the logistic regression. To our knowledge, the comparison with the second version of the model is even less relevant since it did not include the quality of the inner cell mass. In that case, KIDScore D5 v2 should be considered as an additional score to morphology instead of a substitute.

A major limitation of our study is its retrospective nature. A prospective randomized study would be needed to confirm the clinical relevance of KIDScore D5™ v3. Although ours is a large external validation with an unselected ICSI population, its single-center design should be taken into account when considering the universal application of the model. Also, specific culture conditions should be addressed when considering the generalized application of a prediction model. Our data reveal that both methods (conventional morphological grading and automatic embryo scoring) exhibit only poor performance, indicating that further work is required to improve embryo selection methods. The design of the comparison between the automated and the conventional grading systems may introduce bias to the study since the KIDScore D5™ value is a continuous outcome and ASEBIR's grading is a factorial outcome. Moreover, implantation and live birth rates are multifactorial, depending not only on the variables included in the logistic regression performed in this study but also on several clinical factors.

In conclusion, we endorse the clinical efficiency of the KIDScore D5 v3 model for automatically ranking embryos according to implantation and live birth potential. Furthermore, this model provides additional information that could quite conceivably improve consistency in embryo selection. This capacity was strictly observed only in those cycles where preimplantation genetic testing of embryos was not indicated. According to the preferences of each laboratory, this embryo scoring model can be user-dependent or user-independent, based on manual or automatic annotations. Despite observing similar AUCs to conventional embryo selection methodologies, the use of this automatic algorithm should improve workflow and allow embryologists to spend their time on other tasks. Therefore, automatic embryo scoring is a useful decision support tool for embryologists that does not compromise clinical outcomes.

Supplementary data

Supplementary data are available at *Human Reproduction* online.

Data availability

The data underlying this article will be shared on reasonable request to the corresponding author.

Acknowledgements

We acknowledge the contribution of the IVF laboratory staff at IVI-RMA Global Valencia for their clinical support.

Authors' roles

L.B. was responsible for carrying out the statistical analysis and the manuscript drafting. F.M. and M.A.V. were responsible for preparing data. A.G. and J.R. contributed to the study design and its execution. M.M. was responsible for coordinating the study and contributed to the analysis of the project.

Funding

This research has been funded by a grant from the Ministry of Science, Innovation and Universities FIS (PI21/00283) awarded to M.M.

Conflict of interest

Authors have none to declare.

References

Adolfsson E, Porath S, Andershed AN. External validation of a time-lapse model; a retrospective study comparing embryo evaluation

using a morphokinetic model to standard morphology with live birth as endpoint. *J Bras Reprod Assist* 2018;**22**:205–214.

Ahlström A, Lundin K, Lind A-K, Gunnarsson K, Westlander G, Park H, Thurin-Kjellberg A, Thorsteinsdottir SA, Einarsson S, Åström M *et al*. A double-blind randomized controlled trial investigating a time-lapse algorithm for selecting day 5 blastocysts for transfer. *Hum Reprod* 2022;**37**:708–717.

Amir H, Barbash-Hazan S, Kalma Y, Frumkin T, Malcov M, Samara N, Hasson J, Reches A, Azem F, Ben-Yosef D. Time-lapse imaging reveals delayed development of embryos carrying unbalanced chromosomal translocations. *J Assist Reprod Genet* 2019;**36**: 315–324.

Aparicio-Ruiz B, Basile N, Pérez Albalá S, Bronet F, Remohí J, Meseguer M. Automatic time-lapse instrument is superior to single-point morphology observation for selecting viable embryos: retrospective study in oocyte donation. *Fertil Steril* 2016;**106**: 1379–1385.

Azzarello A, Hoest T, Mikkelsen AL. The impact of pronuclei morphology and dynamicity on live birth outcome after time-lapse culture. *Hum Reprod* 2012;**27**:2649–2657.

Barberet J, Bruno C, Valot E, Antunes-Nunes C, Jonval L, Chammas J, Choux C, Ginod P, Sagot P, Soudry-Faure A *et al*. Can novel early non-invasive biomarkers of embryo quality be identified with time-lapse imaging to predict live birth? *Hum Reprod* 2019;**34**: 1439–1449.

Barrie A, Homburg R, McDowell G, Brown J, Kingsland C, Troup S. Examining the efficacy of six published time-lapse imaging embryo selection algorithms to predict implantation to demonstrate the need for the development of specific, in-house morphokinetic selection algorithms. *Fertil Steril* 2017;**107**:613–621.

Basile N, Vime P, Florensa M, Aparicio Ruiz B, García Velasco JA, Remohí J, Meseguer M. The use of morphokinetics as a predictor of implantation: a multicentric study to define and validate an algorithm for embryo selection. *Hum Reprod* 2015;**30**:276–283.

Bori L, Dominguez F, Fernandez EI, Gallego R, Del Alegre L, Hickman C, Quiñonero A, Nogueira MFG, Rocha JC, Meseguer M. An artificial intelligence model based on the proteomic profile of euploid embryos and time-lapse images: a preliminary study. *Reprod Biomed Online* 2020a;**42**:340–350.

Bori L, Meseguer F, Cerdá Alegre VM, Tejera L, Remohi A, Meseguer JM. A universal algorithm is available in last generation timelapse incubators: embryo score provided by the KIDScoreD5 is strongly correlated with chromosomal status and clinical outcomes. Abstr 36th Virtual Annu Meet ESHRE. *Hum Reprod* 2020b; **35**:i48–i49.

Campbell A, Fishel S, Bowman N, Duffy S, Sedler M, Hickman CFL. Modelling a risk classification of aneuploidy in human embryos using non-invasive morphokinetics. *Reprod Biomed Online* 2013;**26**: 477–485.

Cerrillo M, Herrero L, Guillén A, Mayoral M, García-Velasco JA. Impact of endometrial preparation protocols for frozen embryo transfer on live birth rates. *Rambam Maimonides Med J* 2017;**8**: e0020.

Chamayou S, Patrizio P, Storaci G, Tomaselli V, Alecci C, Ragolia C, Crescenzo C, Guglielmino A. The use of morphokinetic parameters to select all embryos with full capacity to implant. *J Assist Reprod Genet* 2013;**30**:703–710.

Conaghan J, Chen AA, Willman SP, Ivani K, Chenette PE, Boostanfar R, Baker VL, Adamson GD, Abusief ME, Gvakharia M *et al*. Improving embryo selection using a computer-automated time-lapse image analysis test plus day 3 morphology: results from a prospective multicenter trial. *Fertil Steril* 2013;**100**:412–419.

Coticchio G, Ezoe K, Lagalla C, Shimazaki K, Ohata K, Ninomiya M, Wakabayashi N, Okimura T, Uchiyama K, Kato K *et al*. Perturbations of morphogenesis at the compaction stage affect blastocyst implantation and live birth rates. *Hum Reprod* 2021;**36**: 918–928.

Cozzolino M, Franasiak J, Andrisani A, Ambrosini G, Vitagliano A. "Delayed start" gonadotropin-releasing hormone antagonist protocol in Bologna poor-responders: a systematic review and meta-analysis of randomized controlled trials. *Eur J Obstet Gynecol Reprod Biol* 2020;**244**:154–162.

Cruz M, Garrido N, Herrero J, Pérez-Cano I, Muñoz M, Meseguer M. Timing of cell division in human cleavage-stage embryos is linked with blastocyst formation and quality. *Reprod Biomed Online* 2012;**25**:371–381.

Dahdouh EM, Balayla J, García-Velasco JA. Impact of blastocyst biopsy and comprehensive chromosome screening technology on preimplantation genetic screening: a systematic review of randomized controlled trials. *Reprod Biomed Online* 2015;**30**:281–289.

Dal Canto M, Bartolacci A, Turchi D, Pignataro D, Lain M, Ponti E, De Brigante C, Mignini Renzini M, Buratini J. Faster fertilization and cleavage kinetics reflect competence to achieve a live birth after intracytoplasmic sperm injection, but this association fades with maternal age. *Fertil Steril* 2021;**115**:665–672.

Dal Canto M, Coticchio G, Mignini Renzini M, Ponti E, De Novara PV, Brambillasca F, Comi R, Fadini R. Cleavage kinetics analysis of human embryos predicts development to blastocyst and implantation. *Reprod Biomed Online* 2012;**25**:474–480.

Desai N, Goldberg JM, Austin C, Falcone T. Are cleavage anomalies, multinucleation, or specific cell cycle kinetics observed with time-lapse imaging predictive of embryo developmental capacity or ploidy? *Fertil Steril* 2018;**109**:665–674.

Desai N, Ploskonka S, Goodman L, Attaran M, Goldberg JM, Austin C, Falcone T. Delayed blastulation, multinucleation, and expansion grade are independently associated with live-birth rates in frozen blastocyst transfer cycles. *Fertil Steril* 2016;**106**:1370–1378.

ESHRE Working Group on Time-Lapse Technology, Apter S, Ebner T, Freour T, Guns Y, Kovacic B, Clef N, Le Marques M, Meseguer M, Montjean D *et al*. Good practice recommendations for the use of time-lapse technology. *Hum Reprod Open* 2020;**4**:hoz025.

Ferrick L, Shan Y, Lee L, Gardner DK. Metabolic activity of human blastocysts correlates with their morphokinetics, morphological grade, KIDScore and artificial intelligence ranking. *Hum Reprod* 2020;**35**:2004–2016.

Fishel S, Campbell A, Montgomery S, Smith R, Nice L, Duffy S, Jenner L, Berrisford K, Kellam L, Smith R *et al*. Live births after embryo selection using morphokinetics versus conventional morphology: a retrospective analysis. *Reprod Biomed Online* 2017;**35**: 407–416.

Fishel S, Campbell A, Montgomery S, Smith R, Nice L, Duffy S, Jenner L, Berrisford K, Kellam L, Smith R *et al*. Time-lapse imaging algorithms rank human preimplantation embryos according to the probability of live birth. *Reprod Biomed Online* 2018;**37**:304–313.

Fréour T, Fleuter N, Lammers J, Splingart C, Reignier A, Barriere P. External validation of a time-lapse prediction model. *Fertil Steril* 2015;**103**:917–922.

Gallego R, Del Remohí J, Meseguer M, Affiliations A, Valencia IG. Time-lapse imaging: the state of the art. *Biol Reprod* 2019;**101**: 1146–1154.

Gazzo E, Peña F, Valdéz F, Chung A, Bonomini C, Ascenzo M, Escudero E. The Kidscore TM D5 algorithm as an additional tool to morphological assessment and PGT-A in embryo selection: a time-lapse study. *J Bras Reprod Assist* 2020;**24**:55–60.

Goodman LR, Goldberg J, Falcone T, Austin C, Desai N. Does the addition of time-lapse morphokinetics in the selection of embryos for transfer improve pregnancy rates? A randomized controlled trial. *Fertil Steril* 2016;**105**:275–285.

Inoue T, Taguchi S, Uemura M, Tsujimoto Y, Miyazaki K, Yamashita Y. Migration speed of nucleolus precursor bodies in human male pronuclei: a novel parameter for predicting live birth. *J Assist Reprod Genet* 2021;**38**:1725–1736.

Irani M, Zaninovic N, Rosenwaks Z, Xu K. Does maternal age at retrieval influence the implantation potential of euploid blastocysts? *Am J Obstet Gynecol* 2019;**220**:379.e1–379.e7.

Kaser DJ, Farland LV, Missmer SA, Racowsky C. Prospective study of automated versus manual annotation of early time-lapse markers in the human preimplantation embryo. *Hum Reprod* 2017;**32**: 1604–1611.

Khosravi P, Kazemi E, Zhan Q, Malmsten JE, Toschi M, Zisimopoulos P, Sigaras A, Lavery S, Cooper LAD, Hickman C *et al.* Deep learning enables robust assessment and selection of human blastocysts after in vitro fertilization. *NPJ Digit Med* 2019;**2**:1–9.

Kimelman D, Confino R, Okeigwe I, Lambe-Steinmiller J, Confino E, Shulman LP, Zhang JX, Pavone ME. Assessing the impact of delayed blastulation using time lapse morphokinetics and preimplantation genetic testing in an IVF patient population. *J Assist Reprod Genet* 2019;**36**:1561–1569.

Kirkegaard K, Campbell A, Agerholm I, Bentin-Ley U, Gabrielsen A, Kirk J, Sayed S, Ingerslev HJ. Limitations of a time-lapse blastocyst prediction model: a large multicentre outcome analysis. *Reprod Biomed Online* 2014;**29**:156–158.

Kragh MF, Rimestad J, Berntsen J, Karstoft H. Automatic grading of human blastocysts from time-lapse imaging. *Comput Biol Med* 2019; **115**:103494.

Liu Y, Chapple V, Roberts P, Matson P. Prevalence, consequence, and significance of reverse cleavage by human embryos viewed with the use of the embryoscope time-lapse video system. *Fertil Steril* 2014;**102**:1295–1300.

Liu Y, Qi F, Matson P, Morbeck DE, Mol BW, Zhao S, Afnan M. Between-laboratory reproducibility of time-lapse embryo selection using qualitative and quantitative parameters: a systematic review and meta-analysis. *J Assist Reprod Genet* 2020;**37**:1295–1302.

Magli M, Gianaroli L, Ferraretti A, Lappi M, Ruberti A, Farfalli V. Embryo morphology and development are dependent on the chromosomal complement. *Fertil Steril* 2007;**87**:534–541.

Majumdar G, Majumdar A, Verma I, Upadhyaya K. Relationship between morphology, euploidy and implantation potential of cleavage and blastocyst stage embryos. *J Hum Reprod Sci* 2017;**10**:49–57.

Martínez-Granados L, Serrano M, González-Utor A, Ortíz N, Badajoz V, Olaya E, Prados N, Boada M, Castilla JA; on behalf of Special Interest Group in Quality of ASEBIR (Spanish Society for the Study of Reproductive Biology). Inter-laboratory agreement on embryo classification and clinical decision: conventional morphological assessment versus time lapse. *PLoS One* 2017;**12**:e0183328.

Meseguer M, Herrero J, Tejera A, Hilligsøe KM, Ramsing NB, Remoh J. The use of morphokinetics as a predictor of embryo implantation. *Hum Reprod* 2011;**26**:2658–2671.

Milewski R, Kuć P, Kuczyńska A, Stankiewicz B, Łukaszuk K, Kuczyński W. A predictive model for blastocyst formation based on morphokinetic parameters in time-lapse monitoring of embryo development. *J Assist Reprod Genet* 2015;**32**:571–579.

Minasi MG, Colasante A, Riccio T, Ruberti A, Casciani V, Scarselli F, Spinella F, Fiorentino F, Varricchio MT, Greco E. Correlation between aneuploidy, standard morphology evaluation and morphokinetic development in 1730 biopsied blastocysts: a consecutive case series study. *Hum Reprod* 2016;**31**:2245–2254.

Mizobe Y, Oya N, Iwakiri R, Yoshida N, Sato Y, Miyoshi K, Tokunaga M, Ezono Y. Effects of early cleavage patterns of human embryos on subsequent in vitro development and implantation. *Fertil Steril* 2016;**106**:348–353.

Motato Y, de los Santos MJ, Escriba MJ, Ruiz BA, Remohí J, Meseguer M. Morphokinetic analysis and embryonic prediction for blastocyst formation through an integrated time-lapse system. *Fertil Steril* 2016;**105**:376–384.

Petersen BM, Boel M, Montag M, Gardner DK. Development of a generally applicable morphokinetic algorithm capable of predicting the implantation potential of embryos transferred on day 3. *Hum Reprod* 2016;**31**:2231–2244.

Reignier A, Girard J-M, Lammers J, Chtourou S, Lefebvre T, Barriere P, Freour T. Performance of Day 5 KIDScore™ morphokinetic prediction models of implantation and live birth after single blastocyst transfer. *J Assist Reprod Genet* 2019;**36**:2279–2285.

Reignier A, Lammers J, Barriere P, Freour T. Can time-lapse parameters predict embryo ploidy? A systematic review. *Reprod Biomed Online* 2018;**36**:380–387.

Rienzi L, Cimadomo D, Delgado A, Minasi MG, Fabozzi G, Gallego RD, Stoppa M, Bellver J, Giancani A, Esbert M *et al.* Time of morulation and trophectoderm quality are predictors of a live birth after euploid blastocyst transfer: a multicenter study. *Fertil Steril* 2019; **112**:1080–1093.e1.

Rubio I, Kuhlmann R, Agerholm I, Kirk J, Herrero J. Limited implantation success of direct-cleaved human zygotes: a time-lapse study. *Fertil Steril* 2012;**98**:11–15.

Sundvall L, Ingerslev HJ, Breth Knudsen U, Kirkegaard K. Inter- and intra-observer variability of time-lapse annotations. *Hum Reprod* 2013;**28**:3215–3221.

Tran D, Cooke S, Illingworth PJ, Gardner DK. Deep learning as a predictive tool for fetal heart pregnancy following time-lapse incubation and blastocyst transfer. *Hum Reprod* 2019;**34**:1011–1018.

VerMilyea MD, Tan L, Anthony JT, Conaghan J, Ivani K, Gvakharia M, Boostanfar R, Baker VL, Suraj V, Chen AA *et al.* Computer-automated time-lapse analysis results correlate with embryo implantation and clinical pregnancy: a blinded, multi-centre study. *Reprod Biomed Online* 2014;**29**:729–736.

Wong CC, Loewke KE, Bossert NL, Behr B, Jonge CJ, De Baer TM, Pera RAR. Non-invasive imaging of human embryos before

embryonic genome activation predicts development to the blastocyst stage. *Nat Biotechnol* 2010;**28**:1115–1121.

Wu L, Han W, Zhang X, Wang J, Liu W, Xiong S, Huang G. A retrospective analysis of morphokinetic parameters according to the implantation outcome of IVF treatment. *Eur J Obstet Gynecol Reprod Biol* 2016;**197**:186–190.

Zaninovic N, Irani M, Meseguer M. Assessment of embryo morphology and developmental dynamics by time-lapse microscopy: is there a relation to implantation and ploidy? *Fertil Steril* 2017;**108**:722–729.

Zhan Q, Ph D, Sierra ET, Ph D, Malmsten J, Ph D, Ye Z. Blastocyst score, a blastocyst quality ranking tool, is a predictor of blastocyst ploidy and implantation potential. *FS Rep* 2020;**1**:133–141.

Human Reproduction, pp. 1–1, 2022
https://doi.org/10.1093/humrep/deac066

human reproduction

SUPPLEMENTARY DATA

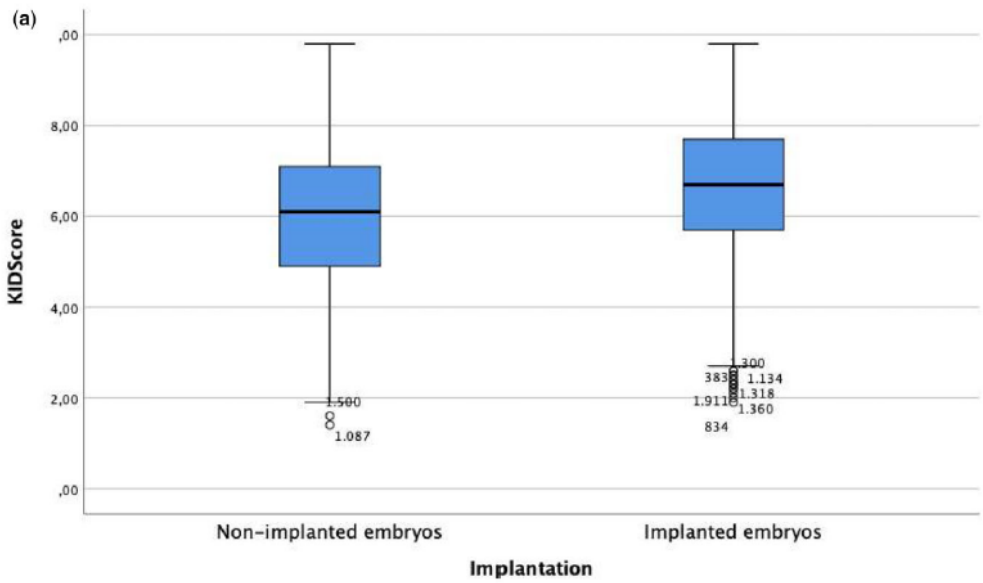

Supplementary Figure S1. Distribution of automatically scored embryos according to two outcomes. (**a**) Implantation success, (**b**) live birth.

Human Reproduction, pp. 1–1, 2022
https://doi.org/10.1093/humrep/deac066

human reproduction

SUPPLEMENTARY DATA

Supplementary Table SI Categories and characteristics of embryonic inner cell mass according to ASEBIR criteria 2015.

Category	Inner cell mass size (μm^2)	Cohesion
A	3800–1900	Compact
B	3800–1900	Non compact
C	<1900	
D	Degeneration signs	Indifferent
Excluded	Degenerated	

Human Reproduction, pp. 1–1, 2022
https://doi.org/10.1093/humrep/deac066

human reproduction

SUPPLEMENTARY DATA

Supplementary Table SII Categories and characteristics of the trophectoderm according to ASEBIR criteria 2015.

Category	Trophectoderm description
A	Homogeneous, united and full of cells
B	Homogeneous, less cells
C	Few cells
D	Degeneration signs
Excluded	Degenerated

Human Reproduction, pp. 1–1, 2022
https://doi.org/10.1093/humrep/deac066

human reproduction

SUPPLEMENTARY DATA

Supplementary Table SIII Embryo classification on Day 5 of development, according to ASEBIR criteria 2015, based on expansion grade, inner cell mass (ICM) and trophectoderm quality.

D + 5			
Expansion grade	**ICM**	**Trophectoderm**	**ASEBIR**
Since 'starting expansion' Up to 'hatched'	A	A	A
		B	B
		C	C
		D	D
	B	A	A
		B	B
		C	C
		D	D
	C	A	A
		B	B
		C	C
		D	D
	D	A, B, C or D	D
Early blastocyst (Thick pellucid zone)			C
Morula		Excluded	

Human Reproduction, pp. 1–1, 2022
https://doi.org/10.1093/humrep/deac066

human reproduction

SUPPLEMENTARY DATA

Supplementary Table SIV Embryo classification on Day 6 of development, according to ASEBIR criteria 2015, based on expansion grade, inner cell mass (ICM) and trophectoderm quality.

D + 6			
Expansion grade	**ICM**	**Trophectoderm**	**ASEBIR**
Since 'starting expansion' Up to 'hatched'	A	A	B
		B	
		C	C
		D	D
	B	A	B
		B	
		C	C
		D	D
	C	A	B
		B	
		C	C
		D	D
	D	A, B, C or D	D
Early blastocyst (Thick pellucid zone)			D
Morula		Excluded	

Human Reproduction, pp. 1–1, 2022
https://doi.org/10.1093/humrep/deac066

human reproduction

SUPPLEMENTARY DATA

Supplementary Table SV Multivariate analysis for implantation and live birth outcome in different patient populations, including automatic embryo score by quartiles.

	Implantation			Live birth		
	OR*	95% CI	*P*-value	OR*	95% CI	*P*-value
All treatments (n = 1952 SETs)						
KIDScore D5 v3 Quartile 2 vs. 1	1.656	[1.288–2.128]	<0.001	1.638	[1.265–2.121]	<0.001
KIDScore D5 v3 Quartile 3 vs. 1	1.989	[1.544–2.562]	<0.001	2.141	[1.655–2.770]	<0.001
KIDScore D5 v3 Quartile 4 vs. 1	2.917	[2.245–3.791]	<0.001	2.946	[2.267–3.829]	<0.001
PGT-A tested (15.7%) vs. non-tested (84.3%)	1.402	[1.080–1.820]	0.011	1.533	[1.178–1.994]	0.001
Embryo transfer fresh (46.5%) vs. frozen (53.5%)	0.714	[0.582–0.877]	0.001	0.661	[0.538–0.813]	<0.001
BMI	–	–	–	0.969	[0.947–0.991]	0.005
Oocyte donation program (n = 1165 SETs)						
KIDScore D5 v3 Quartile 2 vs. 1	1.592	[1.125–2.252]	0.009	1.623	[1.135–2.321]	0.008
KIDScore D5 v3 Quartile 3 vs. 1	1.891	[1.331–2.688]	<0.001	2.160	[1.509–3.092]	<0.001
KIDScore D5 v3 Quartile 4 vs. 1	2.709	[1.926–3.810]	<0.001	2.584	[1.832–3.644]	<0.001
Embryo transfer fresh (54.7%) vs. frozen (45.3%)	0.675	[0.530–0.859]	0.001	0.605	[0.476–0.770]	<0.001
BMI	0.970	[0.944–0.997]	0.028	0.966	[0.940–0.993]	0.014
Autologous oocytes, non-PGT-A (n = 480 SETs)						
KIDScore D5 v3 Quartile 2 vs. 1	2.538	[1.577–4.085]	<0.001	2.237	[1.340–3.735]	0.002
KIDScore D5 v3 Quartile 3 vs. 1	3.000	[1.791–5.025]	<0.001	3.522	[2.044–6.068]	<0.001
KIDScore D5 v3 Quartile 4 vs. 1	4.325	[2.495–7.497]	<0.001	5.495	[3.113–9.701]	<0.001
Oocyte age	–	–	–	0.911	[0.854–0.972]	0.005

OR, odds ratio; PGT-A, preimplantation genetic testing for aneuploidy; SET, single embryo transfer.
*ORs computed from stepwise multivariate logistic regression.
KIDScore D5 v3 Quartile 1= embryo score ≤ 5.4; KIDScore D5 v3 Quartile 2= embryo score 5.5–6.4; KIDScore D5 v3 Quartile 3= embryo score 6.5–7.4; KIDScore D5 v3 Quartile 4= embryo score ≥7.5.
– Variables not considered by the model.

Human Reproduction, pp. 1–1, 2022
https://doi.org/10.1093/humrep/deac066

human reproduction

SUPPLEMENTARY DATA

Supplementary Table SVI **Multivariate analysis of both grading methodologies (conventional morphological categories + automatic embryo score) with respect to implantation and live birth outcome in different patient populations.**

	Implantation			Live birth		
	OR[a]	95% CI	*P*-value	OR[a]	95% CI	*P*-value
All treatments (n = 1952 SETs)						
Automatic embryo score	1.175	[1.074–1.286]	<0.001	1.288	[1.215–1.364]	<0.001
Conventional morphology A-embryos (19.6%) vs. C-embryos (14.3%)	1.970	[1.160–3.347]	0.012	–	–	–
Conventional morphology B-embryos (66.0%) vs. C-embryos (14.3%)	1.489	[1.056–2.098]	0.023	–	–	–
PGT-A Tested (15.7%) vs. non-tested (84.3%)	1.469	[1.128–1.912]	0.004	1.544	[1.189–2.006]	0.001
Embryo transfer fresh (46.5%) vs. frozen (53.5%)	1.387	[1.129–1.703]	0.002	1.510	[1.228–1.857]	<0.001
BMI	–	–	–	0.968	[0.947–0.990]	0.005
Oocyte donation program (n = 1165 SETs)						
Automatic embryo score	1.285	[1.189–1.390]	<0.001	1.260	[1.166–1.362]	<0.001
Embryo transfer fresh (54.7%) vs. frozen (45.3%)	1.451	[1.139–1.848]	0.003	1.642	[1.291–2.088]	<0.001
BMI	0.970	[0.944–0.997]	0.029	0.966	[0.940–0.993]	0.014
Autologous oocytes, non-PGT-A (n = 480 SETs)						
Automatic embryo score	1.381	[1.236–1.543]	<0.001	1.465	[1.298–1.653]	<0.001
Oocyte age	–	–	–	0.909	[0.853–0.969]	0.003

OR, odds ratio; PGT-A, preimplantation genetic testing for aneuploidy; SET, single embryo transfer.
[a]ORs computed from stepwise multivariate logistic regression.
– Variables not considered by the model.

Artículos como coautora no incluidos en esta tesis

I. Soler C, Contell J, **Bori L**, Sancho M, García-Molina A, Valverde A, Segarvall J. Sperm kinematic, head morphometric and kinetic-morphometric subpopulations in the blue fox (Alopex lagopus). Asian J Androl. 2017 Mar-Apr;19(2):154-159. doi: 10.4103/1008-682X.188445. PMID: 27751987; PMCID: PMC5312211.

II. Rodrigo L, Meseguer M, Mateu E, Mercader A, Peinado V, **Bori L**, Campos-Galindo I, Milán M, García-Herrero S, Simón C, Rubio C. Sperm chromosomal abnormalities and their contribution to human embryo aneuploidy. Biol Reprod. 2019 Dec 24;101(6):1091-1101. doi: 10.1093/biolre/ioz125. PMID: 31318411.

III. Alegre L, Del Gallego R, **Bori L**, Loewke K, Maddah M, Aparicio-Ruiz B, Palma-Govea AP, Marcos J, Meseguer M. Assessment of embryo implantation potential with a cloud-based automatic software. Reprod Biomed Online. 2021 Jan;42(1):66-74. doi: 10.1016/j.rbmo.2020.09.032. Epub 2020 Oct 10. PMID: 33189576.

IV. Payá E, **Bori L**, Colomer A, Meseguer M, Naranjo V. Automatic characterization of human embryos at day 4 post-insemination from time-lapse imaging using supervised contrastive learning and inductive transfer learning techniques. Comput Methods Programs Biomed. 2022 Jun; 221:106895. doi: 10.1016/j.cmpb.2022.106895. Epub 2022 May 16. PMID: 35609359.

V. Valera MÁ, Albert C, Marcos J, Larreategui Z, **Bori L**, Meseguer M. A propensity score-based, comparative study assessing humid and dry time-lapse incubation, with single-step medium, on embryo development and clinical outcomes. Hum Reprod. 2022 Aug 25;37(9):1980-1993. doi: 10.1093/humrep/deac165. PMID: 35904473.

CAPÍTULO 1: Introducción

1.1 Técnicas de reproducción asistida (TRA).

1.1.1 Hitos en la historia de la reproducción humana asistida.

La posibilidad de realizar tratamientos médicos con el objetivo de obtener descendencia causaba interés entre la sociedad desde hace siglos. Sin embargo, la carencia de determinadas herramientas elementales impedía el conocimiento en este sentido. Por ello, no se determinó la existencia de los gametos masculinos (espermatozoides) ni femeninos (óvulos, ovocitos u oocitos), como responsables del proceso reproductivo, hasta el desarrollo del microscopio óptico.

Las primeras técnicas de reproducción humana asistida empezaron cerca del siglo XIX, aunque existe la posibilidad de que se realizaran anteriormente y no se hubieran descrito por la dificultad para reconocer públicamente este tipo de actividades en aquella época. El primer relato publicado de una inseminación artificial humana realizada por un médico fue un tratamiento realizado el 5 de junio de 1838 en Francia por el Dr. Girault. (L'Abeille Medicale, volumen 25, páginas 409-17; citado en Poynter, 1968). La primera publicación acerca de una inseminación con semen de donante fue hecha por el italiano Paolo Mantegazza en 1887 (Clarke, 2006). En lo que a la crioconservación se refiere, los primeros nacimientos humanos resultantes de la inseminación artificial con semen criopreservado fueron comunicados por Bunge y Sherman en 1953 (Sherman, 1976).

El primer éxito publicado del proceso de fecundación in vitro (FIV) en humanos fue llevado a cabo por Edwards y colaboradores en 1969, quiénes observaron la formación de pronúcleos en los ovocitos (Edwards *et al.*, 1969). En 1970 consiguieron desarrollar embriones hasta 16 células (Edwards *et al.*, 1970), y en 1978 reportaron el primer nacimiento en el mundo de un “bebe probeta” (Steptoe and Edwards, 1978). Seis años más tarde, se describieron los dos primeros embarazos resultantes de la transferencia de embriones humanos criopreservados (Zeilmaker *et al.*, 1984).

En 1992 se lograron los primeros embarazos mediante la micromanipulación de gametos, inyectando espermatozoides dentro de óvulos (Palermo *et al.*, 1992b). En cuanto al análisis genético, el primer diagnóstico preimplantacional fue llevado a cabo en 1990 para determinar el sexo (Handyside *et al.*, 1990) y en 1992 para descartar embriones portadores de fibrosis quística (Handyside *et al.*, 1992). Un año más tarde fue publicado otro hito para tratar los casos severos de infertilidad masculina, se realizaron las primeras biopsias de testículo por parte del Dr. Silber (Silber *et al.*, 1994).

1.1.2 Inseminación artificial.

La inseminación artificial se define como el depósito de forma no natural de espermatozoides en el útero femenino. Normalmente, suele ser la primera línea de tratamiento frente a la infertilidad. Siempre tras un estudio previo a la pareja, en el que se demuestra que no tienen motivos más severos de infertilidad que contraindiquen ser tratados mediante esta técnica.

Por un lado, el procedimiento habitual implica una estimulación ovárica suave para evitar el desarrollo folicular múltiple. Además, durante el ciclo se realizan controles ecográficos y analíticas de estradiol. Por otro lado, el día de la inseminación se procesa la muestra de semen en el laboratorio mediante una técnica conocida como capacitación.

1.1.3 Fecundación in vitro (FIV).

El procedimiento de fecundación in vitro implica la inseminación del óvulo fuera del cuerpo femenino, en el laboratorio de FIV. Esta metodología empieza con la obtención de los gametos femeninos por punción (o aspiración) folicular. Se utiliza un transductor vaginal que lleva acoplada una aguja, especialmente diseñada para perforar los folículos del ovario y aspirar el líquido folicular junto con el óvulo de su interior.

Los ovocitos pueden ser inseminados con distintas técnicas. La diferencia entre la inseminación convencional y el resto de las técnicas es el grado de contribución a la fecundación y la complejidad. La FIV convencional consiste en la incubación

conjunta de ovocitos y espermatozoides facilitando el proceso de la interacción entre los gametos (Edwards *et al.*, 1969). Debido al fracaso de esta técnica en casos de factor masculino grave, se empezaron a utilizar otros métodos que exigían mayor manipulación del ovocito para facilitar su fusión con los espermatozoides. Se desarrollaron varias técnicas de inseminación, tales como la perforación parcial de la zona pelúcida (PZD) (Gordon *et al.*, 1988), la inseminación subzonal (SUZI) (Palermo *et al.*, 1992a) o la inyección intracitoplasmática (ICSI) (Palermo *et al.*, 1992b). La PZD consistía en la creación de un orificio pequeño en la zona pelúcida, mediante un procedimiento mecánico o químico. La SUZI implicaba la inyección de espermatozoides dentro del espacio perivitelino. La ICSI consiste en la introducción de un espermatozoide dentro del óvulo mediante un micromanipulador. Esta última técnica supuso una revolución para el tratamiento del factor masculino severo, ya que sólo requiere un espermatozoide vivo por ovocito.

Desde 1997 hasta 2017, el Consorcio europeo de fecundación in vitro (EIM) de la Sociedad Europea de Reproducción Humana y Embriología ha registrado más de 10 millones de tratamientos (10.713.407) que han dado lugar al nacimiento de más de 2 millones de bebés (Wyns *et al.*, 2017). La mayoría de los tratamientos notificados a la EIM se realizaron mediante inyección intracitoplasmática de espermatozoides y posterior cultivo de embriones in vitro. La selección del embrión más adecuado para transferencia de toda una cohorte es un factor relevante para el éxito de un tratamiento de infertilidad.

1.2 Selección de embriones en tratamientos de FIV.

Los ovocitos inseminados y subsiguientes embriones se incuban en el laboratorio de FIV, emulando las condiciones del tracto femenino, hasta el momento óptimo para su transferencia al útero materno. Los medios de cultivo ofrecen la capacidad de sustentar el ambiente idóneo para conseguir la fecundación de los ovocitos y

permitir el desarrollo de los embriones hasta su transferencia. Los embriones deben ser evaluados durante su crecimiento para decidir su destino. Al finalizar el cultivo in vitro los embriólogos seleccionan qué embriones transferir, criopreservar o descartar.

1.2.1 Métodos no invasivos.

Morfología convencional

La morfología ha sido el criterio por excelencia para evaluar el desarrollo del embrión desde el principio de la práctica de la FIV (Edwards *et al.*, 1984). La evaluación convencional de los preembriones in vitro se suele realizar bajo un microscopio óptico a 400 aumentos para observar características morfológicas, tales como el conteo del número de células o blastómeros, el nivel de fragmentación o la multinucleación (Baczowski *et al.*, 2004).

En España, el criterio más utilizado es el descrito por ASEBIR (Asociación para el estudio de la biología de la reproducción) (Cuevas *et al.*, 2018). Los criterios ASEBIR de valoración morfológica de oocitos, embriones tempranos y blastocistos humanos proponen la gradación en los distintos días de desarrollo embrionario (ASEBIR, 2015). Aunque consta literalmente que "la decisión clínica sobre el destino de un embrión de determinada categoría pertenece exclusivamente al laboratorio". Para el sistema de gradación se emplearon 4 categorías divididas en función del potencial de implantación esperado:

Categoría A: embrión de óptima calidad con máxima capacidad de implantación.

Categoría B: embrión de buena calidad con elevada capacidad de implantación.

Categoría C: embrión regular con una probabilidad de implantación media.

Categoría D: embrión de mala calidad con una probabilidad de implantación baja o nula.

Durante el estadio de división celular, se propone la observación de los blastómeros en el segundo (D+2) y tercer día (D+3) de desarrollo (Figura 1, anexo). En el cuarto

día de desarrollo (D+4) se observa la adhesión celular y la compactación (Figura 2, anexo). Finalmente, en el quinto (D+5) (Figura 3, anexo) y sexto día (D+6) (Figura 4, anexo) del desarrollo embrionario se evalúa la estructura del blastocisto, considerando la expansión del blastocele, el grosor de la zona pelúcida, el trofoectodermo (TE) y la masa celular interna (MCI) (Figura 5 y 6, anexo). Se considera que un embrión incubado in vitro con buen pronóstico de implantación alcanza el estadio de blastocisto en D+5 o D+6 y su observación debe realizarse en el intervalo recomendado: 114-118h postinseminación para D+5 y 136-140h postinseminación para D+6. El grado de expansión permite la distinción entre blastocisto cavitado (BC), blastocisto temprano (BT), blastocisto expandido (BE), blastocisto eclosionando (BHi) y blastocisto eclosionado (BH). La MCI se evalúa en función de su tamaño y cohesión de las células; y la calidad del TE varía según el número de células, su homogeneidad y cohesión.

La clasificación morfológica convencional sigue siendo hoy en día el estándar de referencia. Sin embargo, sólo el 30% de las transferencias de embriones dan lugar a un embarazo en curso (Kupka *et al.*, 2014). Además, la tasa de gestación múltiple asociada a los tratamientos de FIV sigue siendo elevada, debido a las transferencias de más de un embrión para conservar o aumentar las tasas de embarazo. Aunque las gestaciones múltiples conllevan riesgos maternos y neonatales (Committee and Society, 2012; Norwitz *et al.*, 2005). Las principales limitaciones de esta metodología de evaluación están asociadas tanto a la subjetividad del embriólogo (Ferraretti *et al.*, 2012), como a la evaluación en sí misma. Dado que, aunque el incubador ofrece condiciones óptimas de cultivo, las concentraciones y la temperatura de los gases se alteran al sacar los embriones de la incubadora (Zhang *et al.*, 2010). Por este motivo, los embriones se evalúan en periodos de tiempo limitados y se pierde mucha información entre las observaciones (Cruz *et al.*, 2012). De hecho, ha sido reportado que el estadio y la clasificación del embrión puede variar en pocas horas (Kirkegaard, Agerholm, *et al.*, 2012; Montag *et al.*, 2011), lo que podría dar lugar a una selección de embriones no satisfactoria.

Sistemas *time-lapse* y parámetros morfocinéticos

La introducción de incubadoras con sistemas de lapso de tiempo o *time-lapse* (TL) en los laboratorios de FIV permitió la monitorización continua del crecimiento del embrión en tiempo real. Esta tecnología se ha convertido en una herramienta útil para estudiar el desarrollo dinámico del embrión sin alterar las condiciones de cultivo. Además, ofrece información objetiva y precisa de forma cualitativa y cuantitativa (Aparicio *et al.*, 2013). La determinación de los parámetros morfocinéticos del desarrollo embrionario fue de la mano de la introducción de la tecnología *time-lapse* en los laboratorios de FIV. La combinación de parámetros morfológicos y morfocinéticos ha dado lugar a la creación de varios algoritmos para explorar variables relevantes en la selección de embriones (Cruz *et al.*, 2012; Dal Canto *et al.*, 2012; Meseguer *et al.*, 2011; Motato *et al.*, 2016).

Las anotaciones manuales de parámetros cuantitativos y cualitativos han sido propuestas para predecir la formación de blastocistos, el potencial de implantación o incluso el nacimiento vivo. La escisión temprana (Milewski *et al.*, 2015) y el tiempo de formación de la mórula (Motato *et al.*, 2016) se han utilizado para predecir la formación de blastocistos. Según la revisión acerca de la tecnología *time-lapse* realizada por del Gallego et al., 2019, la duración del segundo ciclo celular, el tiempo de división a cinco células, la segunda sincronía (el intervalo de tiempo entre división de tres a cuatro células) y el tiempo de desvanecimiento de los pronúcleos son los parámetros que más influyen en el potencial de implantación del embrión (Goodman *et al.*, 2016; Meseguer *et al.*, 2011; Petersen *et al.*, 2016; Vermilyea *et al.*, 2014). Los eventos del desarrollo embrionario tardío (por ejemplo, el inicio de la blastulación, el tiempo de formación de la mórula o la calidad del trofoectodermo) se han descrito como los predictores más fiables de recién nacidos vivos (Fishel *et al.*, 2017, 2018; Rienzi *et al.*, 2019). Además, patrones de división anormales, multinucleación, fragmentación, o colapso son algunos de los parámetros considerados de mal pronóstico para clasificar la calidad del embrión (Zaninovic *et al.*, 2017). Estos eventos han sido asociados con formación inadecuada de blastocistos (Wirka *et al.*, 2014), baja tasa de euploidía (Zhan *et al.*, 2016) y bajas tasas de implantación y de recién nacidos vivos (Aguilar

et al., 2016; Azzarello *et al.*, 2017; Desai *et al.*, 2014, 2016; Desch *et al.*, 2017; Ebner *et al.*, 2017; Goodman *et al.*, 2016; Rubio *et al.*, 2012; Zhan *et al.*, 2016).

El principal obstáculo para generalizar el uso de los algoritmos de evaluación y selección embrionaria es la falta de reproducibilidad (Barrie *et al.*, 2017; Fréour *et al.*, 2015). Se han descrito posibles factores de confusión que podrían afectar al rendimiento de los algoritmos de sistemas TL: el entorno y las técnicas utilizadas en cada laboratorio, las características de los pacientes, y/o la subjetividad de las anotaciones manuales (ESHRE Working group on time-lapse technology *et al.*, 2020; Martínez-Granados *et al.*, 2017; Sundvall *et al.*, 2013).

Mediciones en medio de cultivo: secretoma embrionario

Años más tarde surgieron nuevos métodos no invasivos para evaluar la viabilidad del embrión y mejorar los resultados clínicos basados en las ciencias "-ómicas", como la metabolómica y la proteómica (Krisher *et al.*, 2015). Actualmente, existe evidencia científica de la importancia de los ligandos y receptores solubles tanto en el embrión como en el tracto reproductor femenino durante la fase de preimplantación embrionaria (Thouas *et al.*, 2015). Este grupo de proteínas secretadas o metabolizadas por el embrión se conoce como secretoma (Hathout, 2007). Por tanto, el medio de cultivo en el que se desarrollan los embriones es una fuente de información sobre el estado proteico y metabólico de éstos (Hollywood *et al.*, 2006).

Hace treinta años, la primera evidencia del secretoma embrionario fue el factor activador de plaquetas analizado en el medio de cultivo (Punjabi *et al.*, 1990). Desde entonces, se han identificado varias proteínas durante la fase preimplantatoria, como el IFN-α2 (interferón-α2; Jones et al., 1992), la SP1 (glicoproteína P-1 específica del embarazo; Saith et al., 1994), el HLA-G (antígeno leucocitario humano G; Noci et al., 2005), la Apo-A1 (apolipoproteína A1; Mains et al., 2011), la HCG (gonadotropina coriónica humana; Butler et al., 2013) y el GM-CSF (factor estimulante de colonias de granulocitos y macrófagos; Ziebe et al., 2013). La sensibilidad de los métodos de análisis ha mejorado notablemente,

permitiendo el estudio simultáneo de múltiples proteínas (por ejemplo, mediante técnicas de espectrometría de masas o de microarrays). Dicha evolución ha determinado la asociación entre los patrones de expresión proteica y la morfología del embrión (Katz-Jaffe and Gardner, 2007; Katz-jaffe and Mcreynolds, 2013).

El análisis del medio de cultivo embrionario ha revelado la secreción y el consumo de varias proteínas por parte del embrión. El aumento en el medio de cultivo de TNF (factor de necrosis tumoral) R1, IL (interleucina) 10, IL-6 VEGFA (factor de crecimiento endotelial vascular endotelial vascular A), EMMPRIN (inductor de inductor de la metaloproteinasa de la matriz), PLGF (factor de crecimiento placentario), EpCAM (molécula de adhesión de células epiteliales), caspasa-3, HE-4 (proteína 4 del epidídimo humano) e IL-6 sugiere que el embrión ha secretado esas proteínas (Dominguez *et al.*, 2008, 2015; Lindgren *et al.*, 2018). Del mismo modo, una disminución de CXCL (ligando de quimioquinas con motivo C-X-C) 13, SCF (factor de células madre), TRAIL-R3 (receptor para el ligando citotóxico TRAIL), MIP-1β (proteína inflamatoria de macrófagos-1β) y MSP-α (proteína estimulante de macrófagos-α) en el medio de cultivo sugiere que el embrión ha consumido o metabolizado esas proteínas (Dominguez *et al.*, 2008). Además, se han observado distintos patrones de expresión proteica según la calidad del embrión y su potencial de implantación. Los embriones que implantaron consumieron más CXCL13 y GM-CSF que los no implantados (Dominguez *et al.*, 2010; Robertson, 2007). Además, el medio de cultivo de blastocistos mostró mayores concentraciones de EMMPRIN que las muestras de embriones arrestados en estadios tempranos. En cuanto a la calidad de los embriones en D+5 o D+6, se han reportado mayores concentraciones de caspasa-3 en el medio de cultivo de blastocistos de buena calidad (Lindgren *et al.*, 2018).

1.2.2 Métodos invasivos

Se presume que la transferencia de embriones cromosómicamente anormales al endometrio es la principal causa de aborto tras los tratamientos de FIV (van den Berg *et al.*, 2012; Ljunger *et al.*, 2005; Martínez *et al.*, 2010). La evaluación genética de los embriones preimplantatorios previene la transmisión de

enfermedades monogénicas (test genético preimplantatorio para enfermedades monogénicas: PGT-M) antes de la transferencia y permite identificar los embriones cromosómicamente normales de cada cohorte materna (test genético preimplantatorio para aneuploidías: PGT-A). En este sentido, muchas familias han aprovechado los métodos de PGT para conseguir nacimientos sanos (De Rycke et al., 2017).

En los últimos treinta años, se han desarrollado diversos métodos para analizar genéticamente los embriones y deducir su estado de viabilidad. Por ejemplo, el análisis cromosómico a partir de la biopsia del cuerpo polar es un método propuesto de PGT, pero no proporciona información sobre la contribución del espermatozoide al perfil genético del embrión. Durante las primeras fases de las pruebas PGT, la metodología por excelencia implicaba la extracción de uno o dos blastómeros del embrión en división. Sin embargo, esta práctica se ha asociado a una importante reducción del potencial de implantación (Scott, Upham, Forman, Zhao, *et al.*, 2013) y a una elevada tasa de errores de diagnóstico (Fragouli *et al.*, 2019; Piyamongkol *et al.*, 2003). La introducción del cultivo extendido de embriones permitió el análisis genético de las células del trofoectodermo, tomadas por biopsia directa del trofoectodermo en el día 5 o 6 del desarrollo del embrión. Dado que los blastocistos son menos vulnerables que los embriones en división se pueden biopsiar más células para su evaluación sin comprometer la viabilidad. Por tanto, es probable que se reduzcan los errores de diagnóstico debidos al mosaicismo (Fragouli *et al.*, 2017; Kokkali *et al.*, 2007; Scott, Upham, Forman, Hong, *et al.*, 2013). En la actualidad, la gran mayoría de los procedimientos de PGT se realizan con células de trofoectodermo biopsiadas. Sin embargo, la extracción de material genético ya sea del ovocito, del cigoto o del embrión ha implicado el uso de equipos especializados y técnicas invasivas para realizar el procedimiento de biopsia. Además, el procedimiento debe ser realizado por profesionales altamente capacitados para garantizar la viabilidad de los embriones (Cohen *et al.*, 2007; Kirkegaard, Hindkjaer, *et al.*, 2012; Levin *et al.*, 2012; Neal *et al.*, 2017).

1.3 Inteligencia artificial (IA) aplicada a medicina reproductiva.

1.3.1 Aspectos generales.

La inteligencia artificial (IA) se define como la capacidad de un sistema computacional para aprender y ejercer un comportamiento inteligente (Simopoulou *et al.*, 2018). Las primeras evidencias de IA en el área de medicina se registraron en la década del 1960, con los clasificadores bayesianos. Las técnicas asociadas a la IA han evolucionado a lo largo de los años en dirección al *deep learning* (aprendizaje profundo). El aprendizaje simbólico, mediante *decision trees* (árboles de decisión) o el *machine learning* (aprendizaje automático), han formado parte del progreso de los sistemas computacionales en el campo de la embriología.

Clasificadores Bayesianos

Los clasificadores bayesianos simples, son métodos estadísticos clásicos y supervisados basados en el Teorema de Bayes o teorema de la probabilidad condicionada. Se trata de prever la probabilidad de que ocurra un evento "A" dada una información "B", calculándola al revés (Dale, 2005). La limitación, es la suposición de independencia de cada condicionante propuesto como información "B". Un ejemplo, es el uso de clasificadores bayesianos para la selección embrionaria: el evento "A" sería el embarazo (Si o No) y la información de grosor de la zona pelúcida, grado de fragmentación, multinucleación y tamaño de blastómeros se representaría como "B" (Morales *et al.*, 2007).

Árboles de decisión

Los árboles de decisión son algoritmos de aprendizaje supervisado que crean diagramas de construcciones lógicas a partir de una base de datos. Los nodos son las variables de entrada, las ramas representan los posibles valores de las variables de entrada y las hojas son los posibles valores de la variable de salida. Un ejemplo, es el uso de árboles de decisión para prever la probabilidad de embarazo ectópico: la variable salida sería el embarazo ectópico (si o no), los

nodos serían la hormona gonadotropina coriónica (hCG), una kisspeptina (KiSS) y un microRNA (miR-324-3p) y las ramas, corresponderían a sus niveles en el tejido embrionario/placentario (Romero-ruiz *et al.*, 2019).

Machine learning

Machine Learning (ML) utiliza algoritmos para recopilar datos, aprender de ellos y luego hacer una determinación o predicción. Las técnicas convencionales de ML consisten en extraer características "manualmente" para intentar encontrar patrones repetidos que ayuden a realizar de forma automática una tarea específica. Dicha metodología se basa en las *Artificial Neural Networks* (ANNs; redes neuronales artificiales). Se trata de un sistema que toma como analogía las redes neuronales biológicas, de forma que adquiera una gran colección de unidades neuronales interconectadas para permitir la comunicación. Estas unidades son nodos o neuronas que funcionan como procesadores simples en paralelo.

Las ANNs, son sistemas inteligentes utilizados en el aprendizaje automático que combinan hardware (por ejemplo, unidades de procesamiento gráfico) y software (*big data*), para simular el cerebro humano (Curchoe and Bormann, 2019). Las redes neuronales artificiales aplican algoritmos que simulan los procesos de neuronas reales para resolver problemas complejos a través del aprendizaje supervisado. Estas redes están formadas por distintas capas compuestas por neuronas encargadas de recibir las señales (variables o datos), asignarles un peso o valor, y transmitirlas a la siguiente capa (Figura 7). La composición de las ANNs puede dar lugar a diferentes estructuras o arquitecturas de red.

Para desarrollar la estructura más efectiva, se pueden utilizar algoritmos genéticos, es decir, métodos computacionales basados en mecanismos naturales (Takahashi *et al.*, 2016). Con el entrenamiento de las redes neuronales, basado en el aprendizaje de propagación hacia atrás (*Backpropagation*), el sistema llega a minimizar el error en la predicción del resultado deseado (Krogh, 2008; Lecun *et al.*, 2015). Por ejemplo, para el entrenamiento de una ANN que prediga calidad de los embriones en día 5 de desarrollo, se utilizarían imágenes de blastocistos categorizados por

embriólogos. Además, se extraerían características de las imágenes que serían las variables de entrada de las ANNs. Este procedimiento se ha llevado a cabo con embriones de bovino, consiguiendo una precisión de 76,4% en la detección de blastocistos de calidad baja, media y alta (Rocha *et al.*, 2017).

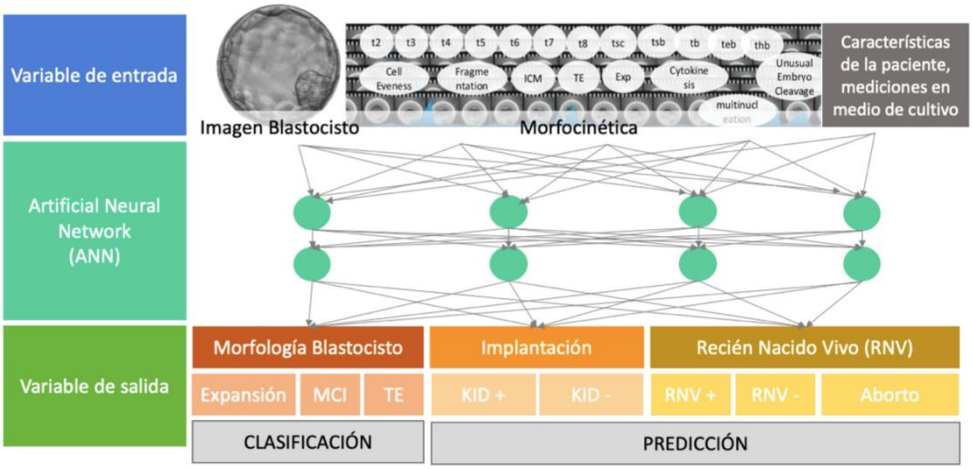

Figura 7. Esquema gráfico de la estructura de una red neuronal artificial (o *Artificial Neural Network; ANN*) con distintos tipos de variables de entrada y de salida. MCI, masa celular interna; TE, trofoectodermo; KID+, datos de implantación positivos - del inglés - *positive known implantation data*); KID-, datos de implantación negativos – del inglés- *negative implantation data*); RNV+, recién nacido vivo positivo; RNV-, recién nacido vivo negativo.

Deep learning

El *deep learning* (DL) es un subcampo o una técnica dentro del ML considerada como la evolución de este. Esta metodología reconoce un dato en un gran conjunto de datos al hacer cambios en sus parámetros para acercarse al valor real (Lecun *et al.*, 2015). La repetición de una circunstancia es responsable del aprendizaje, como si fuera un sistema nervioso biológico (Kim, 2016). De forma general, el cerebro trata de descifrar la información que recibe a través del etiquetado y la asignación de elementos en categorías, es decir, al recibir información nueva, el cerebro intenta compararla con los elementos conocidos antes de darle un sentido. Este concepto

es el utilizado en los algoritmos de DL (Garbade, 2018). Dicha metodología se basa en ANNs complejas, como las redes neuronales convolucionales (Matusevičius *et al.*, 2017). En cuanto al análisis de imagen, se necesitarían muchos casos para el entrenamiento y no habría extracción previa de características. Por ejemplo, para predecir la calidad de blastocistos, mediante esta técnica, el aprendizaje se llevaría a cabo con miles de embriones sin extraer variables de las imágenes (Khosravi *et al.*, 2019).

1.3.2 Inteligencia artificial en el laboratorio de fecundación in vitro.

Las imágenes del desarrollo embrionario permiten la identificación de parámetros involucrados en el proceso de implantación. Para ello, la embriología se puede beneficiar del análisis de imagen por visión computacional, técnica ya utilizada para resolver problemas médicos y biológicos a nivel molecular, sub- y supra-celular (Peng *et al.*, 2016). La visión computacional es la aplicación de sistemas artificiales sobre imágenes, para extraer información y decidir qué eventos son relevantes para resolver una cuestión específica (Danuser, 2011). El objetivo de un programa de visión computacional es aprender de forma interactiva sobre el contenido de una imagen. Una de las utilidades más antiguas de los sistemas de visión computacional en medicina, fue el conteo y seguimiento de células en secciones de encías (Farnoush, 1977).

Los vídeos de los sistemas TL, están compuestos por imágenes tomadas a intervalos de tiempo definidos (por ejemplo, 10 o 15 minutos). Dichas imágenes pueden ser procesadas y analizadas en función de sus píxeles. La diferencia entre una imagen, y la anterior o posterior, define patrones de desarrollo. Si un determinado comportamiento se produce frecuentemente en los embriones que consiguen implantar, y no en el resto, podríamos identificar un nuevo marcador de implantación.

Las imágenes deben ser normalizadas, es decir, procesadas (por ejemplo, convertidas a escala de grises) y estandarizadas antes de someterse a cualquier técnica de análisis. Es importante conocer que, para las herramientas de análisis de

imagen, las imágenes son matrices de píxeles representadas con valores de intensidad. Por ejemplo, para imágenes de 1 canal, que serían en blanco y negro, los valores oscilarían entre 0 y 255 (Figura 8).

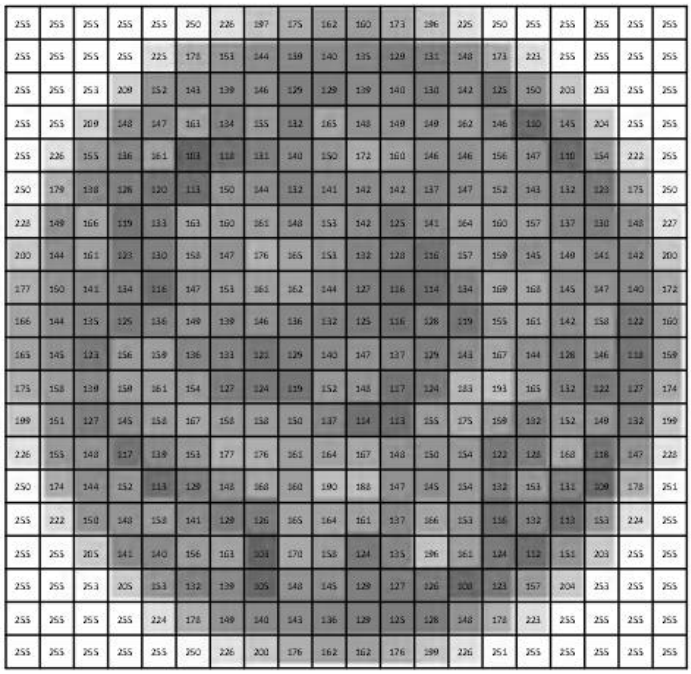

Figura 8. Ejemplo de matriz de píxeles sobre la imagen de un blastocisto. Valores cercanos a 0 indican oscuridad y valores cercanos a 255 indican luminosidad.

La aplicación de filtros sobre las imágenes permite la identificación de bordes o estructuras que facilitan la detección del embrión en el pocillo, como se puede observar en la Figura 9, con el “filtro Gaussiano” (utilizado en análisis de imagen para disminución de la nitidez, aumento de borrosidad y pérdida de detalles). A partir de ese punto, el análisis de imagen puede tanto identificar divisiones embrionarias, como reconocer las partes de un blastocisto. Por ejemplo, la técnica de segmentación ha sido utilizada para reconocer estructuras como la zona pelúcida, la masa celular interna y el trofoectodermo (Arsalan *et al.*, 2022).

La aplicación de filtros sobre las imágenes permite la identificación de bordes o estructuras que facilitan la detección del embrión en el pocillo, como se puede

observar en la Figura 9 con el "filtro Gaussiano" (utilizado en análisis de imagen para disminución de la nitidez, aumento de borrosidad y pérdida de detalles). A partir de ese punto, el análisis de imagen puede tanto identificar divisiones embrionarias, como reconocer las partes de un blastocisto. Por ejemplo, la técnica de segmentación ha sido utilizada para reconocer estructuras como la zona pelúcida, la masa celular interna y el trofoectodermo (Arsalan *et al.*, 2022).

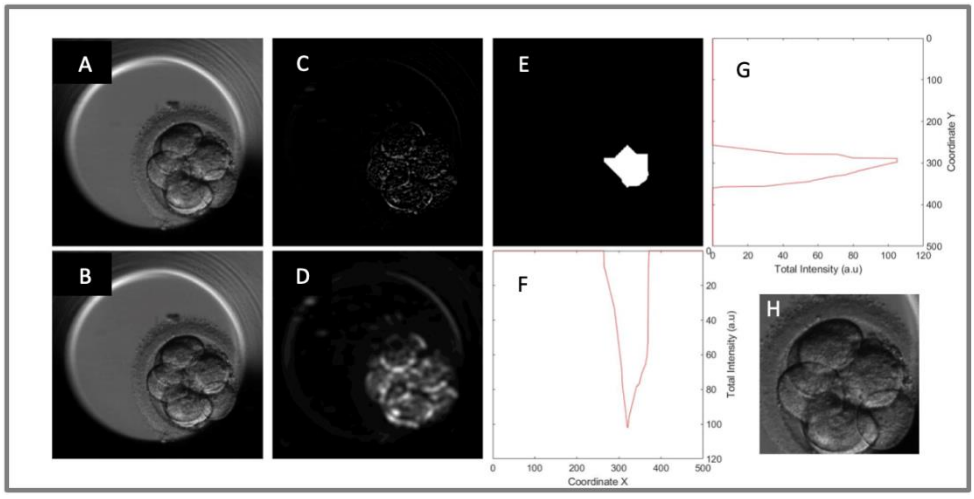

Figura 9. Pasos en la identificación de un embrión en un pocillo. A y B: imágenes de dos fotogramas consecutivos. C: diferencia de B-A, es decir, la resta píxel por píxel; las zonas más oscuras indican menos cambio entre fotogramas. D: aplicación de un filtro Gaussiano para suavizar la imagen. E: imagen con filtro de erosión, se resalta la zona central. F: coordenadas de la suma del eje Y. G: coordenadas de la suma del eje X. H: recorte del embrión identificado.

Anotaciones automáticas

La introducción de sistemas con visión computacional, capaces de extraer información objetiva y estandarizada de imágenes (Danuser, 2011), puede reducir la subjetividad en la selección de embriones (Manna *et al.*, 2013) mediante las anotaciones automáticas.

En el campo de la embriología humana, la primera aproximación predictiva desde imágenes proporcionadas por sistemas TL, fue realizada por Wong et al., (2010). El equipo desarrolló un algoritmo capaz de cuantificar automáticamente la duración de las citocinesis y los tiempos entre mitosis, hasta el estadio de 4 células. Este sistema se comercializó con el nombre de Eeva™ (del inglés Early Embryo Viability Assessment), siendo la primera plataforma validada clínicamente que integra *time-lapse*, 2 parámetros predictivos y un software automático. Se puede incorporar a un incubador convencional y obtiene imágenes digitales de alta resolución, en un único plano y a intervalos de 5 minutos. Dispone de un microscopio invertido digital de campo oscuro, de una cámara digital y del software de adquisición de imágenes; además de una placa para el cultivo de los embriones en grupo (Conaghan *et al.*, 2013).

Asimismo, el incubador Geri® (Merck, Darmstadt, Alemania), tiene incorporado un sistema de anotaciones automáticas en su software de monitorización digital Geri® Connect and Assess 2.0 (Figura 10). Es capaz de detectar automáticamente el tiempo de aparición de los pronúcleos y su desaparición (tPNa y tPNf), los tiempos de división a 2, 3, 4, 5 y 6 células (t2, t3, t4, t5 y t6), la formación de morula (tM), la llegada a blastocisto temprano (tSB), blastocisto expandido (tEB), y el inicio de eclosión a través de la zona pelúcida (tHiB). Además, tiene la capacidad de detectar eventos de división reversa o presencia de fragmentación. Dichas anotaciones se pueden modificar manualmente si el embriólogo considera que no son correctas. Además, el propio *software* muestra una señal de advertencia cuando cierta anotación está fuera del rango temporal establecido por la compañía comercial. Actualmente, los intervalos de tiempo definidos para cada evento son los siguientes: desaparición de los pronúcleos, 17-30 horas; división a 2 células, 20-40 horas; a 3 células, 30-48 horas; a 4 células, 32-54 horas; a 5 células, 38-68 horas; a 6 células, 46-78 horas; formación de mórula, 64-100 horas, formación de blastocisto temprano, 86-126 horas; formación de blastocisto expandido, 86-192 horas y el inicio de eclosión a través de la zona pelúcida, 86-192 horas (Alpha Scientists, 2011; Ciray *et al.*, 2014)

Figura 10. Demostración del software Geri Connect and Assess 2.0® con las anotaciones realizadas automáticamente y las modificaciones realizadas por los embriólogos. La flecha verde marca la casilla de anotaciones manuales; la flecha azul, la casilla de anotaciones automáticas y la flecha rosa, el software Eeva®. La señal de advertencia indica una anotación fuera del rango temporal establecido.

Los incubadores EmbryoScope® y EmbryoScope Plus® (Vitrolife, Copenhague, Dinamarca) también poseen un sistema de anotación automática (Guided Anotations) en su software EmbryoViewer®. Dicha herramienta está diseñada para proporcionar un flujo de trabajo de anotación simplificado y coherente. Esta estrategia de anotación determina qué variables deben anotar los usuarios y en qué orden.

Una vez definida la estrategia de anotación (o algoritmo de selección), la herramienta guía a los embriólogos en el proceso de realizar las anotaciones reales. Todas las variables incluidas en la estrategia de anotación seleccionada se presentan automáticamente junto con una imagen del embrión es ese mismo evento. La serie de imágenes se envía automáticamente a un punto estimado en el tiempo donde debe comenzar el proceso de anotación. Finalmente, el usuario completa el flujo de

trabajo, bien evaluando el embrión y realizando la anotación o confirmando las anotaciones sugeridas por la herramienta.

La función detecta automáticamente la división celular y los eventos morfológicos e inserta estimaciones de tiempos de división y parámetros morfológicos (PN, MCI y TE). El análisis automático de imágenes estima los tiempos de división celular y los parámetros morfológicos con distintos grados de certeza (niveles de confianza). Si establece un umbral de confianza alto, la mayoría de las veces las estimaciones de tiempos y parámetros morfológicos serán correctas. Sin embargo, tendrá que comprobar manualmente más estimaciones. Si establece un umbral de confianza bajo, las estimaciones serán, más a menudo, menos precisas. Sin embargo, los trabajadores tendrán menos estimaciones que comprobar. Dicho umbral debe basarse en la propia tolerancia de la clínica.

Algoritmos de IA para la selección embrionaria

En la actualidad, el sistema Eeva™ está incorporado en el incubador Geri®. El uso de este software predictivo, en combinación con la morfología en día 3 de desarrollo, demostró mejorar la capacidad del embriólogo para identificar embriones capaces de formar blastocistos de buena calidad. De esta manera, se mejora la selección entre embriones de morfología adecuada y se reduce la variabilidad interoperador (Conaghan *et al.*, 2013). Además, el software Eeva también se ha correlacionado con mejora en la tasa de implantación y en la tasa de embarazo clínico (Adamson *et al.*, 2016; Vermilyea *et al.*, 2014) y embarazo evolutivo (Aparicio-Ruiz *et al.*, 2016).

Asimismo, los sistemas *time-lapse* de Vitrolife contienen una herramienta de apoyo a la decisión de los embriólogos, el KIDScore D5™ (software EmbryoViewer; Vitrolife), que aumenta la objetividad y la coherencia en la evaluación de los embriones al clasificarlos según la probabilidad de implantación. La primera versión del algoritmo (KIDScore D5™ v1) se basaba en el número de pronúcleos (PN), la morfología del blastocisto y ocho parámetros morfocinéticos: tiempo de desvanecimiento de los PN (tPNf); tiempo de división en dos células (t2), tres

células (t3), cuatro células (t4), cinco células (t5) y ocho células (t8); tiempo hasta la blastulación temprana (tSB); y tiempo hasta la formación completa del blastocisto (tB). Para la segunda versión del algoritmo (KIDScore D5™ v2) las variables de entrada se redujeron a cinco parámetros morfocinéticos (t2, t3, t4, t5 y tB). Ambas versiones han sido recientemente validadas de forma retrospectiva como herramienta de toma de decisiones para ayudar a los embriólogos (Reignier et al., 2019; Gazzo et al., 2020).

La última versión, el KIDScore™ D5 versión 3, clasifica los embriones en función del ritmo de desarrollo y calidad del blastocisto (Figura 11). Se diseñó con una base de datos multicéntrica de más de 5.000 embriones con datos de implantación conocidos (embriones KID). Según los desarrolladores, la última versión de este modelo tiene en cuenta el número de PN, t2, t3, t4, t5, tB, la masa celular interna y la calidad del trofoectodermo.

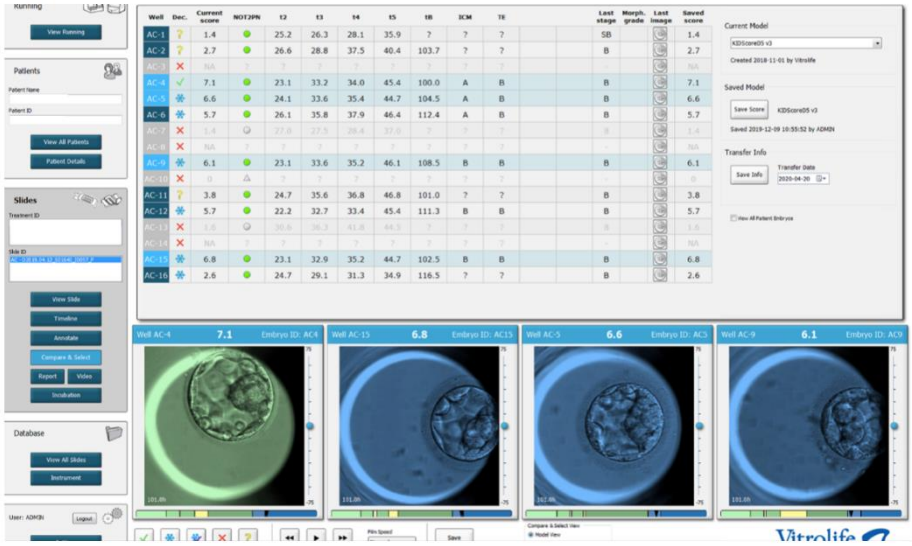

Figura 11. Demostración de la categorización proporcionada por el algoritmo KIDScore D5 v3 para una cohorte de 16 embriones en el software EmbryoViewer®. La parte superior muestra las anotaciones automáticas realizadas en cada embrión. La parte inferior muestra los cuatro embriones con máxima puntuación.

Se genera una puntuación lineal final que oscila entre 1 y 9,9 para cada embrión, que corresponde a una probabilidad de implantación de baja a alta. La puntuación automática de los embriones se recomienda para embriones procedentes de la FIV convencional o de la ICSI e incubados en condiciones reducidas de oxígeno (4-6%). Esta última versión ha sido validada en la presente tesis y su publicación corresponde al artículo III.

CAPÍTULO 2: Hipótesis, objetivos y justificación de compendio de artículos

.1 Hipótesis

Las técnicas de reproducción asistida han ido evolucionando de forma constante en los últimos años. Sin embargo, los procedimientos del laboratorio de fecundación in vitro se siguen realizando manualmente. La evaluación y selección de embriones son procedimientos decisivos en los tratamientos de infertilidad que podrían beneficiarse de nuevas tecnologías basadas en inteligencia artificial. Por lo tanto, consideramos que es necesario investigar en este campo para mejorar la evaluación embrionaria con métodos no invasivos y precisos que aumenten el éxito de la transferencia de un único embrión.

.2 Objetivos

Objetivo general

En esta tesis el objetivo general es definir nuevas metodologías no invasivas como herramienta de apoyo en los laboratorios de fecundación in vitro para seleccionar qué embrión transferir a la paciente, desarrollando y aplicando innovadoras tecnologías como la inteligencia artificial para automatizar y mejorar la evaluación in vitro. Para ello, nos planteamos los siguientes objetivos específicos.

Objetivos específicos

- Describir parámetros del desarrollo embrionario y su relación con el potencial de implantación.
- Identificar marcadores no invasivos del secretoma embrionario y su asociación con el éxito de un tratamiento de reproducción asistida.
- Desarrollar modelos basados en inteligencia artificial para predecir resultados clínicos.
- Evaluar herramientas para la automatización de la selección embrionaria en los laboratorios de fecundación in vitro.

.3 Justificación de la tesis como compendio de publicaciones.

La presente investigación de tesis doctoral se presenta como un compendio de tres publicaciones con datos relevantes obtenidos recientemente para avanzar en la selección embrionaria con métodos no invasivos, señalando a la inteligencia artificial como herramienta de apoyo fundamental en los laboratorios de fecundación in vitro.

Todos los hallazgos de estos trabajos tienen un mismo punto de convergencia: mejorar la evaluación y selección embrionaria en los tratamientos de reproducción asistida, como se resume brevemente a continuación.

En el artículo I, **Novel and conventional embryo parameters as input data for artificial neural networks: an artificial intelligence model applied for prediction of the implantation potential**, fuimos capaces de identificar parámetros morfodinámicos del desarrollo embrionario que funcionaban como variables de entrada de modelos basados en redes neuronales artificiales para predecir la implantación.

La combinación de características morfológicas (extraídas de imágenes del desarrollo embrionario) con mediciones no invasivas de proteómica en el medio de cultivo permitió desarrollar un modelo predictivo de recién nacido vivo en el artículo II, **An artificial intelligence model based on the proteomic profile of euploid embryos and blastocyst morphology: a preliminary study**.

En el artículo III, **The higher the score, the better the clinical outcome: retrospective evaluation of automatic embryo grading as a support tool for embryo selection in IVF laboratories**, se evaluó la utilidad de la puntuación embrionaria automática como herramienta de apoyo a la toma de decisiones en los laboratorios de fecundación in vitro.

CAPÍTULO 3: Resultados y discusión

Los artículos anexados que constituyen el cuerpo de la presente tesis exponen la metodología y los resultados de nuestra investigación de forma detallada. En este capítulo, se describen y discuten, a modo de resumen, los principales hallazgos obtenidos para cada objetivo específico:

3.1 Descripción de parámetros del desarrollo embrionario y su relación con el potencial de implantación.

En el artículo I se analizaron retrospectivamente los siguientes parámetros morfodinámicos del desarrollo embrionario: migración pronuclear, diámetro de expansión del blastocisto, área de la masa celular interna y duración del ciclo celular del trofoectodermo. Los resultados obtenidos se resumen a continuación:

Migración pronuclear

Los pronúcleos de los embriones analizados recorrieron distancias de 2 a 38 µm. No se encontraron diferencias significativas entre los embriones implantados y los no implantados, en términos de distancia y velocidad.

Diámetro de expansión del blastocisto

Los blastocistos alcanzaron tamaños desde 114 a 225 µm de diámetro. Los embriones implantados tenían diámetros significativamente mayores que los no implantados. La tasa de implantación también mejoró a medida que la relación BEd/tBEd era mayor: 46,2% para ≤1,37, 45,3% para 1,37-1,52, 66,7% para 1,52-1,64 y 70,7% para >1,64.

Área de masa celular interna

El área de la MCI evaluada osciló entre 1.051 y 4.847 μm^2. No se encontraron diferencias significativas en relación con la tasa de implantación. Aunque la tendencia fue la siguiente, los embriones con áreas de MCI mayores tuvieron una

mejor tasa de implantación. Se encontraron resultados similares para la relación MCI/tICMa: 52,1% para ≤19,07, 61,00% para 19,07-23,87, 63,8% para 23,87-28,90 y 57,4% para >28,90.

Duración del ciclo celular del trofoectodermo

El ciclo celular de las células del trofoectodermo fue más corto que el de las células blastoméricas. Además, encontramos diferencias significativas entre los embriones implantados y los no implantados.

La media y la desviación estándar de los nuevos parámetros morfodinámicos y de los parámetros morfocinéticos convencionales de los embriones implantados y no implantados se muestran en la Tabla 1.

Tabla 1. Media y desviación estándar para cada parámetro del embrión analizado en el artículo I. El valor p muestra las diferencias estadísticas entre los embriones implantados y los no implantados. PNm, migración pronuclear; BEd, diámetro expandido del blastocisto; ICMa, área de la masa celular interna; ccTroph, ciclo celular del trofoectodermo; tBEd, tiempo transcurrido desde la ICSI hasta la medición de BEd; tICMa, tiempo transcurrido desde la ICSI hasta la medición de ICMa.

Variable	Unidad (SI)	Embriones implantados		Embriones no implantados		P valor
		Media	Desviación estándar	Media	Desviación estándar	
tPB2	h	3,763	1,425	3,858	1,585	0,907
tPNa	h	8,559	2,187	8,735	2,283	0,926
tPNf	h	23,192	2,559	23,508	2,745	0,194
t2	h	25,654	2,956	25,951	2,973	0,383
t3	h	36,219	3,361	36,500	3,817	0,356
t4	h	37,403	3,663	38,154	3,975	0,031*
t5	h	48,801	5,109	49,104	5,812	0,526
t6	h	50,386	5,006	51,519	5,779	0,023*
t7	h	52,777	5,464	54,468	7,031	0,009*
t8	h	56,607	7,817	59,840	10,137	0,003*
t9	h	69,889	8,209	72,800	8,635	<0,001*
tSC	h	80,891	8,757	83,139	9,163	0,012*
tM	h	86,925	8,265	88,689	8,591	0,017*
tSB	h	96,843	6,712	98,978	6,979	0,001*

Variable	Unidad (SI)	Embriones implantados		Embriones no implantados		P valor
		Media	Desviación estándar	Media	Desviación estándar	
tB	h	102,436	6,740	104,326	7,216	0,005*
tEB	h	107,940	6,452	110,274	6,592	0,001*
tHiB	h	110,638	7,694	114,796	9,790	0,418
Distancia PNm	µm	13,649	7,234	13,648	6,898	0,936
Velocidad PNm	µm/h	1,377	1,989	1,174	0,995	0,079
BEd	µm	177,090	21,374	170,830	18,575	<0,001*
ICMa	μm^2	2763,036	707,134	2716,188	830,591	0,069
ccTroph	h	9,945	2,706	9,758	2,702	<0,001*
tICMa	h	113,369	5,419	114,252	9,046	0,184
tBEd	h	113,527	3,787	113,637	2,915	0,461

*p<0.05; diferencias estadísticamente significativas para el valor medio entre embriones implantados y no implantados.

3.2 Identificación de marcadores no invasivos del secretoma embrionario y su asociación con el éxito de un tratamiento de reproducción asistida.

En el artículo II se analizaron los niveles relativos de 92 proteínas en 89 muestras. Del total, 81 fueron medios de cultivo que habían sido incubados con embriones en desarrollo y 8 fueron controles (medios en los que no se incubaron embriones). Se utilizó un inmunoensayo de Proseek Multiplex Assays® (Olink, Bioscience, Suecia) basado en la tecnología Proximity extension assay (PEA). La lectura final del ensayo se presentó en valores de expresión proteica normalizada (NPX). Se trata de una unidad arbitraria en una escala log2, en la que un valor alto corresponde a una mayor expresión proteica. Del total de 92 proteínas, 67 mostraron valores de NPX idénticos en todas las muestras analizadas (medios condicionados y control). Por tanto, solamente 25 de las 92 proteínas medidas tenían valores diferentes entre el total de las muestras. La media de los valores de NPX para estas 25 proteínas en el control y en el medio condicionado se muestra en la Figura 12.

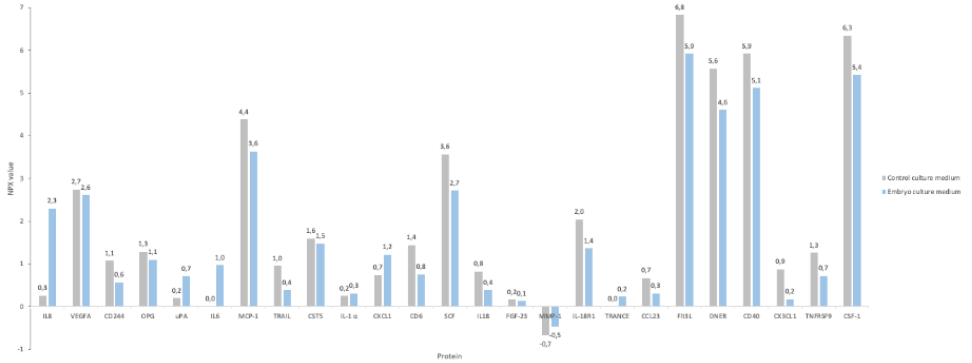

Figura 12. El gráfico de columnas agrupadas del artículo II representa la media del valor NPX obtenido mediante la técnica PEA para las 25 proteínas útiles analizadas en los medios de cultivo de 81 embriones generados a partir de óvulos autólogos. Las columnas grises muestran los medios de control (n = 8) y las azules los medios condicionados recogidos el día 5 de cultivo de los embriones. PEA, ensayo de extensión de proximidad; NPX, expresión proteica normalizada.

En los medios de cultivo con embriones detectamos concentraciones más altas de 3 proteínas en comparación con los niveles de los medios control, indicando una posible secreción por parte de los embriones. Estas proteínas fueron la IL-8 (p=0,025), la IL-6 (p=0,001) y el uPA (activador plasminígeno urocinasa; p=0,006). Además, también detectamos concentraciones más bajas de 14 proteínas en los medios de cultivo de embriones en comparación con los niveles de fondo. Estas proteínas fueron DNER (p<0,001), CSF-1 (p<0,001), Flt3L (p<0,001), SCF (p<0,001), CD40 (p<0,001), MCP-1 (p<0,001), CX3CL1 (p<0. 001), CD6 (p<0,001), TRAIL (p=0,002), TNFRSF9 (p<0,001), CD244 (p<0,001), IL-18 (p<0,001), CCL23 (p<0,001) e IL-18R1 (p<0,001).

La única proteína con valor NPX diferente en los embriones implantados (valor NPX=2,44) y no implantados (valor NPX=2,76) fue la VEGFA (p=0,017).

Posteriormente, se realizó un análisis de colinealidad que demostró que la mayoría de las proteínas estaban muy correlacionadas entre sí. Así, tras corregir la colinealidad, quedaron 7 proteínas independientes y no redundantes: Metaloproteinasa de la matriz-1 (MMP-1), interleucina-6 (IL-6), factor de

crecimiento endotelial vascular A (VEGFA), activador del plasminógeno tipo uroquinasa (uPA), citoquina inducida por la activación relacionada con el TNF (TRANCE), ligando de la tirosina quinasa 3 tipo FMS (Flt3L) y receptor relacionado con el EGF tipo Delta/Notch (DNER). Los niveles relativos de cada proteína se muestran en la Tabla 2, diferenciando entre muestras de embriones que lograron un RNV y los que no.

Tabla 2: Valores NPX obtenidos mediante la técnica PEA para las siete proteínas independientes resultantes del análisis de colinealidad publicado en el artículo II. RNV+, recién nacido vivo posirivo; RNV-, recién nacido vivo negativo; NPX, expresión proteica normalizada PEA, ensayo de extensión de proximidad; DS, desviación estándar.

Proteína	Valor NPX (media ± DS)		
	RNV+	RNV-	P valor
MMP-1	-0,39 ± 0,83	-0,49 ± 0,53	0,579
IL-6	0,94 ± 0,53	0,75 ± 0,67	0,261
VEGFA	2,40 ± 0,37	2,59 ± 0,53	0,137
uPA	0,67 ± 0,42	0,61 ± 0,52	0,634
TRANCE	0,19 ± 0,51	-0,05 ± 0,15	0,023
Flt3L	5,87 ± 0,20	6,00 ± 0,27	0,051
DNER	4,57 ± 0,29	4,71 ± 0,27	0,077

3.3 Desarrollo de modelos basados en inteligencia artificial para predecir resultados clínicos.

En el artículo I se desarrollaron cuatro modelos de selección embrionaria basados en IA para predecir implantación. Se trata de una red neuronal que fue entrenada y

testada utilizando distintos grupos de variables, lo que dio lugar a cuatro modelos con la misma arquitectura y diferentes datos de entrada (Tabla 3): parámetros morfocinéticos convencionales para la ANN1, parámetros morfodinámicos novedosos para la ANN2, parámetros convencionales y novedosos para la ANN3 y aquellos parámetros que presentaban diferencias significativas entre los embriones implantados y los no implantados para la ANN4.

Tabla 3. Variables de entrada para cada arquitectura de red neuronal artificial desarrollada en el artículo I. ANN, red neuronal artificial (del inglés, artificial neural network); tpb2, tiempo de emisión del segundo cuerpo polar; tPNa, tiempo de aparición de los dos pronúcleos; tPNf, tiempo de desvanecimiento de los mismos; t2, tiempo de división a dos células; t3, tiempo de división a tres células; t4, tiempo de división a cuatro células; t5, tiempo de división a cinco células; t6, tiempo de división a seis células; t7, tiempo de división a siete células; t8, tiempo de división hasta ocho células; tSC, tiempo desde la ICSI hasta la compactación temprana; tM, el tiempo hasta la formación de la mórula; tSB, tiempo hasta la blastulación temprana; tB, el tiempo hasta la formación del blastocisto completo; tEB, tiempo hasta el blastocisto expandido; y tHiB, tiempo hasta el incio de eclosión del blastocisto; PNm, migración pronuclear, BEd, diámetro expandido del blastocisto; ICMa, área de la masa celular interna; ccTroph, ciclo celular del trofoectodermo.

Red Neuronal Artificial	Variables de entrada
ANN1	tpb2, tPNa, tPNf, t2, t3, t4, t5, t6, t7, t8, tSC, tM, tSB, tB, tEB, tHiB
ANN2	Distancia PNm, velocidad PNm, BEd, ICMa, ccTroph
ANN3	tpb2, tPNa, tPNf, t2, t3, t4, t5, t6, t7, t8, tSC, tM, tSB, tB, tEB, tHiB, distancia PNm, velocidad PNm, BEd, ICMa, ccTroph
ANN4	t4, t6, t7, t8, t9, tSC, tM, tSB, tB, tEB, Bed, ccTroph

Los resultados en términos de sensibilidad, especificidad, precisión, Valor-F y área bajo la curva de los cuatro modelos en el conjunto de datos de prueba se representan en la Tabla 4. El mayor poder predictivo lo obtuvo la ANN3 con un AUC de 0,77. Asimismo, el modelo más equilibrado también fue la ANN3, presentando la mayor especificidad y una excelente sensibilidad.

Tabla 4. Resultados de los cuatro modelos de selección embrionaria desarrollados en el artículo I. ANN, red neuronal artificial (del inglés, artificial neural network); AUC, área bajo la curva.

Red neuronal artificial	Sensibilidad	Especificidad	Precisión	Valor F	AUC
ANN1	0.88	0.46	0.71	0.78	0.64
ANN2	0.86	0.58	0.75	0.80	0.73
ANN3	0.82	0.67	0.76	0.80	0.77
ANN4	0.85	0.57	0.74	0.79	0.68

La información procedente de las imágenes de los blastocistos y los valores de proteómica obtenidos del análisis del secretoma embrionario se utilizaron para predecir el potencial de un embrión euploide para dar lugar a un nacimiento vivo en el artículo II.

Las tres arquitecturas más eficientes obtenidas se muestran en la Tabla 5. La arquitectura desarrollada con IL-6 y MMP-1 consiguió clasificar correctamente todos los embriones como nacidos vivos positivos y negativos en las fases de entrenamiento, validación y test (éxito total = 100%). El AUC resultante para predecir los nacimientos vivos positivos y negativos alcanzó el valor más alto, 1,0.

Tabla 5. Resultados del test de las tres arquitecturas más eficientes en la predicción de nacimientos vivos publicadas en el artículo II. AUC, área bajo la curva.

Arquitectura de ANN	Datos de entrada		Test	
	Morfología del análisis de imagen[a]	Datos de proteómica	RNV+	RNV -
1	20 variables	MMP-1, IL-6	AUC=1	AUC=1
2	20 variables	MMP-1, IL-6, VEGFA, uPA, TRANCE, Flt3L and DNER	AUC=0.9	AUC=0.9
3	20 variables	25 proteinas[b]	AUC=0.83	AUC=0.84

[a] Las variables se describen en la Tabla Suplementaria 4 del artículo II.

[b] IL-8, VEGFA, CD244, OPG, uPA, IL-6, MCP-1, TRAIL, CST5, IL-1α, CXCL1, CD6, SCF, IL-18, FGF-23, MMP-1, IL-18R1, TRANCE, CCL23, Flt3L, DNER, CD40, CX3CL1, TNFRSF9, CSF-1.

La prueba ciega de la arquitectura 1 realizada con 11 embriones, que no se utilizaron previamente, alcanzó una precisión de predicción del 72,7%. Clasificó correctamente 8 embriones del total.

3.4 Evaluación de herramientas para la automatización de la selección embrionaria en los laboratorios de fecundación in vitro.

En el artículo III se muestra la evaluación de un modelo basado en IA como herramienta de ayuda a la decisión de los embriólogos en el laboratorio de FIV. Un total de 12.468 embriones de 1.678 pacientes fueron calificados automáticamente por el modelo KIDScore™ D5 versión 3 (KIDScore D5™ v3). Se trata de un algoritmo incorporado en los dispositivos *time-lapse* EmbryoScope y EmbryoScope Plus (Vitrolife) que clasifica automáticamente los embriones en función de la regularidad de las divisiones celulares, el ritmo de desarrollo y la calidad de los blastocistos. Dicho modelo genera una puntuación lineal final que oscila entre 1 y 9,9 para cada embrión.

La media de la puntuación fue significativamente diferente ($p<0,001$) entre los embriones clasificados con diferentes categorías morfológicas según los criterios ASEBIR (8,3±1 1 para los embriones clasificados como A, n=640; 5,9±1,3 para los B, n=4.560; 3,7±1,2 para los C, n=2.822; y 2,2±0,9 para los D, n=2.125) y entre los embriones euploides (5,4±1,7, n=674) y aneuploides (4,7±1,8, n=900). La media de la puntuación de los embriones de la población SET fue de 6,6±1,6 para la β-hCG positiva y de 5,9±1,7 para la β-hCG negativa ($p<0,001$); de 6,6±1,6 para la implantación positiva y de 5,9±1,7 para la implantación negativa ($p<0,001$); y de 6,7±1,6 para el nacimiento vivo positivo y de 5,9±1,7 para el nacimiento vivo negativo ($p<0,001$).

A continuación, se realizó un análisis de regresión logística sobre la clasificación KIDScore D5™ v3 teniendo en cuenta posibles factores de confusión: origen de los ovocitos (donados frente a autólogos); tipo de transferencia de embriones (frescos frente a congelados); edad de los ovocitos; IMC de la paciente; PGT-A (embriones probados frente a no probados); día de la transferencia de embriones (quinto frente a sexto día de desarrollo del embrión); estrategia de cultivo (en grupo frente a individual); morfología del blastocisto (embriones clasificados como A frente a C y embriones clasificados como B frente a C); y la morfología del embrión. sexto día de desarrollo del embrión); estrategia de cultivo (grupal vs. individual); morfología del blastocisto (embriones calificados como A vs. C y embriones calificados como B vs. C); e indicación de tratamiento de la infertilidad (factor femenino, masculino, mixto, social o desconocido).

El análisis multivariante por pasos para las diferentes subpoblaciones de pacientes se realizó analizando los resultados de implantación y de recién nacidos vivos. La contribución de la puntuación embrionaria a ambos resultados fue estadísticamente significativa para todos los tratamientos en general, para las pacientes del programa de donación de ovocitos y para los ciclos de ICSI convencionales con ovocitos autólogos y sin PGT-A (Tabla 6). Sin embargo, la puntuación automática del embrión no se relacionó con el resultado de implantación o nacimiento vivo en los

embriones que habían sido analizados genéticamente (n= 307, p=0,226 para la implantación y p=0,731 para el nacimiento vivo).

Tabla 6. Análisis multivariante para la implantación y el resultado de nacidos vivos en diferentes poblaciones de pacientes. OR: odds ratio o razón de probabilidades; IC: intervalo de confianza; SET: transferencia de un solo embrión; PGT-A: pruebas genéticas preimplantacionales para aneuploidía; IMC: índice de masa corporal.

	Implantación			Recién Nacido Vivo		
	OR[a]	95% IC	p-valor	OR[a]	95% IC	p-valor
Todos los tratamientos (n=1,952 SETs)						
Puntuación embrionaria automática	1.285	[1.214-1.360]	<0.001	1.288	[1.215-1.364]	<0.001
PGT-A Testado (15.7%) vs. No testado (84.3%)	1.401	[1.080-1.817]	0.011	1.544	[1.189-2.006]	0.001
Transferencia embrionaria Fresco (46.5%) vs. Congelado (53.5%)	1.389	[1.131-1.705]	0.002	1.510	[1.228-1.857]	<0.001
IMC	-	-	-	0.968	[0.947-0.990]	0.005
Programa de donación de ovocitos (n=1,165 SETs)						
Puntuación embrionaria automática	1.285	[1.189-1.390]	<0.001	1.260	[1.166-1.362]	<0.001
EmbryoTransfer Fresh (54.7%) vs. Frozen (45.3%)	1.451	[1.139-1.848]	0.003	1.642	[1.291-2.088]	<0.001
IMC	0.970	[0.944-0.997]	0.029	0.966	[0.940-0.993]	0.014
	Implantación			Recién Nacido Vivo		
	OR[a]	95% IC	p-valor	OR[a]	95% IC	p-valor
Tratamientos con ovocitos propios, sin PGT-A (n=480 SETs)						
Puntuación embrionaria automática	1.381	[1.236-1.543]	<0.001	1.465	[1.298-1.653]	<0.001
Edad ovocito	-	-	-	0.909	[0.853-0.969]	0.003

[a]ORs calculados a partir de la regresión logística multivariante por pasos.

CAPÍTULO 4: Conclusiones

Lejos de los métodos convencionales para evaluar y seleccionar embriones en los tratamientos de FIV, nuestros estudios proponen una nueva aproximación basada en el uso de la inteligencia artificial. Cada artículo anexado como justificación de la presente tesis muestra sus conclusiones individuales. En este capítulo, se muestran las conclusiones generales de nuestra investigación:

1. Parámetros no convencionales del desarrollo embrionario medidos sobre imágenes *time-lapse* podrían ayudar a predecir el potencial de implantación de los embriones in vitro.

2. Los modelos basados en redes neuronales artificiales permiten analizar y considerar gran cantidad de datos en una predicción específica. Según el artículo I, el modelo más predictivo para implantación es el que está entrenado por más variables del desarrollo embrionario, y no sólo por aquellas que son individualmente discriminatorias.

3. La introducción de la IA en los laboratorios de FIV ayudaría a los embriólogos a predecir el éxito de un embrión para conseguir un recién nacido vivo.

4. La combinación del análisis proteómico del medio de cultivo del embrión y la información morfológica de las imágenes del blastocisto evaluadas mediante técnicas de IA posee poder predictivo sobre el éxito de un tratamiento de reproducción asistida. Los resultados del artículo II, demuestran que una ANN logró detectar embriones euploides capaces de dar lugar a un nacimiento vivo con una excelente precisión, especialmente teniendo en cuenta la IL-6 y la MMP-1.

5. De acuerdo con los hallazgos publicados en el artículo III, aprobamos que la puntuación automática de embriones es una herramienta útil de apoyo a la decisión para los embriólogos sin comprometer los resultados clínicos.

Además, este modelo proporciona información adicional que podría mejorar la coherencia en la selección de embriones. Según las preferencias de cada laboratorio, este modelo de puntuación de embriones puede ser dependiente o independiente del usuario, basado en anotaciones manuales o automáticas. A pesar de observar AUCs similares a las metodologías convencionales de selección de embriones, el uso de este algoritmo automático debería mejorar el flujo de trabajo y permitir a los embriólogos dedicar su tiempo a otras tareas que requieren más atención.

Sugerencias y futuros desarrollos

Durante el transcurso de la presente tesis doctoral la inteligencia artificial ha ido adentrándose en el campo de la reproducción asistida. En esta memoria, se han resaltado algunos avances del uso de esta tecnología en el laboratorio de fecundación in vitro. Del mismo modo, este hecho causa desconfianza a los profesionales del ámbito al tratarse de una innovación que podría alterar la estructura del laboratorio de FIV, el flujo de trabajo, e incluso los resultados clínicos.

La opinión de la candidata acerca de la introducción de la automatización en el laboratorio de FIV ha sido publicada en el artículo IV como una contribución a la contra corriente:

Bori L, Meseguer M. Will the introduction of automated ART laboratory systems render the majority of embryologists redundant? Reprod Biomed Online. 2021 Dec;43(6):979-981. doi: 10.1016/j.rbmo.2021.10.002. Epub 2021 Oct 12. PMID: 34753681.

En este artículo se describe cómo la embriología se está enfrentando a un cambio común a la mayoría de las áreas de la medicina, la introducción de la automatización. El uso de sistemas automatizados en el laboratorio de FIV ya se está produciendo, por ejemplo, con los testigos electrónicos y la clasificación de los embriones. Se espera que en un futuro próximo se automaticen varios sistemas del laboratorio de FIV. De este modo, la manipulación de gametos podría dejar de ser manual y el cultivo y la selección de embriones podrían realizarse mediante microfluidos e inteligencia artificial. Por tanto, las tareas convencionales del embriólogo se reducirían inevitablemente. Sin embargo, surgirán nuevas funciones relacionadas con la captura, gestión y análisis de datos, junto con otras habilidades de investigación y una mayor comunicación con otros profesionales y pacientes.

ARTÍCULO IV

Artículo IV: Will the introduction of automated ART laboratory systems render the majority of embryologists redundant?

Bori L, Meseguer M.

Reprod Biomed Online. 2021 Dec;43(6):979-981. doi: 10.1016/j.rbmo.2021.10.002. Epub 2021 Oct 12. PMID: 34753681.

Factor de impacto 2021: 4,567

5-años factor de impacto: 4,603

RBMO

COUNTERCURRENT

Will the introduction of automated ART laboratory systems render the majority of embryologists redundant?

Lorena Bori[1,2], Marcos Meseguer[1,2,3,*]

ABSTRACT

IVF techniques have changed over time with the aim of improving clinical results. Today, embryology is facing a change common to most areas of medicine, the introduction of automation. The use of automated systems in the IVF laboratory is already happening, for example, with electronic witnessing and the ranking of embryos according to their implantation potential. It is expected that in the near future, various systems in the IVF laboratory will be automated. In this way, gamete manipulation would cease to be manual and embryo culture and selection would be performed by means of microfluidics and artificial intelligence. Therefore, the tasks of the embryologist will inevitably be reduced. However, new functions related to data capture, management and analysis will emerge, along with other research skills and increased communication with other professionals and patients.

Since the first pregnancy was achieved by IVF, there have been many changes in assisted reproduction treatments. Over the past 40 years, laboratory methodologies have been rapidly updated, including intracytoplasmic sperm injection (ICSI), embryo culture extension, embryo biopsy, vitrification, time-lapse systems and electronic witnessing platforms. Further technical innovations, such as microfluidics and noninvasive embryo screening tests, are now being studied for future introduction in assisted reproduction units. Currently, we are seeing the incorporation of automation in some routine processes to minimize the number of steps and the manipulation of gametes and embryos by embryologists. Science and research invite us to constantly update our work in order to improve clinical outcomes, and the time to adapt is now.

MANUAL GAMETE MANIPULATION IS COMING TO AN END

Automation will enter the andrology laboratory in conjunction with microfluidic technologies to facilitate sperm analysis, sperm preparation and sperm selection with minimal manual input. Some preliminary studies have suggested the use of microfluidics for sperm isolation and microrobotic immobilization for ICSI (*Leung et al., 2011*; *Lu et al., 2011*). Thus, future sperm assessment may differ from current evaluation. In addition to concentration and motility, it would analyze the risk of fertilization failure and identify risks to offspring by methylation and mutation loads (*Jenkins et al., 2017*).

Robotics, computerized systems and artificial intelligence integrated with image analysis and biochemical evaluation of oocyte quality could guide patient treatment decisions and automate processes such as oocyte insemination by IVF and ICSI. Finally, systems for intelligent assessment of fertilization could be developed by means of image capture and three-dimensional reconstruction.

IN-VITRO EMBRYO CULTURE AND SELECTION IS DESTINATED TO CHANGE

Currently, in-vitro embryo culture is based on static conditions, while embryos *in vivo* are exposed to dynamic environments that provide stage-specific nutrients. New techniques of manipulation may be used to create microenvironments in the IVF laboratory. In this case, automatic microfluidic-based devices would regulate the culture medium flux, reducing the

[1] IVIRMA Valencia, Spain
[2] IVI Foundation, Valencia, Spain
[3] Health Research Institute la Fe, Valencia, Spain

*Corresponding author. E-mail address: marcos.meseguer@ivirma.com (M. Meseguer). https://doi.org/10.1016/j.rbmo.2021.10.002 1472-6483/

KEYWORDS
Artificial Intelligence
Automation
Embryologist

workload of embryologists. Ideally, the dispute between single or sequential media would end with the addition of biosensors to these devices. In this way, catabolites and supplements would be adapted to the needs of each embryo automatically.

The introduction of continuous monitoring of embryo development in IVF laboratories has already reduced, in part, the time spent by embryologists in moving embryo culture dishes and assessing embryos under optical microscopes at specific time ranges. In addition, time-lapse incubators allow for undisturbed culture conditions and the creation of evaluation and selection models based on the dynamic development of the embryo, with morphological and morphokinetic variables (Del *Gallego et al., 2019*). However, although time-lapse systems are very useful for the accurate evaluation of embryos, most of the existing embryo selection models have not achieved satisfactory results among different laboratories. This may be due to limited interobserver agreement, since the variables used, such as cell division timings or blastocyst morphology, are manually annotated.

Nowadays, embryologists could benefit from artificial intelligence (AI) and computer vision to improve their ability to select the most competent embryo for transfer. Time-lapse videos of embryo development are composed of images taken at defined time intervals (e.g. 10 or 15 minutes). These images can be processed and analyzed on a pixel-by-pixel basis. The difference between one image and the previous or subsequent image defines patterns of development. If a certain behaviour occurs frequently in the embryos that implant successfully, and not in the rest, we could identify a new marker of implantation. Computer vision-based models will apply artificial systems on images to extract information and decide which events are relevant to solve a specific question automatically. Indeed, implementing automation with time-lapse technology is already happening in the IVF laboratory for ranking embryos according to implantation potential. In parallel, automatic models on static embryo images should be developed for laboratories that have not invested in time-lapse systems.

Consideration of the visual dynamics of an embryo could be complemented by non-invasive analysis of embryo-derived factors secreted into the culture medium to assess the embryo's metabolic state. On the one hand, the metabolites involved in oxidative processes have been suggested as predictive of implantation success, in conjunction with morphokinetics (*Alegre et al., 2019*). On the other hand, several patterns of protein expression in spent embryo culture medium have been associated with stages of embryo development, morphology, and even implantation potential. Furthermore, a combination of blastocyst image analysis with proteomic information from the spent culture medium on day 5/6 of development has already been proposed as an initial model that predicts the potential for achieving a live birth (*Bori et al., 2020*).

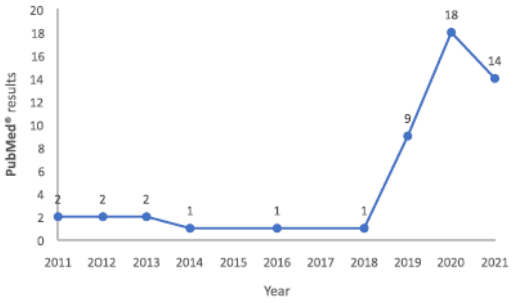

FIGURE 1 Number of publications including the terms 'Artificial intelligence' and 'IVF' in the last decade from a PubMed® search query.

In addition, the ability to identify euploid embryos by non-invasive methods, without need for trophectoderm biopsies, is improving rapidly. Novel techniques range from cell-free DNA collection for chromosomal analysis in spent culture medium to the application of computer vision to detect differences in embryo development that may reveal the embryonic health. Finally, automation will also be used for vitrification as the last step of microfluidic-based devices.

A complex artificial intelligence system based on a combination of microfluidics, biomarkers of embryo metabolism, image analysis and non-invasive PGT-A will serve to create an embryo ranking for each embryo cohort and reduce time to pregnancy.

THE EMBRYOLOGIST'S ROLE WILL ADAPT IN THE FACE OF AUTOMATION

Automation is entering embryology, as revealed by the increase in publications based on artificial intelligence in IVF laboratories (FIGURE 1). In the near future, data collection could be performed automatically in laboratories by voice recognition in electronic medical record systems. In the same way, a facial recognition system could be installed at the workstations that would automatically record the date, time, process and operator. Even the preparation of culture dishes and sampling of the medium for quality control could be automated. In this way, key performance indicators will become increasingly complex and numerous. Big data-based systems could be used as an early warning to detect changes in equipment or operator performance. In addition, AI-driven technologies could improve quality systems in all laboratories, regardless of the number of cycles, by providing sufficient information to optimize procedures. Thus, data integration will encompass all clinical and technical variables to enable AI-based algorithms to 'learn' from these data sets and adjust performance on an ongoing basis.

Electronic witnessing systems are a form of automation used daily in IVF laboratories. Their incorporation reduced the time spent by embryologists and improved the traceability of samples (*Rienzi et al., 2015*). In the short term, it is expected that similar automated systems will be introduced for quality assurance and machine supervision. This will also reduce the time spent by laboratory operators on equipment maintenance and simplify routine procedures.

Automation will increase in several clinical processes, such as embryo scoring, oocyte denudation, and even fertilization checks. Embryo morphology

and morphokinetics will undoubtedly be delegated to AI and computer vision applications, which will be able to detect small developmental aberrations that may affect reproductive success. In addition, information from '-omics' sciences, such as genomics, epigenomics or proteomics will add further value to these novel applications. However, more complex procedures, such as ICSI, trophectoderm biopsy, and vitrification, may not be fully automated in the near future due to their highly technical and variable nature. Although there are researchers working on these types of tools, as they are the most difficult and time-consuming tasks. In any case, the use of an automatic technique should be tested prior to its clinical application to ensure its safety.

These novel technologies will provide us with a wealth of information that we can use for further research and advancement. Nonetheless, the key question is: are embryologists ready for tomorrow? It is inevitable that the implementation of automated and rapid systems will reduce the future demand for embryologists. However, when key tasks are automated, other novel tasks will be created around the increasing amount of data that will be generated per embryo. Therefore, the expertise of embryologists will always be necessary to ensure the successful implementation of any new technology.

The embryologist's profession will inevitably change. There may come a time when human manipulation of embryos will no longer be necessary and all processes will be robotized. In this way, embryology would be much more technological, focused on advising computer scientists and engineers on the development of devices for embryo manipulation. The new role of embryologists will involve exploring the data and determining its relevance, deciding how to use the huge amount of data collected and in what way to combine it to provide an accurate diagnostic of the competence of an embryo.

Embryologists will need to understand how large data sets from different sources, such as a combination of stimulation protocols, patient characteristics, embryo developmental events, and even environmental conditions, are processed using new technologies. Additionally, they will learn how to interpret results, with the capacity to recognize biological and clinical information generated by data fusion. The knowledge gained will facilitate communication between embryologists and patients. The embryologist must be able to broadcast what is 'in action' in the laboratory, to make this information accessible to a growing demand from patients who increasingly want to understand all the procedures occurring in this 'black box' between oocyte retrieval and embryo transfer. The new tasks that embryologists will face will require additional knowledge in statistics and database management.

Future embryologists, apart from having a basic knowledge of the complexity of in-vitro fertilization, should have good communication skills as their new role will also focus on advising colleagues and patients on recommended treatment options. Nonetheless, a few embryologists may still play a more active role in practical laboratory work in the daily clinical routine.

In conclusion, although automated ART laboratory systems will reduce the time spent by embryologists on their current tasks, they will perform new functions focused on clinical and biological aspects of patient care, including quality control and assurance.

REFERENCES

Alegre, L., Gallego, R. Del, Arrones, S., Hernández, P., Muñoz, M., Meseguer, M. **Novel noninvasive embryo selection algorithm combining time-lapse morphokinetics and oxidative status of the spent embryo culture medium.** Fertil. Steril. 2019; 111: 918–927

Bori, L., Dominguez, F., Fernandez, E.I., Gallego, R Del, Alegre, L., Hickman, C., Quiñonero, A., Nogueira, M.F.G., Rocha, J.C., Meseguer, M. **An artificial intelligence model based on the proteomic profile of euploid embryos and time-lapse images: a preliminary study.** RBMO 2020; 42: 340–350

Gallego, R. Del, Remohí, J., Meseguer, M., Affiliations, A., Valencia, I.G. **Time-Lapse Imaging : The State of the Art.** Biol. Reprod. 2019; 101: 1146–1154

Jenkins, T.G., Aston, K.I., James, E.R., Carrell, D.T. **Sperm epigenetics in the study of male fertility, offspring health, and potential clinical applications.** Syst. Biol. Reprod. Med. 2017; 63: 69–76

Leung, C., Lu, Z., Esfandiari, N., Casper, R.F., Sun, Y. **Automated sperm immobilization for intracytoplasmic sperm injection.** IEEE Trans. Biomed. Eng. 2011; 58: 935–942

Lu, Z., Zhang, X., Leung, C., Esfandiari, N., Casper, R.F., Sun, Y. **Robotic ICSI (Intracytoplasmic Sperm Injection).** IEEE Trans. Biomed. Eng. 2011; 58: 2102–2108

Rienzi, L., Bariani, F., Dalla Zorza, M., Romano, S., Scarica, C., Maggiulli, R., Nanni Costa, A., Ubaldi, F.M. **Failure mode and effects analysis of witnessing protocols for ensuring traceability during IVF.** Reprod. Biomed. Online 2015; 31: 516–522

Received 15 September 2021; received in revised form 28 September 2021; accepted 4 October 2021.

Bibliografía

Adamson GD, Abusief ME, Palao L, Witmer J, Palao LM, Gvakharia M. Improved implantation rates of day 3 embryo transfers with the use of an automated time-lapse–enabled test to aid in embryo selection. *Fertil Steril* 2016;**105**:369-375.e6. Available at: http://dx.doi.org/10.1016/j.fertnstert.2015.10.030.

Aguilar J, Rubio I, Muñoz E, Pellicer A, Meseguer M. Study of nucleation status in the second cell cycle of human embryo and its impact on implantation rate. *Fertil Steril* 2016;**106**:291–299.

Alpha Scientists. The Istanbul consensus workshop on embryo assessment: proceedings of an expert meeting Alpha Scientists in Reproductive Medicine and ESHRE Special Interest Group of Embryology. *Human Reproduction* 2011;**26**:1270–1283.

Aparicio B, Cruz M, Meseguer M. Is morphokinetic analysis the answer? *Reprod Biomed Online* 2013;**27**:654–663.

Aparicio-Ruiz B, Basile N, Pérez Albalá S, Bronet F, Remohí J, Meseguer M. Automatic time-lapse instrument is superior to single-point morphology observation for selecting viable embryos: retrospective study in oocyte donation. *Fertil Steril* 2016;**106**:1379–1385.

Arsalan M, Haider A, Choi J, Park KR. Detecting Blastocyst Components by Artificial Intelligence for Human Embryological Analysis to Improve Success Rate of In Vitro Fertilization. *J Pers Med* 2022;**12**.

Azzarello A, Hoest T, Hay-Schmidt A, Mikkelsen AL. Live birth potential of good morphology and vitrified blastocysts presenting abnormal cell divisions. *Reprod Biol* 2017;**17**:144–150.

Baczowski T, Kurzawa R, Wojciech G. Methods of embryo scoring in in vitro fertilization. *Reprod Biol* 2004;**4**:5–22.

Barrie A, Homburg R, McDowell G, Brown J, Kingsland C, Troup S. Examining the efficacy of six published time-lapse imaging embryo selection algorithms to predict implantation to demonstrate the need for the development of specific, in-house morphokinetic selection algorithms. *Fertil Steril* 2017;**107**:613–621.

van den Berg MMJ, van Maarle MC, van Wely M, Goddijn M. Genetics of early miscarriage. *Biochim Biophys Acta Mol Basis Dis* 2012;**1822**:1951–1959. Available at: http://dx.doi.org/10.1016/j.bbadis.2012.07.001.

Butler SA, Luttoo J, Freire MOT, Abban TK, Borrelli PTA, Iles RK. Human chorionic gonadotropin (hCG) in the secretome of cultured embryos: Hyperglycosylated hCG and hCG-free beta subunit are potential markers for infertility management and treatment. *Reproductive Sciences* 2013;**20**:1038–1045.

Ciray HN, Campbell A, Agerholm IE, Aguilar J, Chamayou S, Esbert M, Sayed S. Proposed guidelines on the nomenclature and annotation of dynamic human embryo monitoring by a time-lapse user group. *Human Reproduction* 2014;**29**:2650–2660.

Clarke GN. A.R.T. and history, 1678-1978. *Human Reproduction* 2006;**21**:1645–1650.

Cohen J, Wells D, Munné S. Removal of 2 cells from cleavage stage embryos is likely to reduce the efficacy of chromosomal tests that are used to enhance implantation rates. *Fertil Steril* 2007;**87**:496–503.

Committee P, Society A. Multiple gestation associated with infertility therapy: An American Society for Reproductive Medicine Practice Committee opinion. *Fertil Steril* 2012;**97**:825–834. Available at: http://dx.doi.org/10.1016/j.fertnstert.2011.11.048.

Conaghan J, Chen AA, Willman SP, Ivani K, Chenette PE, Boostanfar R, Baker VL, Adamson GD, Abusief ME, Gvakharia M, *et al.* Improving embryo

selection using a computer-automated time-lapse image analysis test plus day 3 morphology: Results from a prospective multicenter trial. *Fertil Steril* 2013;**100**:412–419.

Cruz M, Garrido N, Herrero J, Pérez-Cano I, Muñoz M, Meseguer M. Timing of cell division in human cleavage-stage embryos is linked with blastocyst formation and quality. *Reprod Biomed Online* 2012;**25**:371–381.

CUADERNOS DE EMBRIOLOGÍA CLÍNICA 3ª Edición · 2015. Available at: www.gobalo.es. Accessed November 8, 2022.

Cuevas I, Pons MC, Vargas MC, Delgado Mendive A, Rives Enedáguila N, Moragas Solanes M, Carrasco Canal B, Teruel López J, Busquets Bonet A, Hurtado de Mendoza Acosta MV. The Embryology Interest Group: updating ASEBIR's morphological scoring system for early embryos, morulae and blastocysts. *Medicina Reproductiva y Embriología Clínica* 2018;**5**:42–54. Available at: https://doi.org/10.1016/j.medre.2017.11.002.

Curchoe CL, Bormann CL. Artificial intelligence and machine learning for human reproduction and embryology presented at ASRM and ESHRE 2018. *J Assist Reprod Genet* 2019;**36**:591–600.

Dal Canto M, Coticchio G, Mignini Renzini M, de Ponti E, Novara PV, Brambillasca F, Comi R, Fadini R. Cleavage kinetics analysis of human embryos predicts development to blastocyst and implantation. *Reprod Biomed Online* 2012;**25**:474–480.

Dale AI. Thomas bayes, an essay towards solving a problem in the doctrine of chances (1764). *Landmark Writings in Western Mathematics 1640-1940* 2005:199–207.

Danuser G. Essay Computer Vision in Cell Biology. *Cell* 2011;**147**:973–978.

Desai N, Ploskonka S, Goodman L, Attaran M, Goldberg JM, Austin C, Falcone T. Delayed blastulation, multinucleation, and expansion grade are independently

associated with live-birth rates in frozen blastocyst transfer cycles. *Fertil Steril* 2016;**106**:1370–1378.

Desai N, Ploskonka S, Goodman LR, Austin C, Goldberg J, Falcone T. Analysis of embryo morphokinetics, multinucleation and cleavage anomalies using continuous time-lapse monitoring in blastocyst transfer cycles. *Reproductive Biology and Endocrinology* 2014;**12**:54.

Desch L, Bruno C, Luu M, Barberet J, Choux C, Lamotte M, Schmutz E, Sagot P, Fauque P. Embryo multinucleation at the two-cell stage is an independent predictor of intracytoplasmic sperm injection outcomes. *Fertil Steril* 2017;**107**:97-103.e4.

Dominguez F, Gadea B, Esteban FJ, Horcajadas JA, Pellicer A, Simon C. Comparative protein-profile analysis of implanted versus non-implanted human blastocysts. *Human Reproduction* 2008;**23**:1993–2000.

Dominguez F, Gadea B, Mercader A, Esteban F, Pellicer A, Simón C. Embryologic outcome and secretome profile of implanted blastocysts obtained after coculture in human endometrial epithelial cells versus the sequential system. *Fertil Steril* 2010;**93**:774-782e1.

Dominguez F, Ph D, Meseguer M, Ph D, Aparicio-ruiz B, Ph D. New strategy for diagnosing embryo implantation potential by combining proteomics and time-lapse technologies. *Fertil Steril* 2015;**104**:908–914.

Ebner T, Höggerl A, Oppelt P, Radler E, Enzelsberger SH, Mayer RB, Petek E, Shebl O. Time-lapse imaging provides further evidence that planar arrangement of blastomeres is highly abnormal. *Arch Gynecol Obstet* 2017;**296**:1199–1205.

Edwards R, Bavister B, Steptoe P. Early stages of fertilization in vitro of human eggs matured in vitro. *Nature* 1969;**221**:632–635.

Edwards R, Steptoe P, Purdy JM. Fertilisation and cleavage in vitro of preovulatory human oocytes. *Nature* 1970;**227**:1307–1309.

Edwards RG, Fishel SB, Cohen J, Fehilly CB, Purdy JM, Slater JM, Steptoe PC, Webster JM. Factors influencing the success of in vitro fertilization for alleviating human infertility. *Journal of In Vitro Fertilization and Embryo Transfer* 1984;**1**:3–23.

ESHRE Working group on time-lapse technology 2020, Apter S, Ebner T, Freour T, Guns Y, Kovacic B, Clef N le, Marques M, Meseguer M, Montjean D, *et al.* Good practice recommendations for the use of time-lapse technology. *Hum Reprod Open* 2020;**4**:hoz025.

Farnoush A. The application of an image analyzing computer (Quantimet 720) for quantitation of biological structures--the automatic counting of mast cells. *Microsc Acta* 1977;**80**:43—47. Available at: http://europepmc.org/abstract/MED/413024.

Ferraretti AP, Goossens V, de Mouzon J, Bhattacharya S, Castilla JA, Korsak V, Kupka M, Nygren KG, Andersen AN. Assisted reproductive technology in Europe, 2008: results generated from European registers by ESHRE. *Human Reproduction* 2012;**27**:2571–2584.

Fishel S, Campbell A, Montgomery S, Smith R, Nice L, Duffy S, Jenner L, Berrisford K, Kellam L, Smith R, *et al.* Live births after embryo selection using morphokinetics versus conventional morphology: a retrospective analysis. *Reprod Biomed Online* 2017;**35**:407–416.

Fishel S, Campbell A, Montgomery S, Smith R, Nice L, Duffy S, Jenner L, Berrisford K, Kellam L, Smith R, *et al.* Time-lapse imaging algorithms rank human preimplantation embryos according to the probability of live birth. *Reprod Biomed Online* 2018;**37**:304–313.

Fragouli E, Alfarawati S, Spath K, Babariya D, Tarozzi N, Borini A, Wells D. Analysis of implantation and ongoing pregnancy rates following the transfer of mosaic diploid–aneuploid blastocysts. *Hum Genet* 2017;**136**:805–819.

Fragouli E, Munne S, Wells D. The cytogenetic constitution of human blastocysts: Insights from comprehensive chromosome screening strategies. *Hum Reprod Update* 2019;**25**:15–33.

Fréour T, Fleuter N, Lammers J, Splingart C, Reignier A, Barriere P. External validation of a time-lapse prediction model. *Fertil Steril* 2015;**103**:917–922.

del Gallego R, Remohí J, Meseguer M, Affiliations A, Valencia IG. Time-Lapse Imaging : The State of the Art . *Biol Repod* 2019;**101**:1146–54.

Garbade DMJ. Clearing the Confusion: AI vs Machine Learning vs Deep Learning Differences. *Towards Data Science* 2018;**14**.

Goodman LR, Goldberg J, Falcone T, Austin C, Desai N. Does the addition of time-lapse morphokinetics in the selection of embryos for transfer improve pregnancy rates? A randomized controlled trial. *Fertil Steril* 2016;**105**:275–285.

Gordon J, Grunfeld L, Garris G, Talansky B, Richards C, Laufer N. Fertilization of human oocytes by sperm from infertile males after zona pellucida drilling. *Fertil Steril* 1988;**50**:68–73.

Handyside A, Lesko J, Tarín J, Winston R, Hughes M. Birth of a Normal Girl after in Vitro Fertilization and Preimplantation Diagnostic Testing for Cystic Fibrosis. *N Engl J Med* 1992;**327**:905–909.

Handyside AH, Kontogianni EH, Hardy K, Winston RML. Pregnancies from biopsied human preimplantation embryos sexed by Y-specific DNA amplification. *Nature 1990 344:6268* 1990;**344**:768–770. Available at: https://www.nature.com/articles/344768a0. Accessed November 8, 2022.

Hathout Y. Approaches to the study of the cell secretome. *Expert Rev Proteomics* 2007;**4**:239–248.

Hollywood K, Brison DR, Goodacre R. Metabolomics : Current technologies and future trends. *Proteomics* 2006;**6**:4716–4723.

Jones K, Warnock S, Urry R, Edwin S, Mitchell M. Immunosuppressive activity and alpha interferon concentrations in human embryo culture media as an index of potential for SUC- cessfal implantation. *Fertil Steril* 1992;**57**:637–640.

Katz-Jaffe M, Gardner DK. Embryology in the era of proteomics. *Theriogenology* 2007;**1**:S125-30.

Katz-jaffe MG, Mcreynolds S. Embryology in the era of proteomics. *Fertil Steril* 2013;**99**:1073–1077.

Khosravi P, Kazemi E, Zhan Q, Malmsten JE, Toschi M, Zisimopoulos P, Sigaras A, Lavery S, Cooper LAD, Hickman C, *et al.* Deep learning enables robust assessment and selection of human blastocysts after in vitro fertilization. *NPJ Digit Med* 2019;**2**:1–9.

Kim KG. Deep Learning. *Healthc Inform Res* 2016;**22**:351–354.

Kirkegaard K, Agerholm IE, Ingerslev HJ. Time-lapse monitoring as a tool for clinical embryo assessment. *Human Reproduction* 2012;**27**:1277–1285.

Kirkegaard K, Hindkjaer JJ, Ingerslev HJ. Human embryonic development after blastomere removal: A time-lapse analysis. *Human Reproduction* 2012;**27**:97–105.

Kokkali G, Traeger-Synodinos J, Vrettou C, Stavrou D, Jones GM, Cram DS, Makrakis E, Trounson AO, Kanavakis E, Pantos K. Blastocyst biopsy versus cleavage stage biopsy and blastocyst transfer for preimplantation genetic diagnosis of β-thalassaemia: A pilot study. *Human Reproduction* 2007;**22**:1443–1449.

Krisher RL, Schoolcraft WB, Katz-jaffe MG. Omics as a window to view embryo viability. *Fertil Steril* 2015;**103**:333–341.

Kupka MS, Ferraretti AP, Mouzon J de, Erb K, Hooghe TD, Castilla JA, Geyter C de, Goossens V. Assisted reproductive technology in Europe , 2010 : results generated from European registers by ESHRE †. *Human Reproduction* 2014;**29**:2099–2113.

Lecun Y, Bengio Y, Hinton G. Deep learning. *Nature* 2015;**521**:436–444.

Levin I, Almog B, Shwartz T, Gold V, Ben-Yosef D, Shaubi M, Amit A, Malcov M. Effects of laser polar-body biopsy on embryo quality. *Fertil Steril* 2012;**97**:1085–1088. Available at: http://dx.doi.org/10.1016/j.fertnstert.2012.02.008.

Lindgren KE, Yaldir FG, Hreinsson J, Holte J, Sundström-poromaa I, Kaihola H, Åkerud H, Lindgren KE, Yaldir FG, Hreinsson J, *et al.* Differences in secretome in culture media when comparing blastocysts and arrested embryos using multiplex proximity assay. *Ups J Med Sci* 2018;**123**:143–152.

Ljunger E, Cnattingius S, Lundin C, Annerén G. Chromosomal anomalies in first-trimester miscarriages. *Acta Obstet Gynecol Scand* 2005;**84**:1103–1107.

Mains LM, Christenson L, Yang B, Sparks AET, Mathur S, Voorhis BJ van. Identification of apolipoprotein A1 in the human embryonic secretome. *Fertil Steril* 2011;**96**:422–427.

Manna C, Nanni L, Lumini A. Artificial intelligence techniques for embryo and oocyte classification. *Reprod Biomed Online* 2013;**26**:42–49.

Martínez MC, Méndez C, Ferro J, Nicolás M, Serra V, Landeras J. Cytogenetic analysis of early nonviable pregnancies after assisted reproduction treatment. *Fertil Steril* 2010;**93**:289–292.

Martínez-Granados L, Serrano M, González-Utor A, Ortíz N, Badajoz V, Olaya E, Prados N, Boada M, Castilla JA. Inter-laboratory agreement on embryo

classification and clinical decision: Conventional morphological assessment vs. time lapse. *PLoS One* 2017;**12**:1–13.

Matusevičius A, Dirvanauskas D, Maskeliūnas R, Raudonis V. Embryo cell detection using regions with convolutional neural networks. *CEUR Workshop Proc* 2017;**1856**:89–93.

Meseguer M, Herrero J, Tejera A, Hilligsøe KM, Ramsing NB, Remoh J. The use of morphokinetics as a predictor of embryo implantation. *Human Reproduction* 2011;**26**:2658–2671.

Milewski R, Kuć P, Kuczyńska A, Stankiewicz B, Łukaszuk K, Kuczyński W. A predictive model for blastocyst formation based on morphokinetic parameters in time-lapse monitoring of embryo development. *J Assist Reprod Genet* 2015;**32**:571–579.

Montag M, Liebenthron J, Köster M. Which morphological scoring system is relevant in human embryo development? *Placenta* 2011;**32**:252–256.

Morales D, Bengoetxea E, Larra P, Merino M, Garc M, Franco Y. Bayesian classification for the selection of in vitro human. *Comput Methods Programs* 2007;**90**:104–116.

Motato Y, de los Santos MJ, Escriba MJ, Ruiz BA, Remohí J, Meseguer M. Morphokinetic analysis and embryonic prediction for blastocyst formation through an integrated time-lapse system. *Fertil Steril* 2016;**105**:376–384.

Neal SA, Franasiak JM, Forman EJ, Werner MD, Morin SJ, Tao X, Treff NR, Scott RT. High relative deoxyribonucleic acid content of trophectoderm biopsy adversely affects pregnancy outcomes. *Fertil Steril* 2017;**107**:731-736.e1. Available at: http://dx.doi.org/10.1016/j.fertnstert.2016.11.013.

Noci I, Fuzzi B, Rizzo R, Melchiorri L, Criscuoli L, Dabizzi S, Biagiotti R, Pellegrini S, Menicucci A, Baricordi O. Embryonic soluble HLA-G as a

marker of developmental potential in embryos. *Human Reproduction* 2005;**20**:138–146.

Norwitz ER, Edusa V, Park JS. Maternal Physiology and Complications of Multiple Pregnancy. *Semin Perinatol* 2005;**29**:338–348.

Palermo G, Joris H, Devroey P, van Steirteghem A. Induction of acrosome reaction in human spermatozoa used for subzonal insemination. *Hum Reprod* 1992a;**7**:248–254.

Palermo G, Joris H, Devroey P, van Steirteghem AC. Pregnancies after intracytoplasmic injection of single spermatozoon into an oocyte. *The Lancet* 1992b;**340**:17–18. Available at: http://www.thelancet.com/article/014067369292425F/fulltext. Accessed November 8, 2022.

Peng H, Zhou J, Zhou Z, Bria A, Li Y, Kleissas DM, Drenkow NG, Long B, Liu X, Chen H. Bioimage Informatics for Big Data. In: *Focus on Bio-Image Informatics*. 2016, 263–272. Available at: http://link.springer.com/10.1007/978-3-319-28549-8.

Petersen BM, Boel M, Montag M, Gardner DK. Development of a generally applicable morphokinetic algorithm capable of predicting the implantation potential of embryos transferred on Day 3. *Human Reproduction* 2016;**31**:2231–44.

Piyamongkol W, Bermúdez MG, Harper JC, Wells D. Detailed investigation of factors influencing amplification efficiency and allele drop-out in single cell PCR: Implications for preimplantation genetic diagnosis. *Mol Hum Reprod* 2003;**9**:411–420.

Poynter F. Hunter, Spallanzani, and the history of artificial insemination. *In Stevenson LG and Multhauf RP (eds) Medicine, Science and Culture The Johns Hopkins Press, Baltimore, MD* 1968.

Punjabi U, Vereecken A, Delbeke L, Angle M, Gielis M, Gerris J, Johnston J, Buytaert P. Embryo-Derived Platelet Activating Factor , a Marker of Embryo Quality and Viability Following Ovarian Stimulation for in Vitro Fertilization. *Journal of in Vitro Fertilization and Embryo Transfer* 1990;**7**:3–8.

Rienzi L, Cimadomo D, Delgado A, Minasi G, Fabozzi G, del Gallego R, Stoppa M, Bellver J, Giancani A, Esbert M, *et al.* Time of morulation and trophectoderm quality are predictors of a live birth after euploid blastocyst transfer : a multicenter study. *Fertil Steril* 2019;**112**:1080-1093.e1.

Robertson SA. GM-CSF regulation of embryo development and pregnancy. *Cytokine Growth Factor Rev* 2007;**18**:287–298.

Romero-ruiz A, Avendaño MS, Dominguez F, Lozoya T. Deregulation of miR-324 / Kiss1 / kisspeptin in early ectopic pregnancy : Mechanistic findings with clinical and diagnostic implications. *Am J Obstet Gynecol* 2019;**5**:e1-480.e17.

Rubio I, Kuhlmann R, Agerholm I, Kirk J, Herrero J. Limited implantation success of direct-cleaved human zygotes : a time-lapse study. *Fertil Steril* 2012;**98**:11–15.

Saith RR, Bersinger NA, Barlow DH. The role of pregnancy-specific P-l glycoprotein (SP1) in assessing human blastocyst quality in vitro. *Human Reproduction* 1994;**11**:1038–1042.

Scott RT, Upham KM, Forman EJ, Hong KH, Scott KL, Taylor D, Tao X, Treff NR. Blastocyst biopsy with comprehensive chromosome screening and fresh embryo transfer significantly increases in vitro fertilization implantation and delivery rates: A randomized controlled trial. *Fertil Steril* 2013;**100**:697–703. Available at: http://dx.doi.org/10.1016/j.fertnstert.2013.04.035.

Scott RT, Upham KM, Forman EJ, Zhao T, Treff NR. Cleavage-stage biopsy significantly impairs human embryonic implantation potential while blastocyst biopsy does not: A randomized and paired clinical trial. *Fertil Steril*

2013;**100**:624–630. Available at: http://dx.doi.org/10.1016/j.fertnstert.2013.04.039.

Sherman J. Clinical use of frozen human semen. *Transplant Proc* 1976:165–170.

Silber SJ, Nagy ZP, Liu J, Godoy H, Devroey P, van Steirteghem AC. Andrology: Conventional in-vitro fertilization versus intracytoplasmic sperm injection for patients requiring microsurgical sperm aspiration. *Human Reproduction* 1994;**9**:1705–1709. Available at: https://academic.oup.com/humrep/article/9/9/1705/609629. Accessed November 8, 2022.

Simopoulou M, Sfakianoudis K, Maziotis E, Antoniou N, Rapani A, Anifandis G, Bakas P, Bolaris S, Pantou A, Pantos K, *et al.* Are computational applications the "crystal ball" in the IVF laboratory? The evolution from mathematics to artificial intelligence. *J Assist Reprod Genet* 2018;**35**:1545–1557.

Steptoe P, Edwards RG. Birth after the reimplantation of a human embryo. *Lancet* 1978;**2**:366.

Sundvall L, Ingerslev HJ, Breth Knudsen U, Kirkegaard K. Inter- and intra-observer variability of time-lapse annotations. *Human reproduction* 2013;**28**:3215–3221.

Thouas GA, Dominguez F, Green MP, Vilella F, Simon C, Gardner DK. Soluble ligands and their receptors in human embryo development and implantation. *Endocr Rev* 2015;**36**:92–130.

Vermilyea MD, Tan L, Anthony JT, Conaghan J, Ivani K, Gvakharia M, Boostanfar R, Baker VL, Suraj V, Chen AA, *et al.* Computer-automated time-lapse analysis results correlate with embryo implantation and clinical pregnancy: A blinded, multi-centre study. *Reprod Biomed Online* 2014;**29**:729–736.

Wirka KA, Chen AA, Conaghan J, Ivani K. Atypical embryo phenotypes identi fi ed by time-lapse microscopy : high prevalence and association with embryo development. *Fertil Steril* 2014;**101**:1637-1648.e5.

Wong CC, Loewke KE, Bossert NL, Behr B, de Jonge CJ, Baer TM, Pera RAR. Non-invasive imaging of human embryos before embryonic genome activation predicts development to the blastocyst stage. *Nat Biotechnol* 2010;**28**:1115–1121.

Wyns C, de Geyter C, Calhaz-Jorge C, Kupka M, Motrenko T, Smeenk J, Bergh C, Tandler-Schneider A, Rugescu I, Vidakovic S, *et al.* results generated from European registries by ESHRE † The European IVF-Monitoring Consortium (EIM) ‡ for the European Society of Human Reproduction and Embryology (ESHRE), ESHRE PAGES. *Hum Reprod Open* 2017;**00**:1–17. Available at: https://orcid.org/0000-0002-6581-5003.

Zaninovic N, Irani M, Meseguer M. Assessment of embryo morphology and developmental dynamics by time-lapse microscopy: is there a relation to implantation and ploidy? *Fertil Steril* 2017;**108**:722–729.

Zeilmaker G, Alberda A, van Gent I. Two pregnancies following transfer of intact frozen-thawed embryos. *Fertil Steril* 1984;**42**:293–296.

Zhan Q, Ye Z, Clarke R, Rosenwaks Z, Zaninovic N. Direct unequal cleavages: Embryo developmental competence, genetic constitution and clinical outcome. *PLoS One* 2016;**11**:1–19.

Zhang JQ, Li XL, Peng Y, Guo X, Heng BC, Tong GQ. Reduction in exposure of human embryos outside the incubator enhances embryo quality and blastulation rate. *Reprod Biomed Online* 2010;**20**:510–515.

Ziebe S, Loft A, Povlsen BB, Erb K, Agerholm I, Aasted M, Gabrielsen A, Hnida C, Zobel D, Mundig B, *et al.* A randomized clinical trial to evaluate the effect of granulocyte-macrophage embryo culture medium for in vitro fertilization. *Fertil Steril* 2013;**99**:1600–1609.

Anexo

- Características morfológicas de la evaluación embrionaria convencional.

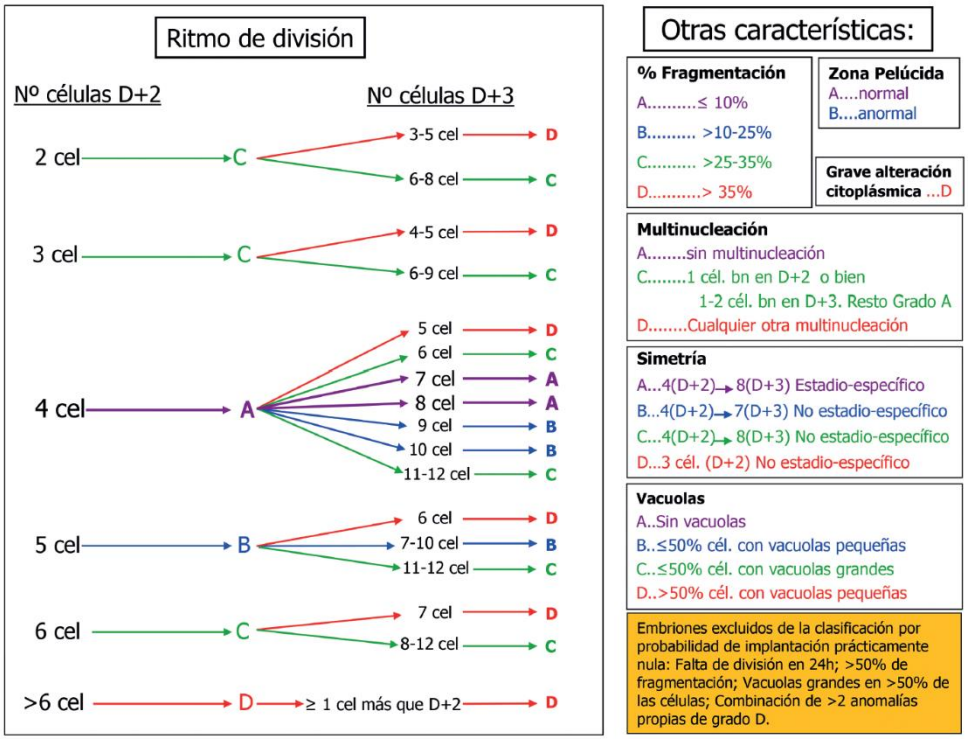

Figura 1. Criterio para la evaluación de embriones in vitro según la asociación para el estudio de la biología de la reproducción (ASEBIR) en el segundo y tercer día del desarrollo embrionario.

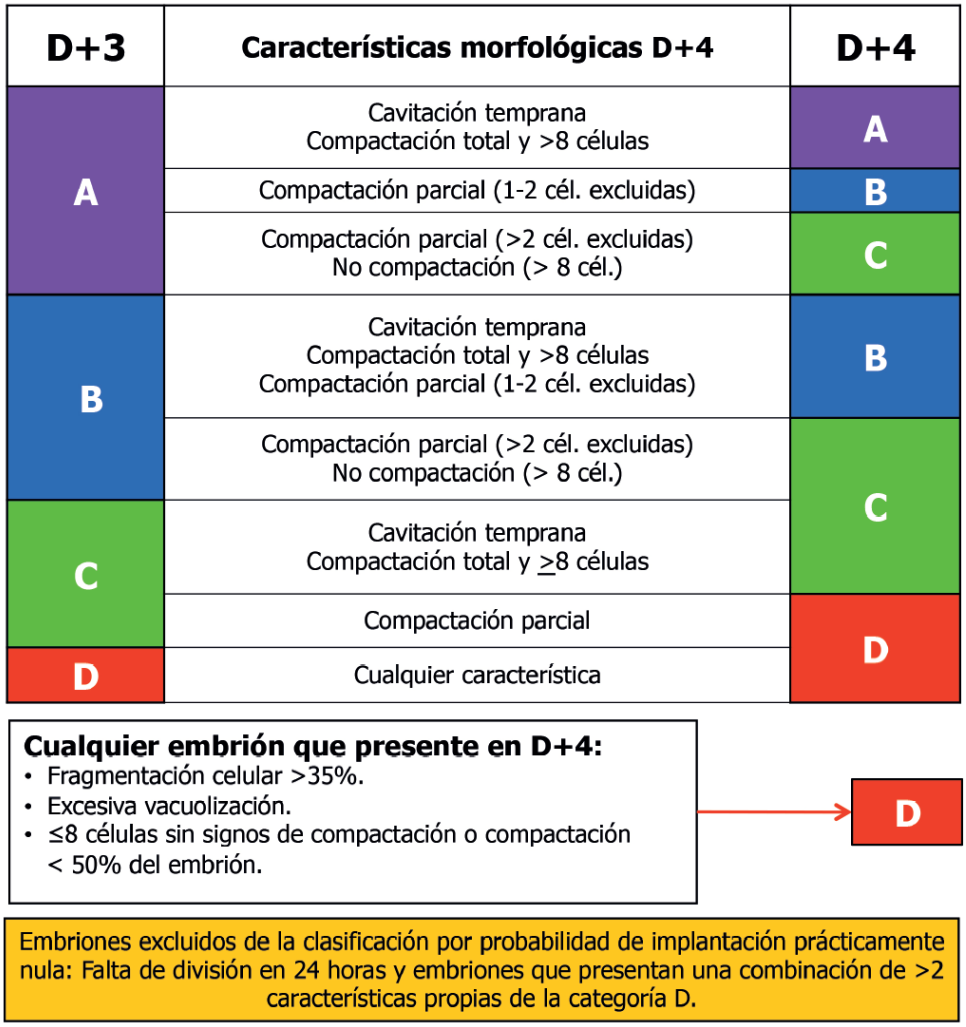

Figura 2. Criterio para la evaluación de embriones in vitro según la asociación para el estudio de la biología de la reproducción (ASEBIR) en el cuarto día del desarrollo embrionario.

<table>
<tr><td rowspan="2">D+4</td><td colspan="4">D+5</td></tr>
<tr><td>Grado de expansión</td><td>MCI</td><td>Trofoectodermo</td><td>ASEBIR</td></tr>
<tr><td rowspan="13">Mórula compacta</td><td rowspan="13">Desde:
"Iniciando la expansión"

Hasta:
"Eclosionando"</td><td rowspan="4">A</td><td>A</td><td>A</td></tr>
<tr><td>B</td><td>B</td></tr>
<tr><td>C</td><td>C</td></tr>
<tr><td>D</td><td>D</td></tr>
<tr><td rowspan="4">B</td><td>A</td><td>A</td></tr>
<tr><td>B</td><td>B</td></tr>
<tr><td>C</td><td>C</td></tr>
<tr><td>D</td><td>D</td></tr>
<tr><td rowspan="4">C</td><td>A</td><td>A</td></tr>
<tr><td>B</td><td>B</td></tr>
<tr><td>C</td><td>C</td></tr>
<tr><td>D</td><td>D</td></tr>
<tr><td>D</td><td>A,B,C o D</td><td>D</td></tr>
<tr><td colspan="3">Blastocisto temprano o cavitando (ZP gruesa)</td><td>C</td></tr>
<tr><td>Mórula no compacta</td><td colspan="3">Mórula</td><td>D</td></tr>
</table>

Figura 3. Criterio para la evaluación de embriones in vitro según la asociación para el estudio de la biología de la reproducción (ASEBIR) en el quinto día del desarrollo embrionario.

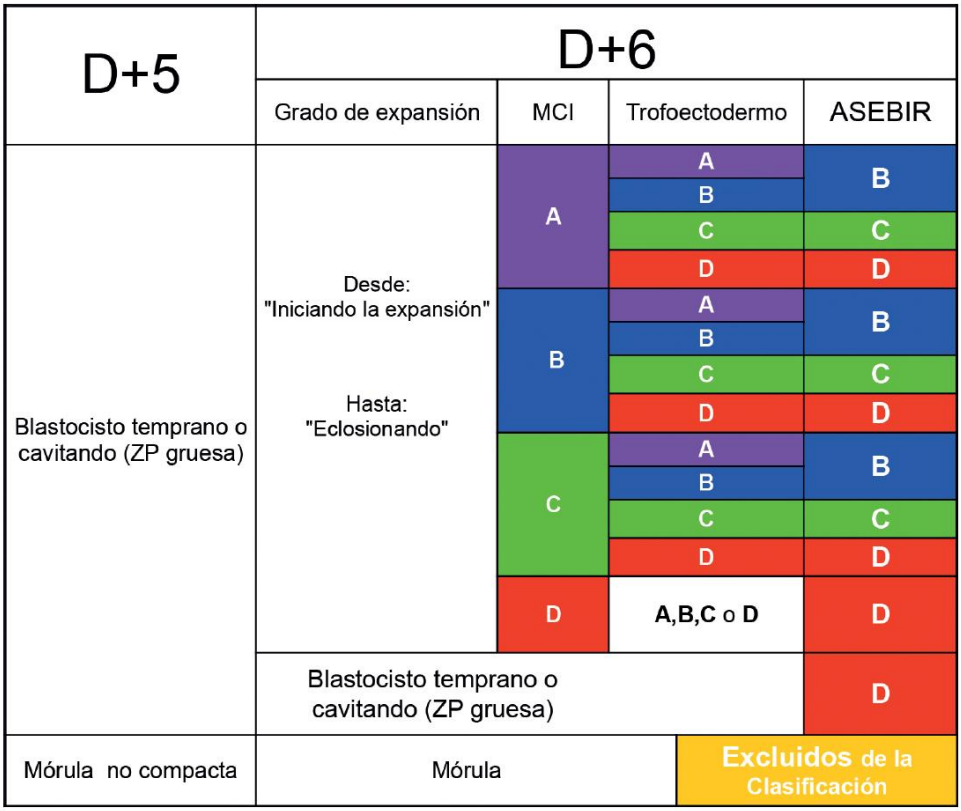

Figura 4. Criterio para la evaluación de embriones in vitro según la asociación para el estudio de la biología de la reproducción (ASEBIR) en el sexto día del desarrollo embrionario.

Categoría	Tamaño MCI (µm²)	Cohesión
A	3800-1900	Compacta
B	3800-1900	No compacta
C	1900	Indiferente
D	Signos de degeneración	
Excluidos	Degenerada	

Figura 5. Criterio para la evaluación de la masa celular interna según la asociación para el estudio de la biología de la reproducción (ASEBIR). MCI, masa celular interna.

Categoría	Descripción del Trofoectodermo
A	Homogéneo, cohesionado y muchas células
B	Homogéneo; menos células
C	Pocas células
D	Signos de degeneración
Excluidos	Degenerado

Figura 6. Criterio para la evaluación del trofoectodermo según la asociación para el estudio de la biología de la reproducción (ASEBIR).

VNIVERSITAT DE VALÈNCIA

Facultat de Medicina i Odontologia

Valencia, Noviembre 2022